Dear Georg,

In this document you will find a brief summary of the main changes made to the manuscript / supplementary information, our response to each of the reviewer's comments and a revised version of the manuscript and SI with track changes highlighted.

Best Wishes,

Ben.

Summary of main revisions

Reporting Fluxes for defined conditions

Alex Guenther's made an excellent suggestion to include a further approach that calculates the emission potential by reporting the average flux for a set of defined (e.g. not standard) conditions. In response to this we have introduced this approach to Section 2.3 where we outline the various options available. We have then added a further section (3.4 – reporting fluxes for a set of defined conditions) to the results section where we discuss our approach to determine the most appropriate set of defined conditions to use (See also Supplementary Information, Section S7, Figs S11-S14) and the advantages and disadvantages of this approach relative to the other methods discussed in the paper. Within this section we include an additional table (4) and figures (8 and 9).

Additional Recommendations

Alex Guenther made several suggestions for further recommendations which we were keen to include in the revised manuscript. These relate to (i) Leaf-level experimentalists reporting emission potentials on both a per mass and per area basis to avoid unnecessary uncertainty when comparing with above canopy fluxes (see Section 3.5) (ii) Modellers providing a single point version of their code to allow experimentalists to more easily translate their above canopy fluxes to isoprene emission potentials (see Section 4) (iii) Experimentalists to no longer use the G06 model in a big leaf format because the resulting emission potentials are typically biased low (see Section 3.3) and (iv) that emission potentials calculated using the weighted average method are also reported for a set of defined conditions to allow modellers to work back to standard conditions themselves (see Section 3.4).

Correction of Castelporziano data

The reviewers noticed that the PPFD data reported for the Castelporziano site looked high. We have checked this with the data provider and the reviewers were correct, the data had been labelled with the incorrect units. We have now reanalysed the Castelporziano data using the correct PPFD data. This has resulted in changes to the Castelporziano results shown in Figs 1, 3, 4, 5, 6 and 7 and discussion of the Castelporziano results made

throughout the text. We have also revised all of the emission potentials and figures presented for the Castelporziano site in the Supplementary Information.

The use of the Weighted Average Method

Two of the reviewers had queries about our decision to recommend the weighted average method over the LSR approach. We discussed our reasoning in detail in our response to the reviewers and have now made changes to the manuscript to make it clear that (i) our reasoning for choosing the weighted average is taken from the perspective of accounting (e.g. we want to ensure the algorithm can reliably reproduce the average flux) and (ii) our reasoning for not adopting the LSR technique is that the regression between flux and gamma is typically non-linear (due to the algorithms inability to properly represent the attenuation of light and temperature through the canopy) and hence violates the fundamental assumptions of a LSR approach (see Section 2.3).

Species composition uncertainties

The reviewers appreciated the fact that we had made an attempt to properly quantify all of the uncertainties associated with derived emission potentials, but questioned if looking at emission potentials by wind sector might give a better approximation of the uncertainty in species composition than assigning a somewhat arbitrary value of 10%. In response to this I have looked at wind roses of emission potential at the Ispra, Bosco fontana and Alice Holt sites and now use the variability between wind sectors as an estimate for species uncertainty (see Section 2.7 and the Supplementary Information (section S6, figure S10). Because the Castelporziano and O3HP sites had much shorter time series it was not possible to perform reliable wind rose analysis at these sites so the uncertainty in species composition was increased to 20% at these sites to reflect the higher values observed at the three other sites.

We thank Alex Guenther and two anonymous referees for their valuable comments on our manuscript. The general feeling seems to be that this paper will form a useful part of the scientific literature but could be further strengthened through the inclusion of emission potentials based on measurements made near a set of defined conditions and through the addition of further recommendations of best-practice for both above-canopy and leaf-level experimentalists. We are, of course, happy to address both of these recommendations in our revised manuscript. In addition we address each of your individual concerns in our more detailed response below.

Response to Reviewer 1, Alex Guenther

General comments

1) The most important comment that I have is that the authors should consider an approach that recognizes that measurements similar to the standard conditions should be used to determine the emission potential. I recognize that this may not result in the best estimate of the daily total emission or the emission at conditions dissimilar to the standard conditions but I would argue that is not the "job" of the emission potential. The emission potential, by definition, is the emission at specified standard conditions and so the best estimate is made by either selecting measurements within some fairly narrow range of conditions or perhaps weighting measurements by how close they are to the standard conditions. It is the "job" of the emission algorithm to go from the emission potential at standard conditions to the emission at other conditions. If the emission algorithm does not do a good job of this then there will be errors but you shouldn't bias the emission potential to try account for this. Instead you should work on developing a better emission algorithm. There will be relatively little difference in the emission potential calculated by different emission algorithms if the emission potential is based on measurements made under conditions similar to the standard conditions. Of course, the problem with applying this approach to canopy scale flux data is that we can't control the measurement conditions and there may not be any that are similar to the standard conditions. If that is the case then the emission potential should be reported for some standard condition that is within the range of the observed conditions. You could then leave it up to the developers/users of a given model to convert this to an emission potential for the standard conditions of their model. Looking at Figure 1, it appears that 3 of the sites would have some measurements at T=30, PPFD=1500 while T=25, PPFD=1500 might be appropriate for the other two. You could report the emission potential for T=25 as the measured emission potential and then also report one or more calculated emission potentials for T=30 along with an exact specification of the model approach used to get there.

AR: In its current form our manuscript is written very much from a measurement perspective so we certainly welcome the opportunity to learn what those involved in BVOC emission model development would find most useful in order to ensure that the recommendations we make are consistent with the needs of the community. We fully agree that if the algorithms were perfectly describing the response to the environmental conditions, the problem our paper discusses would not exist. Thus, developing a better algorithm is a great solution, but until a perfect algorithm is developed the problems we outline will persist.

We also agree with your assertion that each algorithm would derive a similar emission potential when working with only values based close to standard conditions, because the γ factors that account for deviation from the standard conditions would all be small. However, as formulated the standard conditions of most models are far removed from conditions found, e.g., in higher latitudes including at some of our sites. Thus, even if the measurements are made at the reference conditions under laboratory conditions there are two problems: (a) the plant species may not be adapted to these reference conditions and the emissions may not be representative and (b) the algorithm then still needs to correctly extrapolate from those reference conditions to the modelled conditions. The only problem that is solved by this approach is that a different algorithm may otherwise be used in extrapolating from the measurement conditions to the reference conditions than is used for extrapolating from the reference to the modelled conditions, thus duplicating the uncertainty.

Nonetheless, we like your suggestion in principle to report an emission potential together with the conditions that is typical for the measurement dataset and then leave it to the emission modeller to infer the emission potential at their model's reference conditions that is consistent with these emissions under given conditions.

However, there are two problems. As we mention in the manuscript, our reasoning for not including an emission potential based on measurements made close to standard conditions is that the percentage of data that meet these criteria is incredibly low. In addition, as emission algorithms are getting increasingly complex, this is reflected in an increasing number of reference parameters, which means the space of measurement conditions has to be stratified in many dimensions. We had therefore not considered reporting an emission potential for a different set of defined conditions but are happy to do so in the revised manuscript and to include this as a recommendation if you are think this would be useful for the modelling community.

Focussing only on the instantaneous responses to PAR and temperature, we have subsequently re-analysed each data set using a 2d histogram to identify the most appropriate set of conditions to use, e.g a period near the solar maximum with sufficient frequency to provide a robust average flux. We searched for fluxes within windows of ± 0.5 K and ± 100 µmol m^{-2} s^{-1} PPFD. Figure 1 shows the results for the Ispra forest site, which highlights the most abundant set of conditions to use to be between 302-303 K and 1600-1800 µmol m^{-2} s^{-1} PPFD, yielding a total of 19 flux measurements to average. We limit our defined conditions to just current light and temperature as refining the search further to account for the other gamma terms (e.g. T24, T240, PPFD24, PPFD240, RH, wind speed) would limit the available data to little more than n=1. Instead, in Table 1 we list the average fluxes for the defined conditions along with the average of the gamma terms with associated standard deviations.
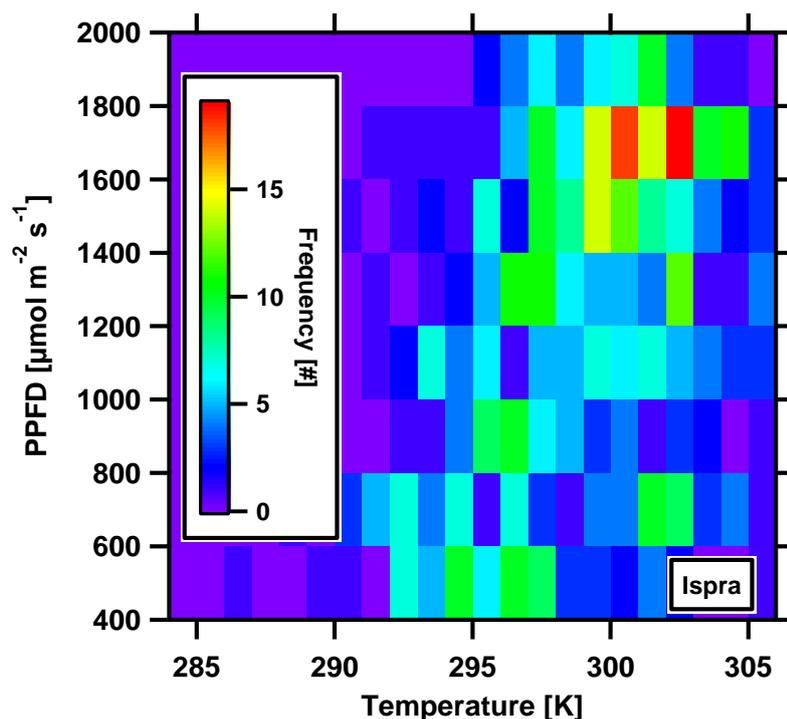
Figure 1. 2d histogram showing the number of flux measurement made at the Ispra forest site that fall within defined light (± 100 PPFD) and temperature (±0.5 K) bins.

As you suggest, reporting fluxes for a set of defined conditions in this way will allow model developers to convert these to the standard conditions used in their model, but, as you point out, will unavoidably introduce further uncertainty. To investigate this further we derived new emission potentials "converted" from the measured values in Table 1 for the G93 and MEGAN 2.1 models (a, b and c) and then compared the performance of these algorithms at replicating our measured fluxes at each site. Figure 2 shows the percentage difference between the averaged measured flux and the averaged modelled flux when using the "converted" isoprene emission potentials. The calculated bias ranged between +29% and -4% for the G93 algorithm and between +9% and -40% for the MEGAN 2.1 approaches. The bias for the G93 algorithm is typically positive which reflects the fact that the algorithm performs well at conditions close to standard conditions but performs worse in the morning and afternoon, overestimating emission fluxes due to its inability to account for the attenuation of light and temperature through the canopy. The observed bias in the MEGAN2.1 simulated isoprene fluxes is driven by two factors (i) the fact that the average flux for the set of defined conditions is based on a limited number of data points (which affects both algorithms), ranging between n=4 to n=19, which may be a poor representation of the typical flux footprint and canopy heterogeneity and (ii) the defined conditions are based on current PPFD and temperature with larger uncertainty on the remaining gamma terms such as past PPFD and temperature.

Thus we conclude that this approach, by definition, succeeds in simulating the emissions at 'typical' conditions encountered at the site, but not in reproducing the average emission.

Table 1. Isoprene emission potentials for each of the five sites for a set of defined conditions. Numbers in brackets show 1 σ.

	Alice Holt	Bosco Fontana	Castelporziano	Ispra	O3HP
IEP (average flux) [µg m^{-2} h^{-1}]	2143	1911	83	9404	2649
σ [µg m^{-2} s^{-1}]	1075	599	102	3593	988
$\overline{RE}$ [µg m^{-2} h^{-1}]	142	443	31	1268	353
N [#]	9	17	5	19	4
Temperature range [K]	293-294	302-303	300-301	302-303	293 - 294
PPFD range [µmol m^{-2} s^{-1}]	800-1000	1800-2000	1400-1600	1600-1800	1800-2000
Mean Temperature [K]	293.4 (0.2)	302.5 (0.3)	300.5 (0.14)	302.6 (0.3)	293.7 (0.16)
Mean PPFD [µmol m^{-2} s^{-1}]	915 (66)	1902 (60)	1523 (44)	1703 (61)	1852 (35)
Mean 24 T [K]	290 (1.1)	299 (1.4)	295 (0.6)	298 (1.6)	290 (0.9)
Mean 240T[K]	290 (0.94)	299 (1.8)	295 (0.25)	297 (1.4)	290 (1)
Mean 24 PPFD [µmol m^{-2} s^{-1}]	432 (84)	680 (70)	424 (31)	556 (3)	625 (54)
Mean 240 PPFD [µmol m^{-2} s^{-1}]	415 (92)	659 (48)	452 (15)	553 (17)	591 (0.7)
Humidity [g/kg]	7.9 (1.2)	11.9 (1.6)	13.5 (1)	11.4 (1.7)	6.5 (0.8)
Wind Speed [m s^{-1}]	2.19 (1)	2 (0.81)	1.8 (0.5)	1.4 (0.5)	4.1 (1.4)

As we discuss in the original manuscript, if emission potentials are calculated using all measured flux data and not just those obtained at a set of defined conditions, then the average measured flux can be replicated by the algorithm with zero bias assuming the weighted average approach has been used to derive the emission potential. The drawback to this approach is that that emission potential cannot then be easily converted for use in different emission models. We agree with you that publishing an average flux for a set of defined conditions may be more readily used by model developers and hence have a wider impact, but we believe it is necessary to highlight that this approach results in emission potentials that are inherently more uncertain, especially for the more complex algorithms where not all of the gamma terms can be controlled. In the revised manuscript we will have a further section to discuss the findings shown here and will recommend experimentalists to adopt both approaches. In addition, we will further stress the importance of researchers submitting their observational data sets to online, publically accessible, data repositories such as the VOCsNET database, as we believe a well populated community database would be a far more valuable resource to model developers and would support further improvement in emission algorithms.
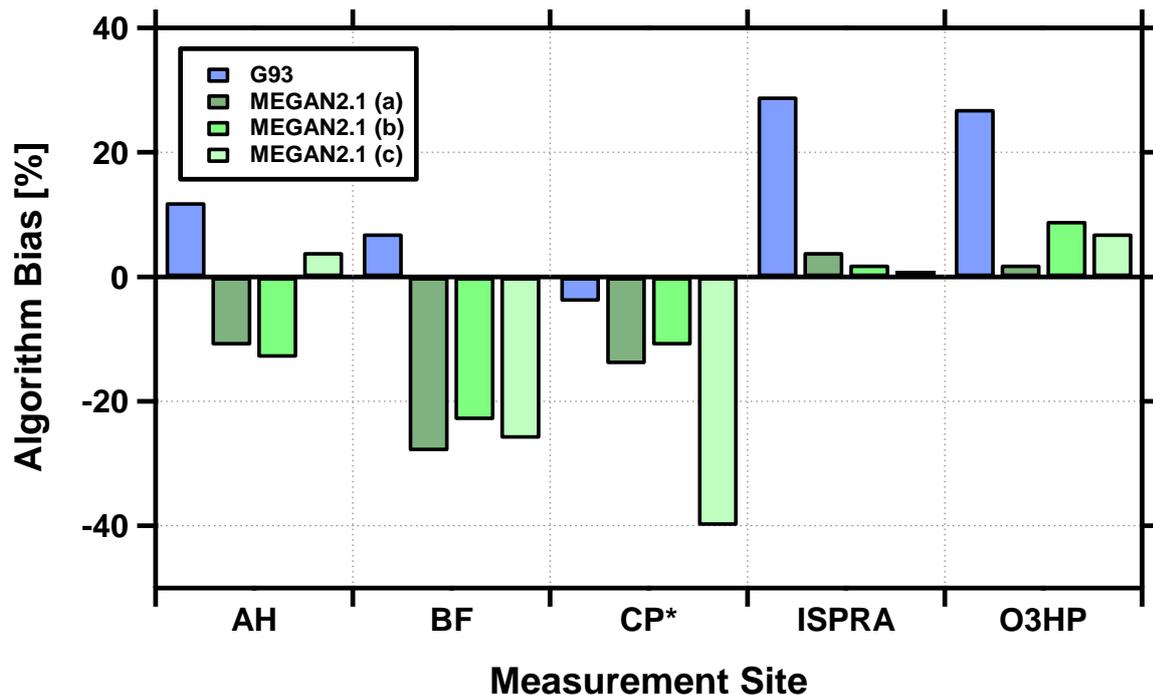
Figure 2. Percentage bias of the average isoprene emission flux simulated by the G93 and MEGAN2.1 emission algorithms at the five measurement sites, Alice Holt (AH), Bosco Fontana (BF), Castelporziano (CP), Ispra forest (ISPRA) and the Observatoire de Haute Provence (O3HP), compared to the measured average flux when using a "converted" emission potential.

2) I assume that there is at least some landscape heterogeneity at some of these sites. The authors should consider binning measurements for different "footprints" associated with different wind directions that represent different oak fractions. This could provide "replicates" with emission potentials for a larger range of oak fraction values that may provide some insights into the value and variability in the leaf-level emission potential. Of course, this assumes that there is some information on the landscape heterogeneity at these sites.

AR: We agree that such an approach could prove useful where there is very detailed species composition data available. Unfortunately, the information we have on species composition at each site is for the forest as a whole and not spatially resolved. Nonetheless, calculating an emission potential by wind sector does provide some information on the spatial variability of the emission potential. For each site we will investigate to see if there is sufficient variability in the wind direction to enable us to infer a species composition uncertainty based on the variability of emission potentials calculated for each wind sector. We have explored the spatial aspects of species composition for the Bosco Fontana field site in a separate paper (Acton et al., 2016) and will refer to the main messages in the revised manuscript.

Specific comments

Page 2, line 28: "In the Guenther algorithms, isoprene emission rates are modelled by assessing the emission potential". This is not something specific to these algorithms all isoprene emission models include some term of this type, although they may not call it an emission factor.

AR: We will change this to " In most BVOC emission algorithms…"

Page 4, line 31: delete "to" in "Castelporziano has to a Thermo-Mediterranean"

AR: This will be changed

Page 6, line 18 and line 33: Be more specific about how the tendencies for studies to use a big leaf approach and using leaf temperature equals air temperature. For example, how many of the studies listed in line 16/17 do this? It may be useful to consider that at least one reason investigators do is because of the considerable effort involved in applying the full inverse canopy algorithm to their dataset and it would be useful to have an easier way to do this. For example, Yu et al. al 2017 (http://doi.org/10.1016/j.scitotenv.2017.03.262) calculated emission factors using an aircraft flux measurement dataset by using the single point version of MEGAN2.1 that you mention on page 7 line 9, and is relatively easy to use, and compare this with emission factors estimated using the regional MEGAN2.1 FORTRAN code, which is relatively difficult to use. A possible recommendation from your study is that BVOC emission modelers should provide a single point version of their code that can more easily be used to derive emission potentials from tower and aircraft flux data.

AR: We agree wholeheartedly with you on this point. The big leaf G93 approach is undoubtedly the most widely used method to calculate emission potentials due to its simplicity. Our investigation of different algorithms was only made possible through the use of the "Pocket MEGAN" you provided so we will ensure the revised manuscript includes a recommendation for model developers to provide a single point version of their code to enable experimentalists to more easily calculate emission potentials.

Page 8, line 32-36: The statement that "Measurements of the emission potential made using leaf-cuvette systems on a single leaf or branch gives a direct measurement of the isoprene emission rate that inherently excludes the deposition process." seems inconsistent with "but it may still be offset slightly as some of the isoprene may undergo dry deposition to leaf surfaces". The leaf cuvette measurement excludes deposition to other leaves and to the soil but there is the possibility of uptake by the emitting leaf including by phyllosphere microbes on the leaves.

AR: You are correct. We will amend the text accordingly

Page 10, line 27: what is the basis for the 10% uncertainty assigned to species composition and 15% to LAI? Does this consider landscape heterogeneities and the uncertainty associated with differences in the LAI and species composition within the footprint of each measurement in comparison to the average for the whole area?

AR: The species composition data and information we have on LAI for each measurement site did not come with associated uncertainties and therefore these values are fairly arbitrary. As discussed above, we will revise the 10% species composition based on the spatial variation of isoprene emission potentials when broken down by wind sector. An initial analysis of IEP windroses for the AH, BF and Ispra forest sites and shown in Figure 3, reveals that the emission potential is fairly constant with wind direction. Taking the standard deviation of the IEP from different wind sectors and comparing with the site average suggests a variability of 14% to 28%. The largest variability was seen at the BF site (28%), which had the smallest fraction of oak and the smallest was seen at AH (14%) which was composed of 90% oak. Wind rose analysis were not performed on the two remaining sites, Castelporziano and O3HP, because these were much shorter time series with insufficient data coverage to provide meaningful emission potentials for different wind sectors. In the revised manuscript we will increase the uncertainty for these two sites from 10% to 20%.
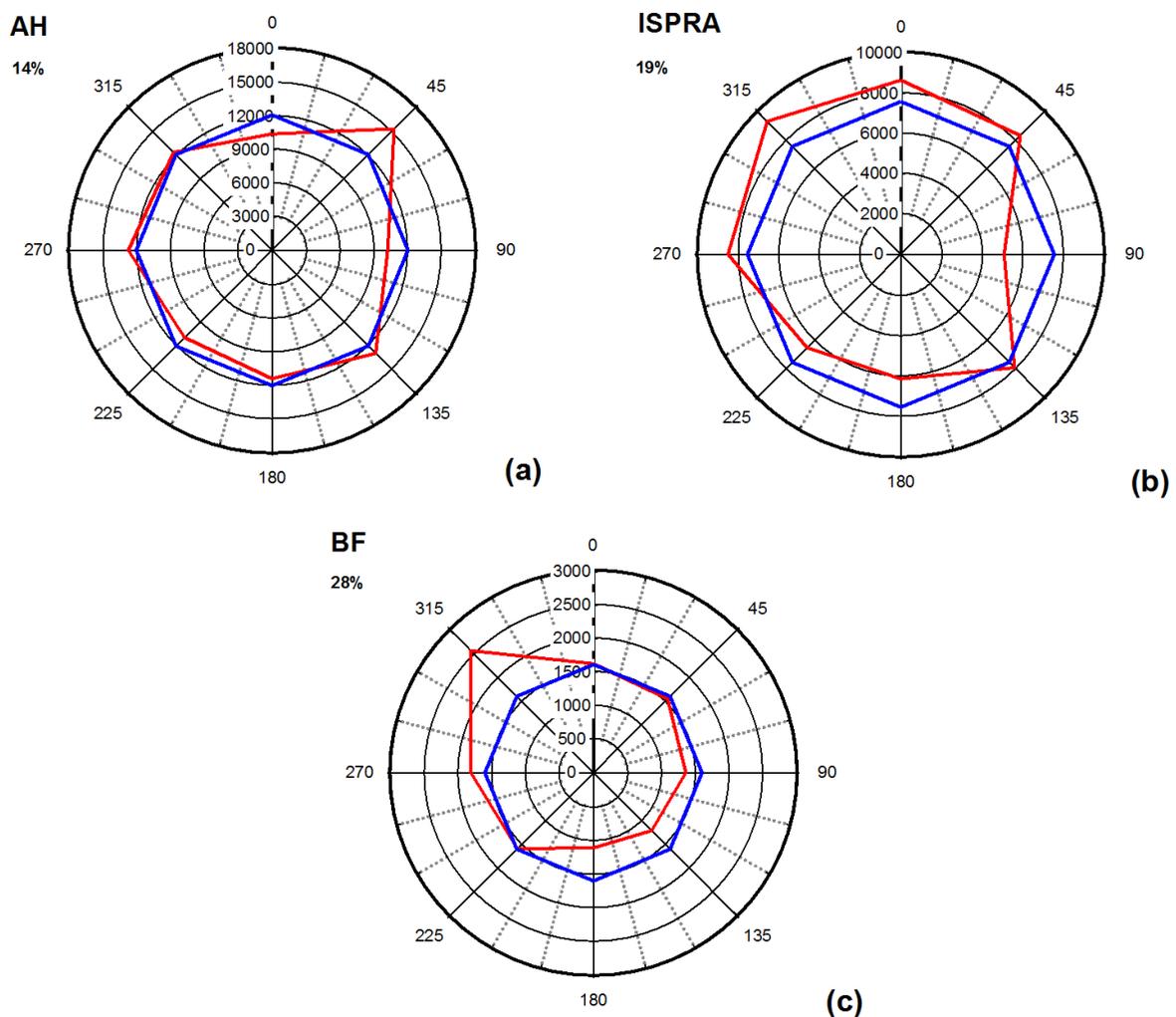
Figure 3. Isoprene emission potentials calculated by wind sector for the Alice Holt (a), Ispra forest (b) and Bosco Fontana (c) sites (red traces) compared to the site average emission potential (blue trace).

Page 10, line 34: The specific leaf mass that you use to convert canopy scale emission potentials to leaf-per-mass emission potentials are arguably as uncertain and variable as isoprene emission potentials. A 25% uncertainty for specific leaf mass may be a reasonable value but you should justify this number and mention how this makes it difficult to compare canopy and leaf scale measurements. This uncertainty could be eliminated if the investigators making leaf level measurements would report emissions as both "per mass" and "per area" leaf emission potentials (i.e., they should provide the specific leaf mass for each measurement) and I suggest that this be a recommendation. If some of the leaf level data that you refer to include measured specific leaf mass (and so direct measurements of per-area leaf emission potentials) then you should make this more direct comparison that does not suffer from the large uncertainties in specific leaf mass estimates (you could do this in addition to the comparison you have already made with the per-mass leaf emission potentials.

AR: This is an important point which we will add to our discussion along with specific recommendation for leaf-level emission potentials to be reported on both a "per mass" and "per area" basis.

Page 11, line 29: Define what you mean by a "wide" range. The range given here of 6750 +/- 1150 is equivalent to +/- 17% which is well within the uncertainties that you discuss. Should that be considered a wide range?

AR: This will be changed to "…the calculated emission potentials span from ~ 5,600 to 7,900 µg m-2 h -1"

Page 12, line 22: "regional or VOC global" should be "regional or global VOC" Page 13, line 26: MEGAN2.1 allows users the option of using a constant value for each of the 15 PFTs but the recommended approach is to use the MEGAN2.1 isoprene emission factor map that accounts for the fraction of isoprene emitters in each landscape based on plant species composition and the species specific emission potential for each location.

AR: We will make the suggested change and highlight the suggested MEGAN best practice in the revised manuscript.

Page 14, line 1: The MEGAN2.1 canopy-scale emission potential for high isoprene emitters is 24000 ug m-2 h-1. The global average temperate broadleaf deciduous tree PFT isoprene emission potential of 10000 thus represents a canopy composed of 41.6% high isoprene emitting trees which is high but not "primarily composed" as stated in the text.

AR: We will make this point clear in the revised manuscript and rephrase our statement accordingly

Page 14, line 17-22: As is pointed out in this manuscript, canopy-average leaf-level PPFD values are considerably lower than above canopy values. Even sun leaves have a PPFD that is typically 50% or less than the above canopy PPFD since they are, on average, at an angle to the sun. The MEGAN2.1 standard condition for the past 24 and 240 hour PPFD refers to the leaf-level value and it is not appropriate (i.e., it just doesn't work) to use the above-canopy value (i.e., a big-leaf model) with this equation (G06). That the G06 past 24/240 hour algorithm should

not be used with the big leaf model is an important point to make in this paper but then going on to compare the MEGAN leaf-level PPFD standard condition with the measured above-canopy PPFD in figures S5 to S9 is comparing "apples and oranges" and may be confusing to some readers. It should be made clear that this is a comparison of two different parameters (above canopy PPFD and leaf-level canopy-average PPFD) and the main point is that the above-canopy value should not be used in the past 24/240 algorithm.

AR: Agreed. We will make this point clear in figures S5 to S9.

Page 14, line 28: Why not just conclude/recommend that the G06 algorithm should not be used with a big leaf model?

AR: Agreed. We will add this recommendation here.

Page 14, line 23 (and Figure 1 and Figure 7): Check on the values of PPFD shown for Castelporziano. They appear to be higher than what would be expected at the top to the atmosphere. Also, note that PAR should always be expressed in units of W/m2 while PPFD is the appropriate term when you use units of micromol/m2/s.

AR: Agreed. We checked with the data owner who has now provided the PAR data in the correct units. We have re-analysed all of the Castelporziano data using the correct PAR data and have updated the text, tables and figures accordingly. Additionally we have now replaced PAR with PPFD throughout the manuscript.

Page 14, line 37: This sentence is confusing.

AR: This will be changed to "Interestingly, when the use of previous light and temperature is switched off (e.g. MEGAN 2.1 (c)) the emission potential increases as the effects of past light and temperature are no longer considered.

Page 14, line 40: This may be because the Castelporziano PPFD solar radiation value is incorrect as mentioned above.

AR: Thank you for pointing out this error. We now have the correct data from the data provider and have recalculated all of the emission potentials and replotted all graphs and tables to account for the adjusted PAR values.

Page 15, line 4-6: or when they are measured under conditions similar to the standard conditions

AR: Agreed, we will stress this point in the revised manuscript.

Page 15, line 9: Leaf-level isoprene emission potential varies considerably between the top and bottom of the canopy and also depending on the past light and temperature environment. Are the leaf level emissions representative of the canopy average, as is the case for the canopy scale measurements, and is the past light and temperature similar? If this is not known, and it is often not reported for leaf-level studies, then this point could be included in the discussion of uncertainties for this comparison.

AR: Agreed we will add this point to our discussion and make a recommendation for past light and temperature to be reported with Leaf-Level emission potentials.

Page 15, line 23: As discussed above, an alternative approach is to select only measurements that are close to the standard conditions.

AR: This will be added.

Page 16, line 37: This is an important point and a good opportunity for you to provide some recommendations for the standardization of flux measurements.

AR: Standardisation of VOC flux measurements is undoubtedly important, but we are not comfortable with making specific recommendations without fully engaging with the community. Encouragingly, some progress in this area is being made with a PTR-MS intercomparison scheduled for later this year in Cabauw as part of the European research infrastructure project ACTRIS. This will hopefully lead to the formation of standard instrument operating procedures but a similar effort is needed for flux measurements and in particular for their post-processing.

Figures 4-6: You were generally consistent in referring to "emission potentials" but these figures refer to "emission factors". Either can be used but be consistent.

AR: These will be changed

Response to Anonymous Reviewer 2

General

1) The authors should try to avoid the confusion between the same parameters derived in a different way/scale/conditions. Alex's point to use the conditions closest to the standard conditions seems like another sensible approach worth evaluating. However, inverting the algorithm even at conditions significantly deviating from standard conditions seems still worth the exercise but must necessarily lead to larger errors from environmental parameters measured simultaneously, and potentially may become inconsistent with original model design or intent. Assuming the measured environmental parameters (e.g. T, PAR) are accurate, the value of inferring about the emission potential at different conditions seems valuable to assess how well the algorithmic activity factor works. If it works well, then the emission potential collected under the conditions close to standard should be similar to that inverted from fluxes measured at different conditions with reverse algorithm within the

same footprint. For example, Figure 2 showing stable measured emission potential during the day is unbelievably encouraging, so this approach in my opinion deserves some greater attention.

AR: We agree that Alex's suggestion is a good one and have added emission potentials for specific light and temperature conditions which we discuss further in our response to Alex and will also include in the revised manuscript.

2) Model parameters which were designed for the leaf level-scale may not always be compatible for comparison or extrapolation with the same parameter obtained from inverting the equation at the ecosystem scale, even if in principle it should work. For this reason, it would be helpful to use a thoughtful system of descriptors for equivalent parameters, e.g. EFcan or EFextrap, so it is clear and distinguishable how the parameter was obtained. This will help the issue which the authors are trying to communicate to modelers (last paragraph in the abstract) that they should be careful about how these parameters were derived before using them.

AR: In the supplementary information we do already make this distinction by presenting emission potentials as E_{eco} (ecosystem emission potential), E_{can} (Oak canopy emission potential) and E_{LL} (Leaf-level equivalent emission potential). We will add the subscripts to figures 4-6 and throughout the text.

3) The abstract seems somewhat heavy for a reader. The take-home message about the differences as large as a factor of four are somewhat scary and confusing. It asks for some further insight as to what exactly causes such a large difference. If you suggest the uncertainties in the inversion of the algorithms are different for different models is it because the inversion does not work perfectly or the specific algorithm does not work well for top-down inference about the emission potential (so would likely not be accurate the other way round – bottom up)? I suggest to focus in the abstract on the major points and progress, and less so much on what you did and technical detail. Specific

AR: Agreed, the abstract will be made more concise with less focus on the technical detail.

4) P5 L33 G93 "Perhaps the most widely used" – did you mean the most highly cited?

AR: I think it is the most highly cited because it is also the most used. We will change to say "…the most widely used and highly cited…"

5) P8 L4-5 Why did you leave out Langford et al. 2010 here? Misztal et al. (e.g. 2011, table 3) used approaches to estimate BER from the regression with measurements, as well as from the middle of the day (11:00 LT; which you show also here agrees well). I think you should add Langford et al., 2010 reference here, because they reported BERs as mid-day average. I would also suggest to be more neutral and refrain from subjective statements about which approaches are more popular.

AR: This reference will be added

6) Abstract. Seems long and overloaded. In particular the last two sentences are rather pessimistic and might agitate modelers unnecessarily, because it is hard to believe you could really be off by a factor of four if everything is done perfectly or at least it is not sufficiently clear why exactly this is the case.

AR: The last two sentences will be removed.

7) In the concluding remarks, you focus on the way the emission potentials are derived. Do you also want to make a bigger point about how the future models could be enhanced to better assimilate observational data at regional scale?

AR: We will stress the point that by providing a consistent and robust approach to calculating emission potentials from top-down flux measurements future models may be better parameterised through the incorporation of regional scale observations.

8) It is great that you include the original definition of emission factor (collected under the standard conditions and leaf scale). I wonder if it would be worth making a distinction between the parameterized algorithm on the full-canopy observations and whether it should be labeled as the same or a modified algorithm.

AR: We are unsure to which part of the manuscript you are specifically referring to here. Please could you provide a specific page and line number?

9) Table 1 – since PTR-TOF-MS was used in Castelporziano, why did you write vDEC? Did you artificially convert the PTRTOF dataset to disjunct to be consistent with other measurements? Either seems fine, as long as it is clear.

AR: This has been changed

10) SI S1.1 Alice Holt – Measurement setup Lag time - as the signal to noise ratio for isoprene was rather very high, why did you use the approach for low signal to noise species? Why did you not use the accurate lag-time from each half hour period?

AR: The signal-to-noise ratio for the isoprene data set was well below 10. According to Langford et al. (2015) a data set with a signal-to-noise ratio in this range and with disjunct sampling interval of 2.5 s could expect a systematic bias of around 50% (see Figures 4 and 6b). For this reason we used a prescribed lag-time as recommended by Langford et al.

11) SI S1.1 "to ensure the reduced electric field strength" seems somewhat random and out of context. Also 2.01 mbar suggests that the pressure was stable to 0.01 mbar. This is rarely the case. I suggest you say 2.0 mbar or 2.01+/-0.XX mbar

AR: The line you refer to simply describes that the E/N ratio was held constant at 127 Td. The E/N ratio is a fundamental parameter which should always be reported so we would be reluctant to remove this. "The PTR-MS operating conditions were held constant throughout the measurement period to ensure the reduced electric field strength (E/N, where E is the electric field strength and N is the buffer gas density) was maintained at 127 Td."

12) SI S.1.1 P.1 L21-22 Instead of the justification it might be appropriate just to write what the consequences are (if any). I do not think it is necessarily bad to use high resolution measurement if it is appropriately post-averaged unless it leads to counting zeros. Otherwise, can you inform what the difference is between fluxes measured at 50 ms and averaged to 200 ms, as opposed to measured at 200 ms?

AR: The consequences are a lower signal-to-noise-ratio and potential systematic bias. We avoid this potential bias by using a prescribed time-lag as recommended by Langford et al. (2015). We will make this point in the revised manuscript.

13) P8 L16-30. Unfortunately, I am extremely confused by the lack of clarity here. In particular, the weighted IEP is concerning. Why do you average the activity factor across the footprints and conditions before taking the ratio? It does not seem appropriate, because, as you say, these processes are nonlinear. For example, you have to use the model to average PAR accurately. It is more intuitive to average the emission potential, because in principle it should be relatively constant for the same vegetation type (as you show in Fig. 2), and you would not have to average nonlinear processes.

AR: We apologise for the lack of clarity as we believe the reviewer may have misunderstood our approach. We are not calculating a gamma for the average meteorological conditions, but calculating the average of all gammas which were explicitly calculated for each individual flux period. Please also refer to our response to reviewer 3 where we further justify this approach. In the revised manuscript we will clarify our approach to avoid any further confusion.

14) Sect. 2.4. Isoprene deposition. Given the large gradient it is interesting that the authors suggest the deposition can be significant even for isoprene. It would be helpful to provide the percentage range of isoprene deposition relative to total flux, in addition to canopy resistance. As Alex wisely points out, you need to be aware of epiphytic microbes whose role is not yet well understood in affecting emission and uptake of isoprene.

AR: This is already stated (5-8%) in both the abstract and results sections. As we point out in the manuscript these estimates are highly dependent on the value of Rc we use, which may not be ideal for our sites but represents the only published value available in the literature. To truly understand how much isoprene is lost due to dry deposition and indeed to microbes on leaf surfaces will require further research,

but the method we outline will become increasingly meaningful as more VOC specific canopy resistances become available in the future.

15) Sect. 2.6 how do you differentiate between the effective LAI and the tree cover area fraction?

AR: Unfortunately we do not have leaf area index measurements for the individual tree species, only the tree cover fraction and hence we cannot differentiate between the two. Upscaling to 100% oak undoubtedly means that changes to the canopy LAI will occur, with the largest changes associated with sites with the lowest fractions of oak. We discuss this uncertainty in Section 2.7 and attempt to scale this relative to how much upscaling is required but recognise that without detailed information on tree species LAI our efforts are somewhat arbitrary.

16) P10 L28 As you did not calibrate isoprene on gas standard at Alice Holt, you had to estimate the concentration from relative transmission. I am generally fine with the approach, but it should be clear in the text whether you have accounted for isoprene fragmentation (mostly to m/z 41) because as you probably know isoprene sensitivity is significantly deviating from transmission estimate vs non-fragmenting species (e.g. MVK). Not accounting for fragmentation would result in underestimating the concentrations but perhaps you derived a fragmentation correction factor for proton reaction rate constant (effective k) in the post-campaign calibration? In either case it is not clear so you should add appropriate detail to SI.

AR: The reviewer is correct about the fragmentation of isoprene to m/z 41 and this was already accounted for in the reaction rate constant k used in our transmission. For completeness, we now include a description of the correction applied.

17) Sect. 3.2 Figure 2a,c is incredibly super cool, and the diurnal emission potential seems relatively constant as expected, except for the morning and evening times. Did you try to filter for low u-star to see how this would affect the diel trend? Maybe you could plot the low ustar data in grey. Do you know why you could not reproduce this stability with G93 as beautifully as with G12?

AR: We are glad the reviewer enjoyed this figure. The fact that the G12 algorithm is able to much better replicate the measured fluxes, even during the evening and morning periods means that low turbulence is not the reasoning for the comparatively poor performance of the G93 algorithm. The G93 is unable to replicate the diurnal pattern because it uses the big-leaf approach and therefore cannot properly capture the effects of light and temperature attenuation through the canopy.

18) Figure 7. This is also an incredibly beautiful figure. In particular the temperature activity factor works shockingly well. In panel a, it might also be useful to add the parameterized G06 line which would better fit the gamma for PAR. It would be nice to further discuss these differences because they show major results from this study

AR: The purpose of this figure is to demonstrate why the G06 algorithm generates emission potentials that are much lower than the other algorithms. We feel it is critical to highlight the problems with this approach because it is becoming more widely used, including by ourselves in the past. We feel that adding the PCEEA approach to this figure, an algorithm that was more consistent with the emission potentials calculated using MEGAN 2.1, may dilute our message.

Technical:

19) G93, G95, G06, G12 need to be defined on their first use and used consistently (e.g. G93 in the abstract).

AR: This will be changed

20) add page numbers in SI

AR: Page numbers will be added

21) Sect. 2.1.1-2.1.5 Significant figures in the coordinates of the locations vary from 3 to 10. Please be consistent.

AR: Changed to 3 SF at each site

22) P6 L13 the unit of the gas constant seems incorrect. Maybe a typo or maybe you intended to refer to 1 mole.

AR: This will be corrected.

Response to Anonymous Reviewer 3

Overall, this is a nice paper that explores a technical aspect of isoprene emission modeling: relating whole-system, measured isoprene fluxes to the emissions capacity used in most isoprene emission frameworks. My biggest concern is that the authors recommend using the means of observations and of the calculated gamma to find the emission capacity (equation 6). On page 13, line 2, the authors' state that the superiority of this technique has been established in the previous results section. Since the least-squares approach has a well-established theoretical justification, the manuscript should do more to explore the advantages of Equation 6. This must be a pretty common issue in modelling. For example, how do ecosystem models of net primary productivity deal with this issue? I think the authors could do more to justify this new approach.

AR: I'm not sure we agree with the reviewer on this point. In the context of calculating emission potentials from eddy covariance flux measurements the least squares approach has been used but to the best of our knowledge its use has never been explicitly justified. Indeed, the lack of justification was the partial

motivation for this work. We would stress that the specific approach you take to calculate your "average" emission potential should depend on your proposed use of the BVOC model. In our manuscript we address this problem from the perspective of accounting, with the aim of producing an emission potential that allows us to properly simulate average or total emissions from a given forest over a given time period. We present eddy covariance flux measurements which we carefully correct for the effects of chemical flux divergence and dry deposition and therefore assume to represent the "best estimate" average emission from the site. Having established this "best estimate" average emission rate we can now use this to first back out an emission potential and secondly to challenge the model (combined with new emission potential). In practice this is no different from using a branch enclosure to measure the isoprene flux and then scaling to standard conditions using the algorithm to estimate the emission potential. Using this approach we have systematically evaluated various techniques for deriving a single "average" emission potential from a time series of flux measurements including through the LSR approach. As the reviewer suggests, the least squares approach has a well-established theoretical justification but only if a number of assumptions are fulfilled, two of which are that the data show a linear relationship and that the residuals are normally distributed. Figure 4 shows a plot of the measured isoprene flux versus the G93 γ term for the Bosco Fontana measurement site. It is clear that (i) the relationship is non-linear, driven by the algorithms inability to account for the attenuation of light and temperature through the canopy particularly during the periods either side of midday and (ii) the residuals are not normally-distributed. These two factors mean that the application of the LSR approach would be inappropriate. Indeed, our analysis shows that when the LSR method is used to estimate the "average" emission potential, then the algorithm subsequently fails to replicate the average observed flux. In contrast, adopting the "weighted average" approach ensures an emission potential with zero bias.

We will include this figure with short explanation in a revised version of the Supplementary Information and will emphasise our justification for choosing the weighted average method in the revised manuscript.
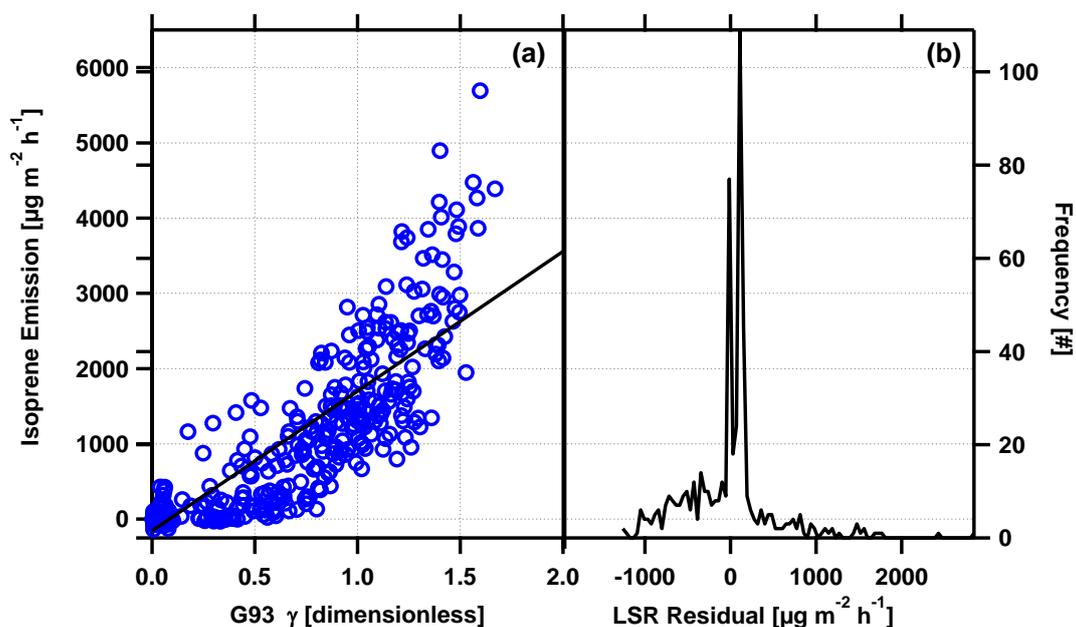
Figure 4. Plot showing (a) the non-linearity in fluxes modelled using the G93 emission algorithm when compared with observations and (b) the distribution of residuals from a least square regression fit.

Major comments

*Figures 2 and 3 pack in too much information. For example, I was interested in comparing the performance of the LSR & ODR approaches with MEGAN. In most cases in Figure 3, I could not distinguish these two cases because of overlapping plotting characters. What's the benefit of plotting all the different time average periods? Couldn't that be conveyed in a separate graph? Near lines 28-31 on page 12, you take away from Figure 3 that the G93 approach difference significantly from the MEGAN approach. This is well known, and could be conveyed more succinctly in a separate figure.

AR: We will replot figure 3 so the points at each site are staggered horizontally to ensure all symbols are visible to the reader. In figure 2, where lines are masked by others we will change the covering lines to dashes.

*The conclusion that "the emission potential is not constant throughout the day" should be refined. Within the modeling framework, the emission potential should be a constant throughout the day. The better way to frame this is that the calculated emission potential is not properly capturing the diurnal cycle. Also, considering just 08:00 to 18:00, there's not much variation in the EIP.

AR: You are correct in the case of Figure 2, but the MEGAN algorithm didn't always perform so well. For example, Figures S1 and S4 showed much greater variation at the Alice Holt and O3HP sites respectively.

*On lines 9-12, page 8, you mention the issue of the intercept for the least-squares approach. For the least-squares calculations in this paper, did you use a zero intercept?

AR: No, in each case we did not force the intercept through zero as we felt this gives the regression only one degree of freedom. However, looking into this further we found that in most cases setting the intercept to zero only resulted in a very minor change to the calculated emission potential.

Minor comments

*The abstract is a bit long. While comprehensive, I counted 660 words. In particular, some of the recommendations at the end repeat material from the abstract (factor of four). A target of 600 words seems more reasonable. With an open-access journal, there is less pressure on fitting so much in the abstract.

AR: Agreed, we shorten the text, primarily through the removal of the last two sentences (which reviewer 2 did not approve of) and look to refine the text.

Page 2, lines 33-34: The article by Arneth would be useful to consider and site at this point in the discussion (http://www.atmos-chem-phys.net/8/4605/2008/).

AR: reference will be added

Page 2, lines 34-36: Very minor point: branch enclosure measurements typically can't be performed at standard conditions. Instead, leaf temperature and light are measured, and often the Guenther algorithms are applied to derive a basal rate.

AR: We will change this to just refer to leaf-level measurements

Page 3, lines 5-7: Again, a good place to refer to Arneth et al 2008.

AR: Reference will be added

Page 3, line 22: Inconsistencies isn't the right notion here. Yes, there are inconsistencies, but there are also different assumptions.

AR: This will be changed to "…inconsistencies and differences in the underlying assumptions…"

Page 4, line 1: Since the algorithms for previous light and temperature are coming to come into play, some mention of the meteorological conditions during the campaigns compared to average climatology is necessary. In particular, where any of the campaigns conducted during times of water stress?

AR: Agreed, where available we will add further details about the meteorological conditions at each site.

Page 7, lines 21-32: This is a lot of text to describe something that wasn't used. Please consider if its necessary to include.

AR: Although the PCEEA method was not shown in Figures 2 and 3, we do use it to derive emission potentials and the results are shown in Figures 4-6 and in the tables of emission potentials listed in the Supplementary Information. We therefore believe the brief description of the algorithm is merited.

Page 8, line 25: Shouldn't this produce the same result as a linear regression with the intercept set to 0?

AR: No, this is not the case because the datasets are never perfectly linear.

Page 11, lines 16-18: "discernable" is subjective. This might be a real effect, or it might be random noise. Also, connect this to the major comment above: this variation represents a failure in the underlying model. Lines 26-27 (page 11) are the proper way to frame this conclusion.

AR: We will remove the term "discernible"

Page 12, lines 36-41: Yes, but this is only true when considering the extreme ends of the day. Typically, the focus is 10:00 – 16:00, when the variability is much lower with MEGAN.

AR: You are correct in the case of Figure 2, but the MEGAN algorithm didn't always perform so well. For example, Figures S1 and S4 showed much greater variation at the Alice Holt and O3HP sites respectively, even within your suggested window of 10:00-16:00.

Technical comments

Page 1, line 34: hyphenate 'site specific'

AR: Done

Page 2, line 18: hyphenate 'ground level'

AR: Done

Page 3, line 39: note explicitly this is ug of isoprene, not carbon (ugC), which has also been used in the past.

AR: This will be changed to "…µg of isoprene m^{-2} h^{-1}…"

Page 4, line 13: be consistent about lat/long significant figures. The two used elsewhere are probably sufficient.

AR: Changed

Page 4, line 23: According to BG style, "32m platform".

AR: Changed

Page 7, line 7: hyphenate "in canopy"

AR: Done

Page 10, lines 6-7: fix grammar

AR: Done

Page 10, line 13: reflect should be reflects

AR: Changed

Isoprene emission potentials from European oak forests derived from canopy flux measurements: An assessment of uncertainties and inter-algorithm variability

Ben Langford[1], James Cash[1, 2], W. Joe F. Acton[3], Amy C. Valach[3*], C. Nicholas Hewitt[3], Silvano Fares[4],
Ignacio Goded[5], Carsten Gruening[5], Emily House[1, 2, 3], Athina-Cerise Kalogridis[6**], Valérie Gros[6],
Richard Schafers[1,2], Rick Thomas[7], Mark Broadmeadow[8] and Eiko Nemitz[1]

[1] Centre for Ecology & Hydrology, Edinburgh, EH26 0QB, U.K.
[2] School of Chemistry, University of Edinburgh, West Mains Road, Edinburgh, EH9 3JJ, U.K.
[3] Lancaster Environment Centre, Lancaster University, Lancaster, LA1 4YQ, U.K.
[4] Council for Agricultural Research and Economics - Research Centre for Forestry and Wood (CREA-FL), Arezzo, Italy
[5] European Commission, Joint Research Centre, Ispra, Italy
[6] Laboratoire des Sciences du Climat et de l'Environnement (LSCE-IPSL), Unite Mixte CEA-CNRS-UVSQ
(Commissariat a l'Energie Atomique, Centre National de la Recherche Scientifique, Universite de Versailles Saint-Quentin-
en-Yvelines), 91198 Gif-sur-Yvette, France
[7] School of Geography, Earth and Environmental Sciences, University of Birmingham, Edgbaston, Birmingham, B15 2TT
~~Forestry Commission, Alice Holt Lodge, Farnham, Surrey, GU10 4LH, UK~~
[8] Forestry Commission, Alice Holt Lodge, Farnham, Surrey, GU10 4LH, UK
~~School of Geography, Earth and Environmental Sciences, University of Birmingham, Edgbaston, Birmingham, B15 2TT~~

* now at: British Antarctic Survey, Cambridge, UK
** now at N.C.S.R. "Demokritos", Institute of Nuclear and Radiological Sciences & Technology, Energy & Safety, 15341
Agia Paraskevi, Attiki, Greece

Correspondence to: Ben Langford (benngf@ceh.ac.uk)

Abstract

Biogenic emission algorithms predict that oak forests account for ~70% of the total European isoprene budget. Yet the isoprene emission potentials that underpin these model estimates are calculated from a very limited number of leaf-level observations and hence are highly uncertain. Increasingly, micrometeorological techniques such as eddy covariance are used to measure whole-canopy fluxes directly, from which isoprene emission potentials can be calculated. Here, we review five observational datasets of isoprene fluxes from a range of oak forests in the UK, Italy and France. We outline procedures to correct the measured net fluxes for losses from deposition and chemical flux divergence, which were found to be on the order of 5-8% and 4-5%, respectively. The corrected observational data were used to derive isoprene emission potentials at each site in a two-step process. Firstly, six commonly used emission algorithms were inverted to back out time series of isoprene emission potential, and then an "average" isoprene emission potential was calculated for each site with an associated uncertainty. We used these data to assess how the derived emission potentials change depending upon the specific emission algorithm used and importantly, on the particular approach adopted to derive an "average" site-specific emission potential. Our results show that isoprene emission potentials can vary by up to a factor of four depending on the specific algorithm used and whether or not it is used in a "big-leaf" or "canopy environment model" format. When using the same algorithm, the calculated "average" isoprene emission potential was found to vary by as much as 34% depending on how the average was derived. ~~In order to best replicate the observed fluxes we propose a new "weighted average" method whereby the isoprene emission potential is calculated as the average of all flux observations divided by the average activity factor (γ) of the emission algorithm. This approach ensures that modelled fluxes always have the same average as the measurements.~~ Using ~~this~~ a consistent ~~approach~~new approach, with version 2.1 of the Model for Emissions of Gases and Aerosols from Nature (MEGAN), we derive new ecosystem-scale isoprene emission potentials for the five measurement sites, Alice Holt, UK (10,500±2,500 µg m^{-2} h^{-1}),

Bosco Fontana, Italy (1,610±420 µg m^{-2} h^{-1}), Castelporziano, Italy (~~43~~121±~~10~~15 µg m^{-2} h^{-1}), Ispra, Italy (7,590±1070 µg m^{-2} h^{-1}) and the Observatoire de Haute Provence, France (7,990±1010 µg m^{-2} h^{-1}). Ecosystem-scale isoprene emission potentials were then extrapolated to the leaf-level and compared to previous leaf-level measurements for *Quercus robur* and *Quercus pubescens*, two species thought to account for 50% of the total European isoprene budget. The literature values agreed closely with emission potentials calculated using the G93 algorithm, which were 85±75 µg g^{-1} h^{-1} and 78±25 µg g^{-1} h^{-1} for *Q. robur* and *Q. pubescens* respectively. By contrast, emission potentials calculated using the G06 algorithm, the same algorithm used in a previous study to derive the European budget, were significantly lower, which we attribute to the influence of past light and temperature conditions. Adopting these new G06 specific emission potentials for *Q. robur* (55±24 µg g^{-1} h^{-1}) and *Q. pubescens* (47±16 µg g^{-1} h^{-1}) reduced the projected European budget by ~17%. Our findings demonstrate that calculated isoprene emission potentials vary considerably depending upon the specific approach used in their calculation. Therefore, it is our recommendation that the community now adopt a standardised approach to the way in which micrometeorological flux measurements are corrected and used to derive isoprene, and other biogenic VOC, emission potentials. ~~Modellers who use derived emission potentials should pay particular attention to the way in which an emission potential was derived and ensure that the algorithm they are using, and the implementation thereof, is consistent with that used to derive the emission potential. Our results show that, in the worst cases, failure to account for this may result in modelled fluxes that differ from observations by up to a factor of four.~~

1. Introduction

Over the past 30 years much attention has been focused on understanding the processes that control emission rates of the C_5H_8 molecule, isoprene, from vegetation (Tingey et al., 1981; Sharkey and Loreto 1993; Guenther et al., 1993; 1995; 2006; 2012; Monson et al 1994; Goldstein et al., 1998; Petron et al., 2001; Sharkey, 2008). Isoprene is a key species in both atmospheric chemistry and climate, acting as a precursor in the formation of ground-level ozone pollution through its interactions with oxides of nitrogen (NO_x) and the hydroxyl radical (OH) and playing an important, but as yet, not fully quantified, role in the formation of secondary organic aerosol (SOA) (Hallquist et al., 2009; Kiendler-Scharr et al., 2009; Carlton et al., 2009). Although our understanding of why plants emit isoprene is still incomplete (Laothawornkitkul et al., 2009), robust relationships between isoprene emissions and the ~~available~~ photosynthetic photon flux density~~ally active radiation~~ (P~~P~~F~~D~~A~~R~~) and ambient temperature have been identified and form the basis of some of the most widely used algorithms used to predict its emissions from the biosphere (Guenther et al. 1991; 1993; 2006; 2012). Although the algorithms of Guenther are perhaps the most widely used and highly cited, numerous other models exist which are formulated on a partial understanding of the underlying metabolic processes that determine production rates of isoprene synthase such as photosynthesis (Arneth et al., 2007; Niinemets et al., 1999; Martin et al., 2000; Zimmer et al., 2000; Bäck et al., 2005 and Pacifico et al., 2011).

In the Guenther algorithms, isoprene emission rates are modelled by assessing the emission potential (also referred to in the literature as an emission factor or the basal emission rate) of plant species for a set of standard environmental conditions (typically 1000 µmol m^{-2} s^{-1} ~~PAR~~ PPFD and 303 K) which is then scaled using parameterisations of the emission response to fluctuations in light and temperature. On this basis, global biogenic isoprene emissions are thought to be on the order of 500 Tg/year (Guenther et al., 2012), accounting for around half of all non-methane VOC emissions to the atmosphere. These estimates are of course only as certain as the underpinning model parameters. Currently, the largest source of uncertainty in global isoprene emission estimates is attributed to emission potentials (Guenther et al., 2012~~;)~~Arneth et al., 2008). Historically, emission potentials have been derived using ~~leaf or branch~~ enclosure measurements, where the emission rate of isoprene was measured from a single leaf or branch at standard conditions. Numerous laboratory and field studies have contributed to an extensive database of isoprene emission potentials from individual plant species which have been used to assign emission potentials to differing plant functional types (PFTs).

Keenan et al. (2009) compiled a database of leaf-level isoprene emission potentials for 80 European plant species which they used in conjunction with three separate BVOC emission models (Niinemets et al., 1999; Martin et al., 2000 and Guenther et al., 1993, 2006) to generate a comprehensive regional isoprene emission inventory for European forests. Their work highlighted the importance of oak trees, which, when averaged over the three models were shown to account for 70% of the total isoprene emissions within Europe, with the bulk (~66% of the total) attributed to just three oak species, *Quercus robur*, *Quercus pubescencs* and *Quercus petrea*. Yet, the emission potentials used in the models for these three species are based on a very limited number of leaf-level measurements and in the case of *Q. petrea*, which accounts for 16% of the total European emissions, the emission potential was taken from just a single leaf-level study. Clearly, the sparse nature of emission potential measurements and high variability between genotypes and also leaves of the same tree (Genard-Zielinski et al., 2015) means the uncertainties associated with the isoprene emission inventory are very large (Arneth et al., 2008).

More recently, micrometeorological methods such as relaxed eddy accumulation (REA) (e.g. Olofsson et al., 2005) and eddy covariance (EC) (Karl et al., 2004; Rinne et al., 2007; Davison et al., 2009; Ruuskanen et al., 2011; Potosnak et al., 2013; Park et al., 2013; Kalogridis et al., 2014; Acton et al., 2016; Rantala et al., 2016) have been used to determine canopy-scale emissions directly. This "top-down" approach is, in principle, favourable because the flux measurements are integrated over a wide source area (the flux footprint) giving an emission potential that is representative of an ecosystem as a whole. This avoids the need to classify and measure individual emission rates for all of the species present and the effect of canopy architecture on the in-canopy profiles of temperature and radiation. In addition, micrometeorological methods do not disturb the ecosystem, avoiding the potential biases to which enclosure methods are vulnerable, and the measured emission rates are those actually leaving the canopy, net of any in-canopy losses from chemical degradation or deposition to surfaces.

While micrometeorological methods offer certain advantages over enclosure techniques they do not provide a direct measurement of the emission potential required in the emission models. Indeed, the derived standardised emission potentials are very much dependent on both the way in which the data are processed (cf. Langford et al., 2015) and the methods used to convert a measured flux into an emission potential that reflects a set of standard conditions. For example, when modelling isoprene emissions using emission potentials derived from canopy-scale measurements, large uncertainties may arise ~~due to inconsistencies~~ between the algorithms used in the model and for the calculation of the emission potential due to differing assumptions of the algorithms. In particular, where standard conditions are very different from the site conditions encountered during the field measurements, the model algorithms need to extrapolate over a wide range from the measurement conditions to the standard conditions for the derivation of the emission potential, and back again to the field conditions where the emissions are to be predicted, potentially using a different algorithm. This maximises the introduction of errors.

The scalability of canopy emission potentials also needs to be considered, as measurements at a given site are not necessarily transferable to similar ecosystems as the leaf area index (LAI) and canopy structure may vary significantly between locations introducing additional uncertainties (~~Niinemets et al., 2010~~; Grote, 2007; Niinemets et al., 2010; Keenan et al., 2011).

In this study, we review (partly, previously unpublished) canopy-scale isoprene flux measurements from five European oak forests located in the UK, Italy and France. At each site we calculate the emission potential of the (sometimes mixed) ecosystem as a whole as well as the oak species separately and then interpolate our findings to the leaf-level for comparison with previous, species specific emission potentials, calculated from leaf cuvette measurements. We do this using several implementations of the most commonly used Guenther emission algorithms (Guenther et al., 1993; 2006; 2012), critically reviewing the differences observed between algorithms and the implications this might have for the modelling community. We carefully evaluate ~~the way~~different ways in which emission potentials can be derived from micrometeorological flux measurements and quantify associated uncertainties, with the aim of guiding the community towards establishing a consistent methodology.

2   Method

In total, five datasets covering a total of 134 days of isoprene flux measurements made by (virtual disjunct) eddy covariance were analysed concurrently to (i) determine best practices for the processing of these data (ii) to establish robust emission potentials suitable for use in atmospheric chemistry and transport models and (iii) to compare the canopy-scale emission
5   potentials with literature leaf-level emission potentials. These data sets comprise measurements above European oak forests in the U.K, France and Italy. All emission rates are displayed in units of μg of isoprene m^{-2} h^{-1} which is consistent with those used within the MEGAN model.

2.1   Measurement sites and datasets

2.1.1   Alice Holt, U.K. (AH)

10   Alice Holt forest is located in the south-east of England (51.17~~68~~° N; 0.85~~0~~° W), lying at an altitude of 80 m above sea level. The forest is dominated by oak trees (*Q. robur* with a scattering of *Q. petraea)* which are interspersed with European ash (*Fraxinus excelsior*, ~10%) a non-isoprene emitting species. The average canopy height is 20.5 m with a single sided leaf area index (LAI, m^2/ m^2) of 4.8. The understory comprises woody shrubs and herbs with hazel (*Corylus avelanna*) and hawthorn (*Crataegus monogyna*) being the most abundant (Wilkinson et al., 2012). Isoprene fluxes were measured between ~~the~~ June 15
15   and August 16, 2005. Measurements were made from a 25 m tall lattice tower. An ultrasonic anemometer (model Solent R2, Gill Instruments) was mounted to a mast at 28.5 m and isoprene concentrations were measured using a high sensitivity proton transfer reaction – mass spectrometer (Ionicon Analytik GmbH). In total, 29 days of isoprene flux data were collected at this site. For specific details of the measurement setup the reader is referred to the Supplementary Information.

2.1.2   Bosco Fontana, Italy (BF)

20   The Bosco Fontana Nature Reserve (45.20~~30556~~° N, 010.74~~47222~~° E), is a primary old-growth semi-natural lowland oak-hornbeam forest located in the heart of the Po Valley, Northern Italy. Pedunculate oak (*Quercus robur*), Northern Red oak (*Quercus rubra*), Turkey oak (Quercus cerris) (upper storey) and H~~h~~ornbeam (*Carpinus betulus*) (under storey) are the dominant species in the forest which covers an area of approximately 2.33 km^2. The forest is isolated in a region now dominated by intensive agricultural and industrial activities and is one of the last remaining areas of flood plain forest in the central Po
25   Valley. The land immediately surrounding the forest is cultivated, becoming increasingly urbanised towards the province of Mantova 5.5 km to the south east. The forest has an average canopy height of approximately 25 m and a single sided leaf area index of 5.5 m^2/ m^2.

Measurements were made from a 40 m tall, freestanding, rectangular (2.5 x 3 m) scaffold structure with platforms at 8, 16, 24, 32, and 40 m. The northwest edge of the tower was instrumented with sonic anemometers and aspirated thermocouples at five
30   heights. Eddy covariance flux measurements were made from the 32-m platform using a HS-50 Gill research anemometer. A gas sampling line (PFA – OD. 18 mm ID. 13 mm) was installed and purged at ~ 60 L min^{-1} from which the PTR-MS subsampled at a rate of 0.3 L min^{-1}. Measurements were made between June 13 – July 12, 2012 and in total, 29 days of isoprene flux data were collected at this site.

A detailed description of the instrument setup, calibration procedures and sensitivities are presented by Acton et al. (2015).

35   ### 2.1.3   Castelporziano, Italy (CP)

The Presidential Estate of Castelporziano covers an area of about 6000 ha located along the Latium coast 25 km SW from the centre of Rome, Italy. The flux tower was located in the "Castello" experimental site (41.74° N, 12.40~~9249~~° E), 80m a.s.l. and 7 km from the seashore of the Thyrrenian Sea. Castelporziano has to a Thermo-Mediterranean climate with prolonged warm

and dry summer periods and mild to cool winters. The soil of the experimental site had a sandy texture (sand content > 60%) with low water-holding capacity.

The experimental site is characterized by a mixed Mediterranean forest dominated by Laurel (*Laurus nobilis*) in the understory and Holm Oak (*Quercus ilex*) in the overstory. There were also large individual trees of Cork oak (*Quercus suber*) and Stone pine (*Pinus pinea*). The mean height of the overstory was 25 m, while the LAI was 4.~~76~~8 m^2/m^2.

Flux measurements were carried out between September 13 and October 1, 2011 from a flux tower 35 m tall. A PTR-TOF-MS (model 8000, Ionicon Analytik GmbH, Innsbruck, Austria) was housed in an air conditioned container at the bottom of the experimental tower. Air was drawn through a 1/4″ PFA-Teflon inlet tube to the PTR-TOF-MS from inlets mounted on top of the tower a few cm below a 3D sonic anemometer (Young, model 8100 VRE) at a flow rate of 18 SLM. The inlet tube inside the container and the drift tube of the PTR-TOF-MS were heated to 50 °C to avoid condensation. No significant line artefacts of the measured BVOCs have been observed during inlet tube tests of the PFA-Teflon material used for this study. To protect the inlet line and the instruments from dust and particles, a 250 nm Teflon particle filter was mounted in front of the inlet tube. In total, 14 days of isoprene flux measurements were collected at this site. More detailed information on the experimental site and flux tower set up can be found in Fares et al. (2013).

2.1.4 Ispra, Italy (Ispra)

The flux station Ispra is situated in a small forest of approximately 10 ha inside the premises of the Joint Research Centre in Ispra, Italy, at the northern edge of the Po Valley (45.81~~27~~° N, 8.63~~40~~° E, 209 m above sea level). The forest is unmanaged since the 1950s and consists of mostly deciduous trees (*Quercus robur*, *Alnus glutinosa*, *Populus alba* and *Carpinus betulus*) with a leaf area index of 4.4 m^2/m^2 as derived from hemispheric photography during the campaign. The average height of the canopy is approximately 26 m.

Eddy covariance measurements were performed on the top of a self-standing tower 37 m above ground, using a Gill HS-100 sonic anemometer for the measurement of high frequency vertical wind velocities. Sample air was drawn from the tower top to an instrument container at the forest ground at a flow rate of 25 ~~slpm~~ SLM through a Teflon tube with an inner diameter of 6 mm. Isoprene concentrations were measured from a 4 ~~slpm~~ SLM sub-sample with a Fast Isoprene Sensor (Hills Scientific) located inside the air-conditioned container. Measurements were made between June 11 and August 8, 2013 and in total 54 days of isoprene flux data were collected at this site. Further details on the measurement setup are given in the Supplementary Information.

2.1.5 Observatoire de Haute Provence, France (O3HP)

The Oak observatory (O3HP) site is located at the Observatoire de Haute Provence (43.93~~16667~~° N, 5.71~~22222~~° E) in the heart of a 70 year old deciduous oak forest in south-east France approximately 650 m above sea level. The 5 m tall forest canopy is dominated by two species, Downy oak (*Quercus pubescens*) and Montpellier maple (*Acer monspessulanum*) which account for 75% and 25% of the foliar biomass, respectively. The understory is dominated by European smoke bush (*Cotinus coggygrian Scop.*) and a multitude of herbaceous species and grasses. The average single sided leaf area index is 2.4 m^2/m^2. Measurements were made between June 9 – 11, 2012 and in total eight days of isoprene flux data were collected at this site. A detailed description of the site and measurements are given by Kalogridis et al. (2014) and Genard-Zielinski et al. (2015).

2.2 Isoprene emission algorithms

In this study we use six separate implementations of the Guenther et al. (1993; 2006; 2012) algorithms to normalise the measured fluxes to standard conditions and to assess the variation in the derived emission potentials. We also focus on the use of the algorithms in both the "big leaf" and detailed "canopy environment model" formats and discuss the performance of

5

each. Below we provide a brief description of each of the algorithms used in this study. For further information the reader should refer to the associated citations.

2.21 Leaf-level algorithms

Perhaps the most widely used isoprene emission algorithm used is the leaf-level model first published by Guenther et al. (1993) hereafter termed G93.

$$F_{iso} = \varepsilon \cdot \gamma \cdot D = \varepsilon D \, \gamma_L \, \gamma_T \tag{1}$$

The algorithm assumes that the emission rate of isoprene (F_{iso}) from individual leaves or plants can be determined by multiplying the emission potential of the vegetation (ε), for a set of standard conditions (303 K and 1000 µmol m^{-2} s^{-1}), by a scaling factor, γ and the biomass density (D in g$_{dw}$ m^{-2}). The scaling factor accounts for fluctuations in both light (γ_L) and temperature (γ_T) which have been demonstrated to account for the majority of short term variation in isoprene emission rates (Guenther et al., 1991; Fall and Monson, 1992).

Isoprene emission rates from vegetation typically demonstrate a linear increase with ~~PAR~~ PPFD up to a saturation point which can be described by:

$$\gamma_L = \frac{\alpha C_{L1} L}{\sqrt{1+\alpha^2 L^2}}. \tag{2}$$

Here, L is the measured PPFD~~PAR~~ (in µmol m^{-2} s^{-1}) and α (= 0.0027) and C_{L1} (=1.066) are empirical coefficients, which describe the initial slope of the curve and normalise the response curve at standard conditions, respectively. These were determined experimentally based on the response curves measured in four plant species (eucalyptus, sweet gum, aspen and velvet bean). The same four species were also used to determine empirical coefficients to describe the temperature response of isoprene emissions which can be expressed as:

$$\gamma_T = \frac{exp\frac{C_{T1}(T-T_s)}{RT_sT}}{1+exp\frac{C_{T2}(T-T_M)}{RT_sT}}, \tag{3}$$

where T is the leaf temperature in K (often assumed to be equivalent to ambient air temperature), T_s is the standard temperature (303 K), R is the universal gas constant (=8.314 J K^{-1} mol^{-1}) and C_{T1} (=95,000 J mol^{-1}), C_{T2} (=230,000 J mol^{-1}) and T_M (= 314 K) are empirical coefficients.

Although this algorithm is optimised for leaf-level emissions it has proved very popular within the flux community due to its relative simplicity and has been routinely used to back out canopy-scale emission potentials based on observed isoprene fluxes (Rinne et al., 2002; Olofsson et al., 2005; Davison et al., 2009; Potosnak et al., 2013; Kalogridis et al., 2014; Valach et al., 2015; Rantala et al., 2016). ~~In most cases the canopy~~In each of these studies the canopy ~~is~~ was treated as a "big leaf" and the leaf temperature ~~is~~ considered to be equivalent to the average air temperature. When inverting Eq. (1) to work back to a canopy-scale emission potential it is typical for the foliar density term to be removed and the canopy-scale emission potential to be reported in terms of mass per unit area of ground (rather than unit mass of biomass dry weight) per unit time which is also the convention adopted by the more recent isoprene emission algorithms.

2.2.2 Canopy-scale algorithms

More recently, Guenther et al. (2006; 2012) introduced the Model of Emission of Gases and Aerosols from Nature (MEGAN) which estimates isoprene emission rates based predominately upon canopy-scale isoprene emission potentials. This model represents a significant progression over the previous leaf-scale emission algorithms as it encompasses our growing understanding of the key driving environmental and meteorological variables that control the emission rates of isoprene from plants, which include the influence of both current and past light (γ_l) and temperature (γ_t), soil moisture (γ_{SM}), leaf age (γ_A) as well as the influence of the steadily increasing CO_2 (γ_C) concentrations in the atmosphere. Although the model takes the same basic form as Eq. (1), the MEGAN model also encompasses a detailed canopy environment (CE) model. This model accounts

for the attenuation of light and temperature through the plant canopy across several discrete layers. In addition, the model also accounts for the effect of changing leaf area index (LAI) and has the flexibility to calculate emission rates based on calculated leaf temperature rather than the more commonly used air temperature,

$$\gamma = C_{CE} \cdot LAI \cdot \gamma_l \cdot \gamma_t \cdot \gamma_{SM} \cdot \gamma_A \cdot \gamma_C. \tag{4}$$

5 The increased number of gamma factors used within MEGAN inevitably means that there is an ever more detailed definition of standard conditions. Table 2 lists the standard conditions, where gamma is equal to unity, for each of the algorithms used in this study. The most noticeable difference between the original leaf-level algorithms and the MEGAN model is the change in standardised ~~PPFD~~PAR from 1000 µmol m^{-2} s^{-1} in the leaf level algorithms to 1500 µmol m^{-2} s^{-1} in the canopy scale emission algorithms. The increase in standard ~~PAR~~ PPFD was made to reflect MEGANs canopy-scale approach, with the larger value
10 thought to better replicate the solar radiation received at the top of a typical plant canopy.

In this study we use MEGAN 2.0 (Guenther et al., 2006, hereafter G06) in a "big leaf" format (e.g. the canopy is treated as a single layer and air temperature is assumed equivalent to the average leaf temperature). This method is similar to the G93 approach but incorporates a more advanced understanding of the influence of previous meteorology on current isoprene emission rates (Sharkey, 1991). This approach has previously been used to back calculate emission potentials from flux
15 measurements made above rainforests (Langford et al., 2010) oil palm plantations (Misztal et al., 2011) and regions of California and the south-east United States (Misztal et al., 2016). As our measured fluxes are already corrected for in-canopy chemical losses and isoprene deposition we do not use the in-canopy production and loss term, ρ, used by Guenther et al in version 2.0 of the MEGAN model.

In our analysis we also explore the use of the more recent MEGAN 2.1 model (Excel version beta 3 provided by A. Guenther),
20 which employs a five layer canopy environment model to better replicate the changes in isoprene emissions that occur as light and temperature are attenuated within the canopy. We utilise this model in three separate configurations which we refer to in the text as MEGAN 2.1 (a), (b) and (c). Configuration (a) is the full implementation of the model, where the air temperature is converted to leaf temperature by calculating the leaf energy balance (Goudriaan and van Laar, 1994) and the effects of both previous light and temperature are included (Sharkey, 1991; Guenther et al., 1999). Implementation (b) uses measured air
25 temperature and assumes this to be constant with height throughout the canopy, but it still accounts for the influence of both current and previous light and temperature. The final implementation (c) uses air temperature but does not account for the influence of previous light and temperature. In each of these three ~~runs~~configurations we do not account for the effects of varying CO_2 concentrations, setting it to 400 ppm, nor do we consider the effects of soil moisture. In both cases this decision was motivated by a lack of the necessary observational data across all sites. Finally, a fixed, site specific leaf area index was
30 used within the canopy environment model for each of the three MEGAN 2.1 implementations.

2.2.3   The parameterised canopy environment emission algorithm

As well as the complete MEGAN 2.0 model and associated canopy environment model, Guenther et al. (2006) also developed a simplified single-layer canopy-scale representation of the full multi-layer model known as the Parameterised Canopy Environment Emission Algorithm which is designed to reduce the computational expense associated with the full model.
35 Emission fluxes are simulated on the basis of current and past (24 h) light and temperature as well as information on the angle of solar elevation. The PCEEA approach uses a modified set of algorithms that describe the canopy-scale isoprene emission response in the absence of a full canopy environment model. Specifically, the algorithms used in the PCEEA approach are based on simulations using the full MEGAN model and canopy environment (CE) model for warm, broad leafed forests. According to Guenther et al. (2006), isoprene emission rates derived using the PCEEA approach match estimates from the full
40 model to within 5% when applied at the global scale but may deviate by >25% at specific locations. This algorithm was used by Langford et al. (2010) to simulate isoprene fluxes in Malaysian Borneo, but the PCEEA approach performed less well than the G06 algorithm and hence was not used for the calculation of the published emission potentials.

2.3   Deriving emission potentials from above canopy flux measurements

Micrometeorological flux measurements of isoprene above forests allow the net mass flux into the atmosphere and its response to the driving meteorological variables to be quantified directly. In order to translate these measurements into ecosystem emission potentials for use in atmospheric chemistry and transport models it is first necessary to somehow normalise the measured fluxes to the set of standard environmental conditions used by the model, i.e. the point at which γ equals unity. One approach is to average only those flux data recorded during periods where standard conditions were met, but in reality this may only constitute a very small fraction of the measured data. More typically, the emission potential (ε) is calculated by normalising the measured fluxes to standard conditions by inverting one of the emission algorithms described above. This generates a time series of isoprene emission potentials, which typically shows systematic patterns, indicating that either the parametrisations imperfectly reflect the response of the emission to the meteorological drivers or that ε is subject to additional biological (e.g. circadian) control (Hewitt et al., 2011). Nevertheless, for the measurements to add to the emission potential database a single value needs to be chosen to represent that site. Various methods have been used to derive this single value, but there is currently no consensus in the literature as to which method is most appropriate. For example, both Misztal et al. (2011, 2014; 2016) and Langford et al. (2010) chose to derive emission potentials as the average of midday emission potentials

$$IEP = \overline{\left(\frac{F_{iso\,h_1\ldots h_n}}{\gamma_{h_1\ldots h_n}}\right)}, \tag{5}$$

where $F_{iso\,h_1\ldots h_n}$ represents the individual above-canopy flux measurements obtained between specific hours of the day ($h_1\ldots h_n$ – typically around midday) and γ is the sum of the isoprene emission rate scaling parameters. By contrast, Rantala et al. (2016) chose to determine the emission potential as the gradient in a least squares regression between F_{iso} and γ. The latter approach, which we hereafter term the LSR method, has gained in popularity (Acton et al., 2016; Valach et al., 2015; Rantala et al., 2016) with some choosing to set the intercept to zero (Kalogridis et al., 2014; Acton et al., 2016) and others leaving it to be determined by the fit (Rantala et al., 2016). Yet, the application of this approach is often questionable, because the relationship between flux and γ is sometimes non-linear and thus violates the assumptions of the least squares approach.

As we will show in this paper, although the 'average' emission potential is derived from the measurement data, over the day, the emission predicted with such 'average' emission potential does not necessarily reproduce the measured emission, because (i) the emission parameterisations are highly non-linear and (ii) the emission values observed during a day are not normally distributed. The inability of this approach to yield emission potentials that replicate the magnitude of the observed flux is a concern, especially when models are to be used for accounting purposes.

Here, we will evaluate both the average and LSR both of these methods alongside two new approaches. The first calculates the emission potential using an orthogonal distance regression (also known as a total least square regression) between F_{iso} and γ. Put simply, the ODR method is a least squares regression that can be weighted based on the errors in both the dependent and independent variables. The random error of individual flux measurements determines the weighting for the fluxes, whereas constant uncertainties of ±25% and ±12% are applied to the values of γ calculated by the G93 and MEGAN emission algorithms respectively and are based on sensitivity studies by Guenther et al., (1993) and Situ et al., (2014). This, and the standard least squares regression approaches are in stark contrast to the average method which weights all data points evenly. The second approach is to use a weighted average to ensure the derived emission potential will always yield fluxes with the same average as the observed fluxes. This is calculated as

$$IEP_{weighted} = \frac{\overline{F_{iso}}}{\overline{\gamma}}. \tag{6}$$

This is similar to the average approach but takes the ratio of the average flux and the average of the γ_i values gammas rather than the average of the ratios and which effectively ensures that the contribution of each single IEP_i is weighted by the magnitude of the associated γ_i.

8

As part of this study we compare the isoprene emission potentials derived through the inversion of the most commonly used isoprene emission algorithms described above and the use of the average, LSR, ODR and weighted average methods in determining single, site specific emission potentials.

The impact of extrapolating from field to standard and back to field conditions can be minimised, by selecting a set of standard deviations that is closer to field conditions. Thus, a further strategy for the reporting of emission ~~factors~~ potentials could be to report emission ~~factors~~potentials together with a set of reference conditions for which the emission ~~factor~~potential is representative and then leave it to the emission modellers to either adapt their algorithm to these reference conditions or to extrapolate to their standard conditions. As this would use the same algorithm that is used for the emission calculations the errors induced by the extrapolation would cancel. This approach is explored in Section 3.4 below.

2.4   Accounting for dry deposition

Measurements of the emission potential made using leaf-cuvette systems on a single leaf or branch gives a direct measurement of the isoprene emission rate that inherently excludes the deposition process. By contrast, micrometeorological flux measurements reflect the net surface exchange of a compound which is a balance between the upward (emissions) and downward (deposition) mass fluxes. At our five measurement sites the flux of isoprene is dominated by the emission process so the net flux is nearly always upwards (positive), but it may still be offset slightly as some of the isoprene may undergo dry deposition to leaf surfaces. In order to calculate an emission potential that accurately reflects what is emitted directly from the vegetation it is therefore necessary to first correct measured fluxes for the effects of deposition. The dry deposition for isoprene is typically assumed to be very small and is often not corrected for, but the effects of deposition may become much more significant for other species such as monoterpenes and methanol which have been seen to be efficiently deposited to vegetation (Bamberger et al., 2011; Ruuskanen et al., 2011; Wohlfahrt et al., 2015).

Our measurements provide the average net isoprene flux for a measurement point above the tree canopy, z_m. The flux at the canopy surface can be defined as

$$F_s = F_m + F_d, \tag{7}$$

where F_m is the measured isoprene flux and F_d is the fraction that is depositing. This depositing fraction can be calculated as

$$F_d = -\frac{x_{(z_0')}}{R_c}, \tag{8}$$

where $x_{(z_0')}$ is the average concentration of isoprene at the notional (micrometeorological) average height of the exchange with the canopy, and R_c is the canopy resistance. Although we did not directly measure the concentration of isoprene at the canopy top we can extrapolate our above-canopy measurements, $x_{(z_m)}$, to the surface using Eq. (9).

$$x_{(z_0')} = x_{(z_m)} + F_m(R_a + R_b) \tag{9}$$

Here, R_a, is the aerodynamic resistance, R_b, is the laminar boundary layer resistance which describes the transport through the laminar region that forms very close to the vegetation surface and both terms are calculated using direct measurements of micrometeorological parameters following Nemitz et al (2009). In the calculation of R_b a value of 9.3×10^{-5} m^{-2} s^{-1} was used as the molecular diffusivity of isoprene, which was calculated using the molecular structure online calculator (EPA, 2007). Accounting for Eq. (9) the calculation of the deposition flux becomes

$$F_d = \frac{x_{(z_m)}}{R_c} + F_m\left(\frac{R_a(zm)+R_b}{R_c}\right). \tag{10}$$

The canopy resistance (R_c) for isoprene was set to 250 s m^{-1} as experimentally determined by Karl et al. (2004) using direct measurements of isoprene fluxes above a tropical forest. This value is perhaps not ideal for use with temperate broad leaf forests and may also vary with canopy morphology and meteorological conditions. However, no further estimates of R_c for isoprene could be found, highlighting the need of further research in this area.

Adding the estimate of the isoprene deposition flux to the observed net isoprene flux gives a closer approximation of what was actually released from the forest canopy but is still not the total isoprene flux as the effects of flux divergence, e.g. the chemical degradation of isoprene before it reaches z_m, must also be estimated and corrected for.

2.5 Accounting for chemical flux divergence

Flux divergence occurs when the scalar of interest is not chemically conserved during the average time it takes for transport between emission and detection at z_m. The magnitude of the effect is proportional to the reactivity of the compound, concentration of atmospheric oxidants (e.g. OH, O_3 and NO_3) and inversely proportional to the turbulent velocity scale which determines the rate of transport through the turbulent boundary layer, as well as measurement height. Schallhart et al. (2016) and Kalogridis et al. (2014) estimated directly the chemical loss of isoprene between canopy and measurement height to be 4% and 5% at the Bosco Fontana and O3HP sites, respectively. For the remaining sites we assume a 5% chemical loss of isoprene which is also consistent with model simulations by Stroud et al. (2005), who predict canopy escape efficiencies for isoprene to be typically greater than 0.9.

2.6 Extrapolating emission potentials to different scales

The ecosystem-scale emission potentials (ε_{eco}) derived from the measurements were extrapolated (i) to derive the emission potential for the oak species (ε_{can}), correcting for the presence of other tree species, and (ii) to provide an emission potential equivalent to a leaf-level measurement (ε_{LL}) that could be compared to literature values. At four of the measurement sites, the only identified isoprene emitting vegetation species were oak, which meant the calculated ecosystem emission potential could be simply scaled based on the known percentage of oak present in relation to the overall tree cover. At the Ispra site the derived emission potential was a composite of the two known isoprene emitting species, *Quercus robur* and *Poplus alba* which represented 80% and 5% of the forest composition respectively. According to Keenan et al. (2009) the emission potentials of these two species on an area basis are 6,820 and 5,109 µg m^{-2} h^{-1} respectively. Based on the known species composition and relative emission potentials of these two species we scaled our ecosystem emission potential to assume a canopy composed of 94% oak and 6% poplar.

Leaf-level equivalent emission potentials were subsequently calculated for each site by dividing the whole-oak canopy emission potentials by values of leaf dry mass per unit area obtained from Keenan et al. (2009) for each species. This converts the canopy scale emission potentials which assume an emission rate on a per area basis to units of µg g^{-1} h^{-1}. Leaf-level emission potentials are typically measured at a ~~PAR~~ PPFD of 1000 µmol m^{-2} s^{-1}, but in five of the algorithms we use, the standard conditions were increased to 1500 µmol m^{-2} s^{-1} to better replicate the solar radiation received towards the top of a tree canopy. Assessing the light response used in each model allowed us to scale γ_i to equal one at 1000 µmol m^{-2} s^{-1} and ensure parity between the both the literature emission factors and those calculated using the G93 leaf-level algorithm.

2.7 Emission potential uncertainties

Emission potentials for VOCs are often reported without full consideration of the associated uncertainties in the derived quantity. Here, we attempt to derive an uncertainty value for all ecosystem, canopy and leaf-scale equivalent emission potentials that accurately reflects the wide range of potential uncertainties in the derived quantity.

There are several sources of uncertainty that are common across the ecosystem, canopy and leaf-scale equivalent emission potentials which include uncertainties in the normalisation of the fluxes to standard conditions, calibration gases used, the canopy resistance used in calculating losses due to deposition and the assumed in-canopy chemical loss of isoprene. Table 3 shows the known (calibration gases) and estimated (chemical loss and canopy resistance) uncertainties used at each of the five measurement sites. An isoprene gas standard was not available during the Alice Holt field measurements. Instead, concentrations were derived on the basis of the instrument transmission curve which according to Taipale et al. (2008) gives

10

an uncertainty of approximately ±25%. The random uncertainty in derived emission potentials for each measurement site is taken as the average uncertainty of the individual flux measurements (Langford et al., 2015):

$$\overline{RE} = \sqrt{\frac{\left(\sum_{i=1}^{N} RE_i\right)^2}{N}},$$
(11)

where RE_i represents the individual flux measurement uncertainty and N is the total number of flux measurements being averaged.

Additional uncertainties are associated with the oak specific canopy emission potentials which include the uncertainty in the species composition data and the change in LAI index that would result from assuming the canopy was comprised of 100%only oak. Wind rose analysis of isoprene emission potentials at the Alice Holt, Ispra and Bosco Fontana sites showed variation of 14%, 19% and 28% respectively (see Supplementary Information). The comparatively short time series of isoprene fluxes at the Castelporziano and O3HP sites meant that wind rose analysis was not possible for these locations, so an uncertainty of 20% was assigned to the species composition data. Similarly, an uncertainty of e assume a 10% uncertainty in the species composition data at each of the five sites and assign a 15% uncertainty in thewas assigned to LAI data at each of the five sites. This value was then scaled based on the percentage of oak present at each site. For example, at Alice Holt the forest is 90% oak so we multiply the estimated 15% uncertainty by 1.1 to give a final uncertainty of 16.5%. By contrast, at Bosco Fontana where oak species only represent 27% of the species present an uncertainty of 26% was derived by multiplying 15% by 1.73. In order to convert from whole-canopy to leaf-level equivalent emission potentials it is necessary to convert from an emission rate measured on a per unit area basis to an emission potential on a gram per dry leaf weight basis. The percentage leaf dry mass assumed for each oak species was taken from Keenan et al. (2009) for each of the tree species and given an assumed uncertainty of 25%. The process of converting from fluxes made on a "per area" to a "per mass" basis is clearly a source of uncertainty, but it is worth noting that this uncertainty could be eliminated if investigators making leaf-level measurements were to report their emission potentials on both a "per mass" and "per area" basis (Niinemets et al., 2011).

Finally, the total emission potential uncertainties for each site were calculated by propagating each of the uncertainties listed in Table 3 with the average random uncertainty in measured fluxes.

3   Results and discussion

3.1   Above-canopy flux measurements

The time series of the five isoprene flux data sets used in this study are shown in Fig. 1. In total 2792 hours of eddy covariance flux data were analysed and reviewed as part of the study. Isoprene fluxes were largest at the Ispra and Alice Holt forest sites with average midday fluxes of ~6,500 and 2,800 μg m^{-2} h^{-1}, respectively. The larger emission rates reflect the canopy composition, which in both cases was > 80% oak, and the warm summer conditions. In contrast, emission rates at the Castelporziano site were comparatively small, typically below 150 μg m^{-2} h^{-1} despite the high temperature and high levels of solar radiation. This lower emission rate is attributable to not only a lower percentage of oak species present (27%) within the canopy, but to the particular species of oak present. At Castelporziano two evergreen oak species, *Quercus ilex* and *Quercus suber,* account for 27% of the forest canopy but both species are relatively minor emitters of isoprene (Keenan et al., 2009).

3.2   Comparison of averaging methods for emission potentials

Measured eddy covariance flux data from each of the five sites were normalised to standard conditions using the G93 algorithm and the MEGAN 2.1 (a) canopy-scale emission algorithm described in Section 2.2. Normalising flux data in this way effectively produces a time series of isoprene emission potentials from which a single value can be chosen that is thought to best represent the canopy. We calculated this site specific emission potential using the LSR, ODR and several variations of

11

the average method, each described in detail in Section 2.3. For the latter approach, the time series of emission potentials were averaged over different time windows which included 08:00 to 18:00, 10:00 to 15:00, 11:00 to 13:00 and all hours.

Figures 2a and 2c show an average diurnal cycle of the isoprene emission potentials (IEPs) calculated at the Ispra forest site using the simplistic G93 "big-leaf" emission algorithm (Panel a) and the more sophisticated MEGAN model (V2.1) (Panel c).

In this example, a clear diurnal pattern is visible in the isoprene emission potential calculated using the G93 algorithm. The emission potential calculated using the MEGAN model shows a slightly different evolution, with a marginal ~~but discernible~~ increase in magnitude from morning to evening. The amplitude of the variability in the calculated emission potential is greatly reduced compared with the performance of the leaf-level algorithm. The non-constancy of the calculated emission potentials was a feature consistent across all of our measurement sites (see Supplementary Information). There is laboratory evidence that isoprene emission potentials from some plant species are subject to circadian control (e.g. Wilkinson et al., 2006). Hewitt et al. (2011) found calculated isoprene emission potentials derived from canopy-scale flux measurements to exhibit a diurnal pattern, peaking at around midday, which they attributed to such circadian control. This assertion was later challenged by Keenan et al. (2012) who suggested the diurnal pattern in the isoprene emission potential could be removed by tuning the light and temperature response curves of the model and its canopy model implementation to better match those typical of tropical vegetation. In either case, and regardless of its cause, a temporal trend in the emission potential means that the emission algorithm does not perfectly describe all of the factors that influence isoprene net emissions at this site.

Also shown on Fig. 2 (a and c) are the average isoprene emission potentials calculated using the LSR, ODR and average methods. For the G93 "big-leaf" algorithm (Fig. 2a) the calculated emission potentials span ~~a wide range~~ from ~ 5,600 to 7,900 μg m^{-2} h^{-1}. Figure 2b shows the resulting average diurnal cycle of modelled isoprene emissions modelled using each derived average isoprene emission potential. When adopting an emission potential calculated with the widely used average approach (11:00 to 13:00) the algorithm replicates the measured average flux reasonably well at around 11 am, but it significantly overestimates emission rates in the morning and afternoon, which is consistent with the diurnal fluctuation of the derived isoprene emission potential. The calculated emission potential decreases as the average method covers a larger proportion of the day, resulting in a significant underestimation of the measured fluxes (Fig. 2b). The isoprene emission rates simulated using the MEGAN 2.1 (a) model (Fig. 2d) are able to better replicate the observed isoprene fluxes in the morning and afternoon periods, but still overestimate fluxes when integrated across the day. The range of calculated isoprene emission potentials, 6,800 – 8,700 μg m^{-2} h^{-1}, is smaller than that of those obtained using the G93 algorithm which reflects the reduced variability in the calculated diurnal profile of isoprene emission potentials.

Emission potentials calculated using the LSR and ODR methods agree closely at the majority of sites, but the ODR method appears very sensitive to the magnitude of the error weighting applied. We assumed a 25% model error for the G93 algorithm, which was consistent with sensitivities studies by Guenther et al. (1993) and 12.5% for the MEGAN model (Situ et al., 2014). For most sites these assumed model errors provide a fit and associated emission potential that is consistent with the other approaches. However, at some sites the ODR could only produce a sensible fit after adjusting the model uncertainty. For the Ispra data, for example, the MEGAN model error had to be reduced to 8% in order to produce a viable fit. The fact that manual adjustment of errors may be required with some data sets means that the ODR is unlikely to produce the consistent results required for a standardised approach.

Isoprene emission potentials were also calculated using the weighted average approach (Eq. 6). Using this method yielded emission potentials that, when used to simulate isoprene fluxes, matched exactly the integrated flux measurements. We calculated the normalised mean square error, or M score, between measured (F_m) and the modelled (F_{mod}) fluxes, using the different IEP methods described above to assess the performance of each.

The M score assess the performance of the model based on the magnitude of the overall bias, the variance of the residuals and the intensity of association or correlation, with the lowest score deemed to indicate the best model performance (Guenther et al., 1993).

$$M = \frac{\overline{(F_m - F_{mod})^2}}{\overline{F_m - F_{mod}}}$$ (12)

In the Guenther algorithms the IEP is simply a constant that is scaled in relation to the changing environmental conditions, so a change in IEP has no effect on the overall correlation between model and measurements. Therefore, in this study, relative changes in the M score only reflect the magnitude of bias and bias variation. We found that the method with the lowest M
5   score varied between sites and algorithms, but was most often associated with the average (11:00 to 13:00) method (see Supplementary Information). This is perhaps not surprising as fluxes were largest during midday, and thus choosing the correct IEP for those conditions resulted in the smallest M score.

The weighted average method, by definition always yielded a zero bias, but the standard deviation is typically lower than the measurements (see Supplementary Information). Providing emission potentials that allow the average flux to be accurately
10   modelled is certainly desirable, especially for regional or global VOC ~~global~~ budget studies. Nonetheless, the use of the weighted average method might not suit all modelling scenarios. For example, local studies of atmospheric chemical process may require simulated isoprene emissions to better replicate midday fluxes. In these limited cases the use of the average midday method might prove more suitable.

Figure 3 shows the same sets of emission potentials shown in Figure 2, but for each of the five measurement sites. Here, the
15   emission potentials have been normalised to that derived using the weighted average method and the MEGAN model (V2.1). When plotted in this way two features become apparent. Firstly, the use of different emission algorithms to convert observed fluxes to emission potentials can result in markedly different results. This is illustrated by the divergence of open circles (G93) and closed triangles (MEGAN 2.1 (a)) and is particularly apparent at the Alice Holt and Castelporziano sites. Secondly, because the emission potential is not constant throughout the day (see Fig. 2) different averaging approaches yield very different
20   average emission potentials even when the same algorithm is used. In these examples, the emission potential varied by as much as 30% at Alice Holt and 34% at Castelporziano. Since in the emission algorithms considered here the flux is proportional to the emission potential (Eq. 1), the same spread applies to the predicted emissions. The fact that the inferred isoprene emission potentials vary significantly by time of day is also of clear importance. Our results indicate that the derived emission potential may vary significantly depending upon the time of day the measurements were made. This is especially relevant when
25   considering measurements made from airborne platforms or individual leaf cuvette systems that only capture a brief snap shot of the diurnal cycle. The magnitude of this effect will differ depending on the methods used, but as an example, at the Ispra site, an emission potential calculated using the G93 algorithm at 08:00 and then again at15:00 would result in values that differ by a factor of 1.5. The use of the more advanced MEGAN 2.1 model would reduce the variability marginally, but still result in emission potentials that differ by a factor of 1.45.

30

3.3   Isoprene emission potentials and inter-algorithm variability

Having established the weighted average method as the most consistent method for deriving an emission ~~factor~~ potentials that reproduces the measured average flux for a given algorithm, several isoprene emission potentials were calculated for each measurement site which reflect: (i) an actual ecosystem emission potential, (ii) an oak canopy-scale emission potential (where
35   the emission potential is scaled to account for the known percentage of isoprene emitting species present within the flux footprint) and (iii) a leaf-level equivalent emission potential, where the whole oak canopy emission potential is converted to leaf-level based on assumed leaf biomass densities. The calculated isoprene emission potentials and their associated uncertainty are reported in tabular form in the Supplementary Information.

Ecosystem isoprene emission potentials for each of the five measurement sites are shown as the sum of the graduated bars in
40   Fig. 4. The emission potential is divided into three parts which denote the "raw" measured ecosystem flux and the two corrections applied to this value which account for losses associated with in-canopy chemistry and the dry deposition of

13

isoprene to the surface. The chemical loss term was ~5%, while the deposition term was calculated to be marginally larger ranging between 5 and 8% across the five sites. This value, however, remains uncertain and there is a clear need for researchers to derive accurate canopy resistance values for isoprene and other bVOCs for both temperate and tropical ecosystems.

Ecosystem emission potentials directly reflect the isoprene emitted from all of the species present within the measurement footprint. The emission is therefore not just dependent on the oak species, but also their abundance.

Consistent with this, the largest emission potentials were observed at Alice Holt which is comprised of 90% of strongly isoprene emitting oak species (*Q. robur* and a scattering of *Q. petraea*). By contrast, Castelporziano had the smallest ~~recorded~~ calculated isoprene emission potential~~s~~; in addition to having only 27% oak cover, it is due to two evergreen species, *Quercus ilex* and *Quercus suber* (Fares et al., 2013), which are known to be very minor emitters of isoprene (Steinbrecher et al., 1997; Bertin et al., 1997; Owen et al., 2001). The fact that isoprene emissions can vary so dramatically within the *Quercus* genus is one of the major challenges for global BVOC emission models. Within the MEGAN framework vegetation is broken down into distinct plant functional types which are classes of vegetation that are thought to share similar biological properties and responses to environmental drivers (Smith et al., 1997). The full MEGAN2.1 uses an isoprene emission potential map that accounts for the fraction of isoprene emitters in each landscape based on the species composition. In our single site version of MEGAN the detailed emission map is not used. Instead, ~~In total,~~ 15 PFTs are used, covering land classes such as temperate and tropical forest, grasses and crops (Guenther et al., 2012). Based on the species composition data reported by Morani et al. (2014) for this site, Castelporziano maps to a blend of three PFTs: 66% "broadleaf evergreen temperate shrubs" (2,000 μg m^{-2} h^{-1}), 6.8% "Needle leaf evergreen temperate tree" (600 μg m^{-2} h^{-1}) and 27.3% "broadleaf evergreen temperate tree" (1,727 μg m^{-2} h^{-1}), which represents the evergreen oak. Combining these PFTs results in an overall emission potential of 1,839 μg m^{-2} h^{-1} for the Castelporziano site. This value greatly exceeds the calculated emission potentials for this site, which is just 43 μg m^{-2} h^{-1} and serves to highlight the very large uncertainties that arise when assigning emission potentials to vegetation on the basis of plant functional characteristics.

The PFTs that describe the other four sites are also shown in Fig. 4 as a horizontal line and can be directly compared with the isoprene emission potentials calculated using the full MEGAN model (e.g. MEGAN 2.1 (a)). The sites with the highest proportion of oak provide the closest match with the PFT estimates. For example, Alice Holt, a site comprising 90% oak had an emission potential of 10,500 μg m^{-2} h^{-1}. By contrast, the emission potential for Bosco Fontana was just 1,610 μg m^{-2} h^{-1} reflecting, mainly, but not fully, the much lower proportion of isoprene emitting species present (27%) at this site. To account for these differences we adjusted for the presence of non-oak tree cover to provide the emission potentials for oak only, the results are shown in Fig. 5.

The oak specific canopy emission potentials at the Ispra (9,495 μg m^{-2} h^{-1}) and Observatoire Haute de Provence (10,654 μg m^{-2} h^{-1}) sites now compare very closely with the broadleaf deciduous forest PFT emission potential of 10,000 μg m^{-2} h^{-1}, and the Alice Holt and Bosco Fontana sites are also both within the range of the PFT emission potential when accounting for uncertainties. These findings suggest that the emission potentials for the "broad leaf deciduous forest" PFT are representative of canopies primarily composed of high isoprene emitting oak species such as *Quercus robur*.~~but should be viewed as an upper limit in situations where the forest is dominated by species other than oak.~~

At each site the derived emission potentials from the different algorithms show considerable variability, with up to a factor of ~~four~~ 2.7 difference seen at the ~~Castelporziano~~ Bosco Fontana site. In each figure two sets of error bars are shown. The black error bars show the total uncertainty, which includes the random error as well as the systematic uncertainties from sources such as calibration gases, species composition and biomass estimates, which affect estimates at each site equally. The smaller, coloured error bars show the random error associated with the flux measurements and it is this value that should be used when comparing emission estimates at a single site for statistical differences. When viewing the emission potentials in conjunction with these errors it becomes apparent that some large statistical differences do exist between some, but not all, emission algorithms. In Figs. 4 and 5 these differences were, in part, due to the different definitions of standard conditions used between

14

G93 and MEGAN algorithms. Yet, the leaf-level equivalent emission potentials shown in Fig. 6 have been adjusted to remain consistent with previous leaf-level observations which are typically obtained at 303 K and 1000 µmol m^{-2} s^{-1} ~~PAR~~PPFD. Interestingly, the G06 method (effectively the use of the MEGAN 2.0 algorithm in a "big leaf" format) yields a much lower IEP than the other algorithms at all but the Alice Holt site. This relates to the algorithms inclusion of the effects of previous

5 light and temperature on isoprene emissions. According to Table 2, γ will equal unity only once the standard conditions are met, which in this case are a PPFD of 1500 µmol m^{-2} s^{-1} ~~of PAR~~ and 303 K for the current light and temperature and a PPFD of 200 µmol m^{-2} s^{-1} ~~of PAR~~ and 297 K for the previous 24 and 240 hours. An assessment of the previous environmental conditions at each of the five measurement sites (Figs. S5 to S9 in the Supplementary Information) reveals that the previous light and temperature regimes are typically much larger than the standard conditions. Therefore, in order to normalise the

10 measured fluxes to standard conditions the light and temperature response curves must yield unity at much lower levels than is achieved using, for example, the G93 or MEGAN2.1 (c) algorithms, which only include responses to the current environmental conditions. Figure 7 shows the light and temperature response curves used in the G06 algorithm at each of the five sites relative to the response curves at standard conditions (black line). The largest deviations from the curves are seen in the light response (Fig. 7a), with ~~Castelporziano~~ Bosco Fontana furthest from standard conditions, followed by ~~Bosco Fontana,~~

15 Observatoire Haute de Provence, Ispra, Castelporziano and then Alice Holt. Deviations from the temperature curve are rather modest by comparison, with the largest positive deviations seen for Bosco Fontana, followed by Ispra, Castelporziano and O3HP. By contrast, data from Alice Holt are generally lower than the standard temperature response curve, which is consistent with the previous 24 and 240 hour temperature measurements at this site being typically 7 K below the standard temperature. From these curves we can conclude that the inclusion of past light and temperature conditions in the G06 "big leaf" algorithm,

20 therefore, requires the standard response curves to increase (decrease) depending upon the relative values of the previous light and temperature and has the potential to deviate significantly to values calculated using the G93 algorithm. In our analysis the largest difference was observed at the ~~Castelporziano~~ Bosco Fontana site with the IEP calculated using the G06 algorithm ~~some 74%~~over two times lower than that calculated using the G93 algorithm. From this analysis we recommend that the G06 algorithm not be applied in a big leaf format because the calculated emission potentials will likely be biased low.

25 Emission potentials calculated using the MEGAN 2.1 algorithms which each use a full canopy environment model were consistently larger than those calculated by the G06 "big leaf" approach. This relates to the treatment of light and temperature attenuation through the canopy which brings the previous environmental conditions in the lower layers of the canopy much closer to standard conditions. Interestingly, when the use of previous light and temperature is switched off (e.g. MEGAN 2.1 (c)) the emission potential increases ~~because~~ as the effects of past light and temperature are no longer considered~~standard~~

30 ~~conditions are now reduced to current light and temperature~~.

~~The parameterised canopy environment emission algorithm tended to agree quite closely with the emission potentials derived using the full MEGAN 2.1 (a) model and was generally within 10%. The largest discrepancy between the full model and PCEEA was at the Castelporziano site where the PCEEA emission potentials were ~50% larger than the MEGAN 2.1(a) model. This difference doubles the upper limit predicted by Guenther et al. (2006) for model bias at individual sites and in this case~~

35 ~~may relate to the very high solar loadings. As already discussed, emission potentials decrease significantly when the past light and temperature conditions are much larger than standard values of 200 µmol m^{-2} s^{-1} PAR and 297 K. The discrepancy may also be exacerbated at this site due to the relatively small size of the dataset and comparatively low emission rates which ultimately lead to additional uncertainties in the derivation of the emission potentials.~~

The fact that the different algorithms and indeed different variations of the same algorithm do not converge on a single IEP is

40 of critical importance. It implies that VOC emission potentials reported in the literature are only representative as long as (i) they are used in conjunction with the same emission algorithm that was used to back out the isoprene emission potentials from the measured fluxes ~~and~~ (ii) derived with an averaging method that correctly reproduces the measured flux or (iii) were measured under conditions similar to standard conditions. Using a different algorithm to simulate emission rates, or indeed a

15

slightly different implementation of the same algorithm to that used to calculate the emission potential will clearly yield a different result. Our results show that the variations in emission potentials calculated using different implementations of MEGAN 2.1 are relatively small when changing between leaf and air temperature ($< 8.5\%$), but still marginally larger than the $<5\%$ suggested by Guenther et al. (2012), but can become much larger when the influence of previous light and temperature are ignored (45%). By contrast, differences between emission potentials calculated using the G93 algorithm and full MEGAN model can vary by more than a factor of two, even after accounting for the differing sets of standard conditions. While this level of uncertainty may be deemed tolerable for global model simulations, where other uncertainties are equally large, it may prove unacceptable for chemical transport models operating at regional or local spatial scales.

~~While our analysis has focused on the calculation of emission potentials from above-canopy flux measurements and their uncertainties, it is important to recognise that the leaf-level emission potentials to which we compare are also highly uncertain. Leaf-level emission potentials vary considerably between the top and bottom of the canopy and for the same species have been shown to range between a factor of 10 (Aydin et al. 2014, van Meeningen et al. 2016) to 100 (e.g. Pokorska et al. 2011, Winer et al. 1983). Therefore, leaf-level measurements may not always reflect the canopy average observed by top down micrometeorological approaches. Furthermore, leaf-level measurements are typically reported for a set of light and temperature conditions but other important environmental parameters including past light and temperature, CO_2 concentration and soil moisture are typically not reported. With this in mind, we would echo the sentiments of Niinemets et al. (2011) who call for the standardisation of leaf-level measurements and would stress the need for the reporting of emission potentials on both a per mass and per area basis and the inclusion of additional environmental parameters (past light and temperature and CO_2 concentrations) to further reduce the uncertainties introduced when comparing the performance of emission algorithms with above canopy flux measurements.~~

3.4 Reporting fluxes for defined conditions

We have demonstrated that emission potentials can vary considerably depending upon which emission algorithm is used to normalise the measured fluxes to standard conditions, especially if the standard conditions are very dissimilar from conditions encountered in the field. As already stated in Section 2.3, standard conditions are typically far removed from conditions found at many measurement sites e.g. at higher latitude sites, which means typically there is no or very little data directly measured under these conditions. One possibility to remove this uncertainty is to report an emission potential as the average flux that corresponds to a set of defined conditions encountered in the field, together with these new reference conditions.

Using a two-dimensional histogram, binning flux data by light (± 100 μmol m^{-2} s^{-1} PPFD) and temperature (± 0.5 K) we selected the most common set of daytime conditions at each of our five measurement sites. An example histogram is shown for the Ispra forest site in Figure 8 and the average fluxes and environmental conditions that corresponded to these sets of conditions are shown in Table 4. In order to compare how emission potentials (extrapolate from the field reference conditions to the algorithm specific standard conditions) calculated using this small fraction of the available data (typically between 1.2-2%) compared with our previously calculated emission potentials, we converted the average fluxes shown in Table 4 to the algorithm standard conditions using both the G93 and MEGAN2.1 algorithms. Using these new emission potentials, we then simulated the isoprene emission fluxes at each site and compared them to the observations.

Figure 9 shows the percentage difference between the averaged measured flux and the averaged modelled flux when using the "converted" isoprene emission potentials. Because the average predicted flux changes linearly with the emission potential, Fig. 9 implicitly also shows how these new emission factors compare with those derived with the weighted average method. The calculated bias ranged between +29% and -4% for the G93 algorithm and between +9% and -40% for the MEGAN 2.1 approaches. The bias for the G93 algorithm is typically positive which reflects the fact that the algorithm performs well at the reference conditions which represent typical daytime conditions but performs worse in the morning and afternoon, overestimating emission fluxes due to its inability to account for the attenuation of light and temperature through the canopy.

Formatted: Subscript

Formatted: Subscript

The observed bias in the MEGAN2.1 simulated isoprene fluxes is driven by two factors (i) the fact that the average flux for the set of defined conditions is based on a limited number of data points (which induces a larger random error for both algorithms), ranging between $n = 4$ to $n = 19$, which may be a poor representation of the typical flux footprint and canopy heterogeneity and (ii) the defined conditions are based on current PPFD and temperature with larger uncertainty on the remaining gamma terms such as past PPFD and temperature. Therefore, we conclude that this approach succeeds in simulating emissions at 'typical' conditions encountered at each site, but less reliably reproduces the average emission.

While the reporting of fluxes at a set of defined reference conditions offers some clear advantages (e.g. the avoidance of two different algorithms being used for the forwards and backwards calculations), our analysis shows that there are also drawbacks that need to be considered. For example, ~~in our analysis~~here, we chose only to bin the measured flux data by the two major drivers of isoprene emissions, current light and temperature, meaning that the corresponding average isoprene emission is only suited for algorithms that use only these two variables (e.g. G93 algorithm). The more complex algorithms have many more reference parameters which means the measurement space becomes increasingly stratified, yielding far fewer flux averaging periods and resulting in larger uncertainties. In addition, with increasing bin width, additional uncertainty is introduced by averaging highly non-linear responses. We recommend future studies report both an emission potential for a set of defined conditions and an emission potential derived using the whole data set in conjunction with the weighted average method, providing a detailed description of exactly how the emission potential was calculated.

3.~~5~~4   Comparison with literature values

The leaf-level emission potentials in Fig. 6 were compared to the literature values compiled by Keenan et al. (2009). Isoprene emission potentials derived using the G93 algorithm, which most closely replicates the standard conditions used in cuvette measurements, agree very closely with the published values. For example, *Quercus pubescens* (81 µg g^{-1} h^{-1}) and *Quercus robur* (79 µg g^{-1} h^{-1}) which are thought to account for some ~50% of total European isoprene emissions, had calculated emission potentials of 78±25 µg g^{-1} h^{-1} and 82±36 µg g^{-1} h^{-1}, respectively, with the latter derived as the average from the Alice Holt, Bosco Fontana and Ispra forest sites. Yet, as we have stressed above, modellers must ensure that the emission potentials used in their model have been derived in a manner compatible with their emission algorithm. According to Keenan et al. (2009), the European isoprene budget was predicted using the G93 algorithm but also incorporating the effects of previous light and temperature as described by the equations in Guenther et al. (2006). This description appears consistent with the G06 approach we outline in Section 2.2.2 and we therefore also compare the published emission potentials against those derived using the G06 algorithm. Our estimates are 31% and 42% lower respectively for *Quercus robur* and *Quercus pubescens*, which, as discussed above, can be explained by the incorporation of additional standard conditions for the previous 24 and 240 hours light and temperature, which typically results in larger values for γ_l and γ_t and subsequently smaller emission potentials. Accounting for the lower emission potentials would see the contribution of *Quercus robur* and *Quercus pubescens* to the annual biogenic isoprene budget decrease from a combined total of 50% to 33%, which equates to an overall reduction in the European total of ~17%. This would give a new average European isoprene budget for the period of 1960-1990 of around 0.85 Tg C a^{-1}.

While our analysis has focused on the calculation of emission potentials from above-canopy flux measurements and their uncertainties, it is important to recognise that the leaf-level emission potentials to which we compare are also highly uncertain. Leaf-level emission potentials vary considerably between the top and bottom of the canopy and for the same species have been shown to range between a factor of 10 (Aydin et al. 2014, van Meeningen et al. 2016) to 100 (e.g. Pokorska et al. 2011, Winer et al. 1983). Therefore, the leaf-level ~~measurements~~emission inventory compiled by Keenan et al. (2009) may not always ~~be~~give IEPs representative of the canopy average flux, which is directly observed by top-down micrometeorological approaches. Furthermore, leaf-level measurements are typically reported for a set of light and temperature conditions but other important environmental parameters including past light and temperature, CO_2 concentration and soil moisture, relevant to the

more advanced emission algorithms, are typically not reported. With this in mind, we would echo the sentiments of Niinemets et al. (2011) who call for the standardisation of leaf-level measurements and would stressreiterate the need for both the reporting of emission potentials on both a per mass and per area basis and the inclusion of additional environmental parameters (past light and temperature and CO_2 concentrations) to further reduce the uncertainties introduced when comparing the performance of emission algorithms (utilising leaf level emission potentials) with above-canopy flux measurements.

3.5 Reporting fluxes for defined conditions

We have demonstrated that emission potentials can vary considerably depending upon which emission algorithm is used to normalise the measured fluxes to standard conditions. One possibility to remove this uncertainty is to simply report those fluxes that correspond to a set of defined conditions. As already stated in Section 2.3, standard conditions are typically far removed from conditions found at many measurement sites e.g. at higher latitude sites, which means typically there is no or very little data directly measured under these conditions. Yet, fluxes may still be reported for a set of average daytime conditions which can then be extrapolated to standard conditions by the modelling community without introducing model specific bias. Using a two-dimensional histogram, binning flux data by light (±100 µmol m^{-2} s^{-1} PPFD) and temperature (± 0.5 K) we selected the most common set of daytime conditions at each of our five measurement sites. An example histogram is shown for the Ispra forest site in figure 8 and the average fluxes and environmental conditions that corresponded to these sets of conditions are shown in Table 4. In order to compare how emission potentials calculated using this small fraction of the available data (typically between 1.2-2%) compared to our previously calculated emission potentials, we converted the average fluxes shown in Table 4 to standard conditions using both the G93 and MEGAN2.1 algorithms. Using these new emission potentials, we then simulated the isoprene emission fluxes at each site and compared them to the observations.

Figure 9 shows the percentage difference between the averaged measured flux and the averaged modelled flux when using the "converted" isoprene emission potentials. The calculated bias ranged between +29% and -4% for the G93 algorithm and between +9% and -40% for the MEGAN 2.1 approaches. The bias for the G93 algorithm is typically positive which reflects the fact that the algorithm performs well at conditions close to standard conditions but performs worse in the morning and afternoon, overestimating emission fluxes due to its inability to account for the attenuation of light and temperature through the canopy. The observed bias in the MEGAN2.1 simulated isoprene fluxes is driven by two factors (i) the fact that the average flux for the set of defined conditions is based on a limited number of data points (which affects both algorithms), ranging between $n = 4$ to $n = 19$, which may be a poor representation of the typical flux footprint and canopy heterogeneity and (ii) the defined conditions are based on current PPFD and temperature with larger uncertainty on the remaining gamma terms such as past PPFD and temperature. Therefore, we conclude that this approach succeeds in simulating emissions at 'typical' conditions encountered at each site, but performs poorly at reproducing the average emission.

While the reporting of fluxes at a set of defined conditions offers some clear advantages (e.g. the avoidance of two different algorithms being used for the forwards and backwards calculations), our analysis shows that there are also drawbacks that need to be considered. For example, in our analysis, we chose only to bin the measured flux data by the two major drivers of isoprene emissions, current light and temperature, meaning that the corresponding average isoprene emission is only suited for algorithms that use only these two variables (e.g. G93 algorithm). The more complex algorithms have many more reference parameters which means the measurement space becomes increasingly stratified, yielding far fewer flux averaging periods and resulting in larger uncertainties. We recommend future studies report both an emission potential for a set of defined conditions and an emission potential derived using the whole data set in conjunction with the weighted average method, providing a detailed description of exactly how the emission potential was calculated.

18

4   Conclusions

Five sets of canopy-scale isoprene flux measurements from European oak forests have been carefully reviewed to determine new ecosystem, oak canopy and leaf-level equivalent emission potentials using different averaging techniques and six implementations of the commonly used Guenther et al. (1993, 2006, 2012) algorithms. New methods to correct derived

5   emission potentials for the effects of chemical flux divergence and the losses of isoprene through dry deposition, two processes that are typically overlooked when determining emission potentials from micrometeorological flux measurements, have been outlined. Furthermore, we have thoroughly assessed the uncertainties in the derivation of ecosystem emission potentials and their subsequent extrapolation to whole-oak canopy and leaf-level estimates. All algorithms fail~~ed~~ to reproduce the diurnal pattern in the flux, resulting in emission potentials being derived that apparently vary over the day, and from these various

10   average emission potentials can be calculated, which result in mean fluxes that vary by up to a factor of two. In this study, we have chosen to calculate average emission potentials using a weighted average approach which ensures modelled fluxes share the same average as the measurements. While we believe this approach gives the most robust and reproducible assessment of the isoprene emission potential, others have used different approaches. We have shown that the isoprene emission potential can vary by more than 30% depending upon which method is used, resulting in additional, but entirely avoidable, uncertainties

15   in emission potentials and hence modelled average emissions. We have also clearly demonstrated that for any given dataset a very wide range of emission potentials can be calculated, the values of which depend upon both the specific algorithm used and how it is implemented to back-out the emission potentials. Some of the variation between algorithms relates to changes in the standard light conditions from 1000 µmol m^{-2} s^{-1} ~~PAR~~ PPFD in leaf-level models to 1500 µmol m^{-2} s^{-1} ~~PAR~~ PPFD in canopy-scale algorithms. However, a comparison of the leaf-level extrapolated emission potentials which were harmonised to

20   a similar set of standard conditions across all algorithms (e.g. 1000 µmol m^{-2} s^{-1} ~~PAR~~PPFD) demonstrated that these algorithms do not always yield similar emission potentials, with up to a factor of ~~four~~ 2.7 difference. Clearly, different emission algorithms and algorithm implementations result in different emission predictions even if the same emission potentials are used, with the variability stated here. If the starting point are canopy-scale rather than leaf-level flux measurements, the emission algorithms are used twice: once for standardisation (backward calculation) and once in the model (forward calculation). If the algorithms

25   and meteorological drivers are identical for both steps then errors in the algorithms cancel each other. By contrast, if different algorithms are used then the uncertainties in both calculations may be additive. This is an important consideration for both the measurement and modelling community. It demonstrates the need for experimentalists to very carefully articulate exactly how published emission potentials were derived and which algorithms and in particular which parameters (e.g. past light and temperature, leaf temperature, CO_2, soil moisture etc.) were used to back out emission potentials. Similarly, the modelling

30   community need to be aware of the uncertainties when using an emission potential derived using a different version, or even implementation, of the algorithm to that used in their model. <u>Using our new, algorithm specific, isoprene emission potentials for *Quercus robur* and *Quercus pubescens* we were able to demonstrate that the previous European isoprene budget may have been systematically overestimated by as much as 17% due to inconsistencies between the emission potentials and emission algorithm used in the model. Therefore, a better estimate of the average European isoprene budget for the period of 1960-1990</u>

35   <u>is 0.85 Tg C a^{-1}.</u>

~~Using our new, algorithm specific, isoprene emission potentials for *Quercus robur* and *Quercus pubescens* we were able to demonstrate that the previous European isoprene budget may have been systematically overestimated by as much as 17% due to inconsistencies between the emission potentials and emission algorithm used in the model. Therefore, a better estimate of the average European isoprene budget for the period of 1960-1990 is 0.85 Tg C a^{-1}.~~

40   In conclusion, we believe the uncertainty in isoprene emission models can be reduced by harmonising the way in which emission potentials are calculated from micrometeorological flux data. We have put forward recommendations for the extrapolation of net above-canopy fluxes back to surface emission fluxes and have outlined a new methodology to calculate the isoprene emission potential with clear justification. Nonetheless, with numerous implementations of the emission

19

algorithms in use and their ever increasing flexibility and complexity there does not appear to be easy solution to avoid intra-algorithm biases. In the past the BVOC flux community has preferred to calculate isoprene emission potentials using the G93 emission algorithm due to its relative simplicity. Yet, our work shows that the emission potentials calculated in this way may not be compatible with more recent emission algorithms. Our recommendation is that model developers now provide single point versions of their code, as has already been done for MEGAN 2.1 (e.g. Pocket MEGAN, Excel beta 3), which can be used by experimentalists to more easily determine emission potentials from their observational data. It is, however, ourFurthermore, we recommend recommendation that all processed canopy-scale flux data from which emission potentials are to be derived should be stored on a common community database. The VOCsNET database (http://vocsnetdata.ceh.ac.uk/) enables others to recalculate emission potentials in a fashion that is compatible for their model application and to enable re-calculation in the future to keep pace with the evolution of models such as MEGAN. All five datasets used in this study can be accessed via the VOCsNET database. In addition to the approaches of how to derive emission potentials from canopy scale flux measurements, further standardisation is also required for the micrometeorological flux measurement itself, including selection of instrumentation, instrument setup and operation, relative height of measurements above the canopy, data processing and reporting of results and uncertainties. In the near future it will also be important to ensure compatibility between traditional tower based flux observations and those made using the emerging technology of airborne eddy covariance flux measurements (Karl et al., 2009; Yuan et al., 2015; Misztal et al., 2014; Misztal et al., 2016; Vaughan et al., 2017). We believe that by developing a consistent and robust approach to calculating emission potentials from top-down flux measurements, future emission algorithms may be better parameterised through the incorporation of regional scale observations.

Whilst this analysis focused on the uncertainties involved in the reverse application of the emission algorithm to back out normalised emission potentials from canopy flux measurements, the variability between different algorithms and their implementation is the same for the forward calculation used in the emission models themselves.

Author Contributions

E. Nemitz and B. Langford designed the research. B. Langford led the data synthesis and analysis and collected the data at the BF site. J. Cash assisted with data synthesis and performed the analysis. W. Acton and A. Valach collected and processed the BF dataset. S. Fares collected and processed the data from the CP site. I. Goded and C. Gruening collected and processed the data from the Ispra site, E. House, R. Thomas and M. Broadmeadow collected the data from the AH site. R. Schafers processed the AH data. A.C. Kalogridis and V. Gros collected and processed the O3HP dataset. B. Langford prepared the manuscript with contributions from all co-authors.

Data Availability

All five data sets can be accessed via the VOCsNET database hosted by the Centre for Ecology and Hydrology (http://vocsnetdata.ceh.ac.uk/)

Competing Interests

The authors declare no competing interests

References

Acton, W. J. F., Schallhart, S., Langford, B., Valach, A., Rantala, P., Fares, S., Carriero, G., Tillmann, R., Tomlinson, S. J., Dragosits, U., Gianelle, D., Hewitt, C. N., and Nemitz, E.: Canopy-scale flux measurements and bottom-up emission estimates of volatile organic compounds from a mixed oak and hornbeam forest in northern Italy, Atmospheric Chemistry and Physics, 16, 7149-7170, 10.5194/acp-16-7149-2016, 2016.

Arneth, A., Niinemets, Ü., Pressley, S., Bäck, J., Hari, P., Karl, T., Noe, S., Prentice, I. C., Serça, D., Hickler, T., Wolf, A., and Smith, B.: Process-based estimates of terrestrial ecosystem isoprene emissions: incorporating the effects of a direct CO_2-isoprene interaction, Atmos. Chem. Phys., 7, 31-53, doi:10.5194/acp-7-31-2007, 2007.

Arneth, A., Monson, R. K., Schurgers, G., Niinemets, Ü., and Palmer, P. I.: Why are estimates of global terrestrial isoprene emissions so similar (and why is this not so for monoterpenes)?, Atmos. Chem. Phys., 8, 4605-4620, https://doi.org/10.5194/acp-8-4605-2008, 2008.

Aydin YM, Yaman B, Koca H, Dasdemir O, Kara M, Altiok H, Dumanoglu Y, Bayram A, Tolunay D, Odabasi M, Elbir T.: Biogenic volatile organic compound (BVOC) emissions from forested areas in Turkey: Determination of specific emission rates for thirty-one tree species. Science of the Total Environment 490: 239-253, 2014

Back, J., Hari, P., Hakola, H., Juurola, E., and Kulmala, M.: Dynamics of monoterpene emissions in Pinus sylvestris during early spring, Boreal Environ. Res., 10, 409–424, 2005.

Bamberger, I., Hortnagl, L., Ruuskanen, T. M., Schnitzhofer, R., Muller, M., Graus, M., Karl, T., Wohlfahrt, G., and Hansel, A.: Deposition fluxes of terpenes over grassland, Journal of Geophysical Research-Atmospheres, 116, 10.1029/2010jd015457, 2011.

Bertin, N., Staudt, M., Hansen, U., Seufert, G., Ciccioli, P., Foster, P., Fugit, J. L., and Torres, L.: Diurnal and seasonal course of monoterpene emissions from Quercus ilex (L.) under natural conditions - Applications of light and temperature algorithms, Atmospheric Environment, 31, 135-144, 10.1016/s1352-2310(97)00080-0, 1997.

Carlton, A. G., Wiedinmyer, C., and Kroll, J. H.: A review of Secondary Organic Aerosol (SOA) formation from isoprene, Atmos. Chem. Phys., 9, 4987-5005, doi:10.5194/acp-9-4987-2009, 2009.

Davison, B., Taipale, R., Langford, B., Misztal, P., Fares, S., Matteucci, G., Loreto, F., Cape, J. N., Rinne, J., and Hewitt, C. N.: Concentrations and fluxes of biogenic volatile organic compounds above a Mediterranean macchia ecosystem in western Italy, Biogeosciences, 6, 1655-1670, 2009.

Fall, R., and Monson, R. K.: ISOPRENE EMISSION RATE AND INTERCELLULAR ISOPRENE CONCENTRATION AS INFLUENCED BY STOMATAL DISTRIBUTION AND CONDUCTANCE, Plant Physiology, 100, 987-992, 10.1104/pp.100.2.987, 1992.

Fares, S., Schnitzhofer, R., Jiang, X. Y., Guenther, A., Hansel, A., and Loreto, F.: Observations of Diurnal to Weekly Variations of Monoterpene-Dominated Fluxes of Volatile Organic Compounds from Mediterranean Forests: Implications for Regional Modeling, Environmental Science & Technology, 47, 11073-11082, 10.1021/es4022156, 2013.

5 Genard-Zielinski, A.-C., Boissard, C., Fernandez, C., Kalogridis, C., Lathière, J., Gros, V., Bonnaire, N., and Ormeño, E.: Variability of BVOC emissions from a Mediterranean mixed forest in southern France with a focus on *Quercus pubescens*, Atmos. Chem. Phys., 15, 431-446, doi:10.5194/acp-15-431-2015, 2015.

Goldstein, A. H., Goulden, M. L., Munger, J. W., Wofsy, S. C., and Geron, C. D.: Seasonal course of isoprene emissions from
10 a midlatitude deciduous forest, Journal of Geophysical Research-Atmospheres, 103, 31045-31056, 10.1029/98jd02708, 1998.

Goudriaan, J. and van Laar, H. H.: Modelling potential crop growth processes, Kluwer Academic Publishers, Dordrecht, 1994.

Grote R.: Sensitivity of volatile monoterpene emission to changes in canopy structure – A model based exercise with a process-
15 based emission model. New Phytologist 173(3): 550-561, 2007.

Guenther, A. B., Monson, R. K., and Fall, R.: ISOPRENE AND MONOTERPENE EMISSION RATE VARIABILITY - OBSERVATIONS WITH EUCALYPTUS AND EMISSION RATE ALGORITHM DEVELOPMENT, Journal of Geophysical Research-Atmospheres, 96, 10799-10808, 10.1029/91jd00960, 1991.
20
Guenther, A. B., Zimmerman, P. R., Harley, P. C., Monson, R. K., and Fall, R.: Isoprene and Monoterpene Emission Rate Variability - Model Evaluations and Sensitivity Analyses, Journal of Geophysical Research-Atmospheres, 98, 12609-12617, 1993.

25 Guenther, A., Hewitt, C. N., Erickson, D., Fall, R., Geron, C., Graedel, T., Harley, P., Klinger, L., Lerdau, M., McKay, W. A., Pierce, T., Scholes, B., Steinbrecher, R., Tallamraju, R., Taylor, J., and Zimmerman, P.: A Global-Model of Natural Volatile Organic-Compound Emissions, Journal of Geophysical Research-Atmospheres, 100, 8873-8892, 1995.

Guenther, A., Baugh, B., Brasseur, G., Greenberg, J., Harley, P., Klinger, L., Serca, D., and Vierling, L.: Isoprene emission
30 estimates and uncertainties for the Central African EXPRESSO study domain, Journal of Geophysical Research-Atmospheres, 104, 30625-30639, 10.1029/1999jd900391, 1999.

Guenther, A., Karl, T., Harley, P., Wiedinmyer, C., Palmer, P. I., and Geron, C.: Estimates of global terrestrial isoprene emissions using MEGAN (Model of Emissions of Gases and Aerosols from Nature), Atmospheric Chemistry and Physics, 6,
35 3181-3210, 2006.

Guenther, A. B., Jiang, X., Heald, C. L., Sakulyanontvittaya, T., Duhl, T., Emmons, L. K., and Wang, X.: The Model of Emissions of Gases and Aerosols from Nature version 2.1 (MEGAN2.1): an extended and updated framework for modeling biogenic emissions, Geoscientific Model Development, 5, 1471-1492, 10.5194/gmd-5-1471-2012, 2012.
40
Hallquist, M., Wenger, J. C., Baltensperger, U., Rudich, Y., Simpson, D., Claeys, M., Dommen, J., Donahue, N. M., George, C., Goldstein, A. H., Hamilton, J. F., Herrmann, H., Hoffmann, T., Iinuma, Y., Jang, M., Jenkin, M. E., Jimenez, J. L., Kiendler-Scharr, A., Maenhaut, W., McFiggans, G., Mentel, T. F., Monod, A., Prevot, A. S. H., Seinfeld, J. H., Surratt, J. D., Szmigielski,

R., and Wildt, J.: The formation, properties and impact of secondary organic aerosol: current and emerging issues, Atmospheric Chemistry and Physics, 9, 5155-5236, 2009.

Hewitt, C. N., Ashworth, K., Boynard, A., Guenther, A., Langford, B., MacKenzie, A. R., Misztal, P. K., Nemitz, E., Owen, S. M., Possell, M., Pugh, T. A. M., Ryan, A. C., and Wild, O.: Ground-level ozone influenced by circadian control of isoprene emissions, Nature Geoscience, 4, 671-674, 10.1038/ngeo1271, 2011.

Kalogridis, C., Gros, V., Sarda-Esteve, R., Langford, B., Loubet, B., Bonsang, B., Bonnaire, N., Nemitz, E., Genard, A. C., Boissard, C., Fernandez, C., Ormeno, E., Baisnee, D., Reiter, I., and Lathiere, J.: Concentrations and fluxes of isoprene and oxygenated VOCs at a French Mediterranean oak forest, Atmospheric Chemistry and Physics, 14, 10085-10102, 10.5194/acp-14-10085-2014, 2014.

Karl, T., Potosnak, M., Guenther, A., Clark, D., Walker, J., Herrick, J. D., and Geron, C.: Exchange processes of volatile organic compounds above a tropical rain forest: Implications for modeling tropospheric chemistry above dense vegetation, Journal of Geophysical Research-Atmospheres, 109, 2004.

Karl, T., Apel, E., Hodzic, A., Riemer, D. D., Blake, D. R., and Wiedinmyer, C.: Emissions of volatile organic compounds inferred from airborne flux measurements over a megacity, Atmos. Chem. Phys., 9, 271-285, doi:10.5194/acp-9-271-2009, 2009.

Keenan, T., Niinemets, U., Sabate, S., Gracia, C., and Penuelas, J.: Process based inventory of isoprenoid emissions from European forests: model comparisons, current knowledge and uncertainties, Atmospheric Chemistry and Physics, 9, 4053-4076, 2009.

Keenan T, Grote R, Sabaté S.: Overlooking the canopy: The importance of canopy structure in scaling isoprenoid emissions from leaf to canopy. Ecological Modelling 222(3): 737-747, 2011.

Keenan, T. F., and Niinemets, U.: Circadian control of global isoprene emissions, Nature Geoscience, 5, 435-435, 10.1038/ngeo1500, 2012.

Kiendler-Scharr, A., Wildt, J., Dal Maso, M., Hohaus, T., Kleist, E., Mentel, T. F., Tillmann, R., Uerlings, R., Schurr, U., and Wahner, A.: New particle formation in forests inhibited by isoprene emissions, Nature, 461, 381-384, 2009.

Langford, B., Misztal, P. K., Nemitz, E., Davison, B., Helfter, C., Pugh, T. A. M., MacKenzie, A. R., Lim, S. F., and Hewitt, C. N.: Fluxes and concentrations of volatile organic compounds from a South-East Asian tropical rainforest, Atmospheric Chemistry and Physics, 10, 8391-8412, 10.5194/acp-10-8391-2010, 2010.

Langford, B., Acton, W., Ammann, C., Valach, A., and Nemitz, E.: Eddy-covariance data with low signal-to-noise ratio: time-lag determination, uncertainties and limit of detection, Atmospheric Measurement Techniques, 8, 4197-4213, 10.5194/amt-8-4197-2015, 2015.

Laothawornkitkul, J., Taylor, J. E., Paul, N. D., and Hewitt, C. N.: Biogenic volatile organic compounds in the Earth system, New Phytologist, 183, 27-51, 2009.

23

Martin, M. J., Stirling, C. M., Humphries, S. W., and Long, S. P.: A process-based model to predict the effects of climatic change on leaf isoprene emission rates, Ecol. Model., 131, 161–174, 2000.

Misztal, P. K., Nemitz, E., Langford, B., Di Marco, C. F., Phillips, G. J., Hewitt, C. N., MacKenzie, A. R., Owen, S. M., Fowler, D., Heal, M. R., and Cape, J. N.: Direct ecosystem fluxes of volatile organic compounds from oil palms in South-East Asia, Atmospheric Chemistry and Physics, 11, 8995-9017, 10.5194/acp-11-8995-2011, 2011.

Misztal, P. K., Karl, T., Weber, R., Jonsson, H. H., Guenther, A. B., and Goldstein, A. H.: Airborne flux measurements of biogenic isoprene over California, Atmos. Chem. Phys., 14, 10631-10647, doi:10.5194/acp-14-10631-2014, 2014.

Misztal, P. K., Avise, J. C., Karl, T., Scott, K., Jonsson, H. H., Guenther, A. B., and Goldstein, A. H.: Evaluation of regional isoprene emission factors and modeled fluxes in California, Atmospheric Chemistry and Physics, 16, 9611-9628, 10.5194/acp-16-9611-2016, 2016.

Monson, R. K., Harley, P. C., Litvak, M. E., Wildermuth, M., Guenther, A. B., Zimmerman, P. R., and Fall, R.: Environmental and Developmental Controls over the Seasonal Pattern of Isoprene Emission from Aspen Leaves, Oecologia, 99, 260-270, 1994.

Morani, A., Nowak, D., Hirabayashi, S., Guidolotti, G., Medori, M., Muzzini, V., Fares, S., Mugnozza, G. S., and Calfapietra, C.: Comparing i-Tree modeled ozone deposition with field measurements in a periurban Mediterranean forest, Environmental Pollution, 195, 202-209, 10.1016/j.envpol.2014.08.031, 2014.

Nemitz, E., Hargreaves, K. J., Neftel, A., Loubet, B., Cellier, P., Dorsey, J. R., Flynn, M., Hensen, A., Weidinger, T., Meszaros, R., Horvath, L., Dammgen, U., Fruhauf, C., Lopmeier, F. J., Gallagher, M. W., and Sutton, M. A.: Intercomparison and assessment of turbulent and physiological exchange parameters of grassland, Biogeosciences, 6, 1445-1466, 2009.

Niinemets, U., Tenhunen, J. D., Harley, P. C., and Steinbrecher, ¨ R.: A model of isoprene emission based on energetic requirements for isoprene synthesis and leaf photosynthetic properties for Liquidambar and Quercus, Plant Cell Environ., 22, 1319– 1335, 1999

Niinemets, U., Seufert, G., Steinbrecher, R., and Tenhunen, J. D.: ¨ A model coupling foliar monoterpene emissions to leaf photosynthetic characteristics in Mediterranean evergreen Quercus species, New Phytol., 153, 257–276, 2002b.

Niinemets, U., Copolovici, L., and Huve, K.: High within-canopy variation in isoprene emission potentials in temperate trees: Implications for predicting canopy-scale isoprene fluxes, Journal of Geophysical Research-Biogeosciences, 115, 10.1029/2010jg001436, 2010.

Niinemets, Ü., Kuhn, U., Harley, P. C., Staudt, M., Arneth, A., Cescatti, A., Ciccioli, P., Copolovici, L., Geron, C., Guenther, A., Kesselmeier, J., Lerdau, M. T., Monson, R. K., and Peñuelas, J.: Estimations of isoprenoid emission capacity from enclosure studies: measurements, data processing, quality and standardized measurement protocols, Biogeosciences, 8, 2209-2246, https://doi.org/10.5194/bg-8-2209-2011, 2011.

Olofsson, M., Ek-Olausson, B., Jensen, N. O., Langer, S., and Ljungstrom, E.: The flux of isoprene from a willow coppice plantation and the effect on local air quality, Atmospheric Environment, 39, 2061-2070, 10.1016/j.atmosenv.2004.12.015, 2005.

5 Owen, S. M., Boissard, C., and Hewitt, C. N.: Volatile organic compounds (VOCs) emitted from 40 Mediterranean plant species: VOC speciation and extrapolation to habitat scale, Atmospheric Environment, 35, 5393-5409, 10.1016/s1352-2310(01)00302-8, 2001.

Pacifico, F., et al. (2011), Evaluation of a photosynthesis-based biogenic isoprene emission scheme in JULES and simulation
10 of isoprene emissions under present-day climate conditions, Atmos. Chem. Phys., 11, 4371–4389, doi:10.5194/acp-11-4371-2011.

Park, J. H., Goldstein, A. H., Timkovsky, J., Fares, S., Weber, R., Karlik, J., and Holzinger, R.: Eddy covariance emission and deposition flux measurements using proton transfer reaction - time of flight - mass spectrometry (PTR-TOF-MS): comparison
15 with PTR-MS measured vertical gradients and fluxes, Atmospheric Chemistry and Physics, 13, 1439-1456, 10.5194/acp-13-1439-2013, 2013.

Petron, G., Harley, P., Greenberg, J., and Guenther, A.: Seasonal temperature variations influence isoprene emission, Geophysical Research Letters, 28, 1707-1710, 2001.

20

Pokorska,O., Dewulf,J., Amelynck,C., Schoon,N., Joo,E., Simpraga,M., Bloemen,J., Steppe,K., Van Langenhove,H.: Emissions of biogenic volatile organic compounds from Fraxinus excelsior and Quercus robur under ambient conditions in Flanders (Belgium). International Journal of Environmental Analytical Chemistry 1-13, 2011

25 Potosnak, M. J., Baker, B. M., LeStourgeon, L., Disher, S. M., Griffin, K. L., Bret-Harte, M. S., and Starr, G.: Isoprene emissions from a tundra ecosystem, Biogeosciences, 10, 871-889, 10.5194/bg-10-871-2013, 2013.

Rantala, P., Jarvi, L., Taipale, R., Laurila, T. K., Patokoski, J., Kajos, M. K., Kurppa, M., Haapanala, S., Siivola, E., Petaja, T., Ruuskanen, T. M., and Rinne, J.: Anthropogenic and biogenic influence on VOC fluxes at an urban background site in
30 Helsinki, Finland, Atmospheric Chemistry and Physics, 16, 7981-8007, 10.5194/acp-16-7981-2016, 2016.

Rinne, J., Taipale, R., Markkanen, T., Ruuskanen, T. M., Hellen, H., Kajos, M. K., Vesala, T., and Kulmala, M.: Hydrocarbon fluxes above a Scots pine forest canopy: measurements and modeling, Atmospheric Chemistry and Physics, 7, 3361-3372, 2007.

35

Rinne, H. J. I., Guenther, A. B., Greenberg, J. P., and Harley, P. C.: Isoprene and monoterpene fluxes measured above Amazonian rainforest and their dependence on light and temperature, Atmospheric Environment, 36, 2421-2426, 2002.

Ruuskanen, T. M., Mueller, M., Schnitzhofer, R., Karl, T., Graus, M., Bamberger, I., Hortnagl, L., Brilli, F., Wohlfahrt, G.,
40 and Hansel, A.: Eddy covariance VOC emission and deposition fluxes above grassland using PTR-TOF, Atmospheric Chemistry and Physics, 11, 611-625, 10.5194/acp-11-611-2011, 2011.

Situ, S., Wang, X. M., Guenther, A., Zhang, Y. L., Wang, X. M., Huang, M. J., Fan, Q., and Xiong, Z.: Uncertainties of isoprene emissions in the MEGAN model estimated for a coniferous and broad-leaved mixed forest in Southern China, Atmospheric Environment, 98, 105-110, 10.1016/j.atmosenv.2014.08.023, 2014.

5 Schallhart, S., Rantala, P., Nemitz, E., Taipale, D., Tillmann, R., Mentel, T. F., Loubet, B., Gerosa, G., Finco, A., Rinne, J., and Ruuskanen, T. M.: Characterization of total ecosystem-scale biogenic VOC exchange at a Mediterranean oak-hornbeam forest, Atmospheric Chemistry and Physics, 16, 7171-7194, 10.5194/acp-16-7171-2016, 2016.

Sharkey, T. D., Loreto, F., and Delwiche, C. F.: HIGH-CARBON DIOXIDE AND SUN SHADE EFFECTS ON ISOPRENE
10 EMISSION FROM OAK AND ASPEN TREE LEAVES, Plant Cell and Environment, 14, 333-338, 10.1111/j.1365-3040.1991.tb01509.x, 1991.

Sharkey, T. D., and Loreto, F.: WATER-STRESS, TEMPERATURE, AND LIGHT EFFECTS ON THE CAPACITY FOR ISOPRENE EMISSION AND PHOTOSYNTHESIS OF KUDZU LEAVES, Oecologia, 95, 328-333, 10.1007/bf00320984,
15 1993.

Sharkey, T. D., Wiberley, A. E., and Donohue, A. R.: Isoprene emission from plants: Why and how, Annals of Botany, 101, 5-18, 10.1093/aob/mcm240, 2008.

20 Smith, T. M., Shugart, H. H., and Woodward, F. I. (Eds.): Plant functional types: Their relevance to ecosystem properties and global change, International geosphere-biosphere programme book series 1, Cambridge University Press, Cambridge, 1997.

Steinbrecher, R., Hauff, K., Rabong, R., and Steinbrecher, J.: Isoprenoid emission of oak species typical for the Mediterranean area: Source strength and controlling variables, Atmospheric Environment, 31, 79-88, 10.1016/s1352-2310(97)00076-9, 1997.
25
Stroud, C., Makar, P., Karl, T., Guenther, A., Geron, C., Turnipseed, A., Nemitz, E., Baker, B., Potosnak, M., and Fuentes, J. D.: Role of canopy-scale photochemistry in modifying biogenic-atmosphere exchange of reactive terpene species: Results from the CELTIC field study, Journal of Geophysical Research-Atmospheres, 110, 2005.

30 Sutton, M. A., Fowler, D., Burkhardt, J. K., and Milford, C.: Vegetation atmosphere exchange of ammonia: Canopy cycling and the impacts of elevated nitrogen inputs, Water Air and Soil Pollution, 85, 2057-2063, 10.1007/bf01186137, 1995.

Taipale, R., Ruuskanen, T. M., Rinne, J., Kajos, M. K., Hakola, H., Pohja, T., and Kulmala, M.: Technical Note: Quantitative long-term measurements of VOC concentrations by PTR-MS - measurement, calibration, and volume mixing ratio calculation
35 methods, Atmospheric Chemistry and Physics, 8, 6681-6698, 2008.

Tingey, D. T., Evans, R., and Gumpertz, M.: EFFECTS OF ENVIRONMENTAL-CONDITIONS ON ISOPRENE EMISSION FROM LIVE OAK, Planta, 152, 565-570, 10.1007/bf00380829, 1981.

40 Valach, A. C., Langford, B., Nemitz, E., MacKenzie, A. R., and Hewitt, C. N.: Seasonal and diurnal trends in concentrations and fluxes of volatile organic compounds in central London, Atmospheric Chemistry and Physics, 15, 7777-7796, 10.5194/acp-15-7777-2015, 2015.

van Meeningen, Y., Schurgers, G., Rinnan, R., Holst, T.: BVOC emissions from English oak (Quercus robur) and European beech (Fagus sylvatica) along a latitudinal gradient. Biogeosciences 13, 6067-6080, 2016.

Vaughan, A. R., Lee, J. D., Shaw, M. D., Misztal, P., Metzger, S., Vieno, M., Davison, B., Karl, T., Carpenter, L., Lewis, A. C., Purvis, R., Goldstein, A., and Hewitt, C. N.: VOC emission rates over London and South East England obtained by airborne eddy covariance, Faraday Discussions, 10.1039/c7fd00002b, 2017.

Wilkinson, M. J., Owen, S. M., Possell, M., Hartwell, J., Gould, P., Hall, A., Vickers, C., and Hewitt, C. N.: Circadian control of isoprene emissions from oil palm (Elaeis guineensis), Plant Journal, 47, 960-968, 2006.

Wilkinson, M., Eaton, E. L., Broadmeadow, M. S. J., and Morison, J. I. L.: Inter-annual variation of carbon uptake by a plantation oak woodland in south-eastern England, Biogeosciences, 9, 5373-5389, doi:10.5194/bg-9-5373-2012, 2012.

Winer, A.M., Fitz,D.R., Miller,P.R.: Investigation of the role of natural hydrocarbons in photochemical smog formation in California. Contract No. AO-056-32. 1983. Riverside, California, U.S.A., Statewide Air Pollution Research Center, 1983.

Wohlfahrt, G., Amelynck, C., Ammann, C., Arneth, A., Bamberger, I., Goldstein, A. H., Gu, L., Guenther, A., Hansel, A., Heinesch, B., Holst, T., Hortnagl, L., Karl, T., Laffineur, Q., Neftel, A., McKinney, K., Munger, J. W., Pallardy, S. G., Schade, G. W., Seco, R., and Schoon, N.: An ecosystem-scale perspective of the net land methanol flux: synthesis of micrometeorological flux measurements, Atmospheric Chemistry and Physics, 15, 7413-7427, 10.5194/acp-15-7413-2015, 2015.

Yuan, B., Kaser, L., Karl, T., Graus, M., Peischl, J., Campos, T. L., Shertz, S., Apel, E. C., Hornbrook, R. S., Hills, A., Gilman, J. B., Lerner, B. M.,Warneke, C., Flocke, F. M., Ryerson, T. B., Guenther, A. B., and de Gouw, J. A.: Airborne flux measurements of methane and volatile organic compounds over the Haynesville and Marcellus shale gas production regions, J. Geophys. Res.- Atmos., 120, 6271–6289, doi:10.1002/2015jd023242, 2015.

Zimmer, W., Bruggemann, N., Emeis, S., Giersch, C., Lehning, A., Steinbrecher, R., and Schnitzler, J.-P.: Process based modelling of isoprene emission by oak leaves, Plant, Cell Environ., 23, 585–595, 2000

Table 1. Detailed breakdown of species composition and measurement approach for each of the five sites used in this study

	Alice Holt, UK		Bosco Fontana, Italy		Castelporziano, Italy		Ispra, Italy		Observatoire de Haute Provence, France	
Species Composition	*Quercus robur** (Pedunculate oak) *Quercus petraea** (Sessile oak) *Fraxinus* (Ash)	*90%* *10%*	*Quercus robur** (Pedunculate oak) *Quercus cerris* (Turkey oak) *Quercus rubra** (Northern Red oak) *Carpinus betulus* (Hornbeam) Other	*17%* *7.1%* *9.6%* *40.2%* *26%*	*Laurus nobilis* (Bay tree) *Quercus ilex** (Holm oak) *Pinus pinea* (Stone pine) *Quercus suber** (Cork oak) Other shrubs	*48.9%* *20.5%* *6.8%* *6.8%* *17%*	*Quercus robur* *(Pedunculate, oak) *Alnus glutinosa* (Black alder) *Popolus alba** (White poplar) *Carpinus betulus* (Hornbeam) Other	80% 10% 5% 3% 2%	*Quercus pubescens** (Downy oak) *Acer monspessulanumk* (Montpellier maple)	75% 25%
LAI [m²/m²]	4.8		5.5		4.6		4.4		2.4	
h_c **[m]**	20.5		28		25		26		5	
z_m **[m]**	28.5		32		35		37		10	
Method	vDEC – PTR-MS		vDEC – PTR-MS		~~v~~DEC – PTR-MS		EC – Fast Isoprene Sensor		vDEC – PTR-MS	
MEGAN PFT classification	7		7, 10		1, 5, 9		7		7	

*Known isoprene emitters

LAI: single-sided leaf area index; h_c: canopy height; z_m: measurement height

Table 2. List of standard conditions used by each of the emission algorithms in this study

Parameter	G93 "Big Leaf"	MEGAN2.0 "Big Leaf"/PCEEA	MEGAN2.1 + C_{CE}
γ_T [K]	303	303	303
• T_{24}, T_{240}	-	297, 297	297, 297
γ_L [μmol m^{-2} s^{-1}]	1000	1500	1500
• L_{24}, L_{240}		200, 200	
• Sun leaves: L_{24}, L_{240}			200, 200
• Shaded leaves: L_{24}, L_{240}			50, 50
LAI [m^2/m^2]	-	-	5
γ_{SM} [m^3 m^{-3}]	-	-	0.3
γ_A [%]	-	-	
• Growing			10
• Mature			80
• Old			10
γ_C [ppb]	-	-	400
C_{CE}	-	-	0.57
• Humidity [g kg^{-1}]			14
• Wind speed [m s^{-1}]			0.3

Table 3. Summary of uncertainties attributed to the various steps used in the calculation of emission potentials for each of the five measurement sites

Site	No. data	Emission potential calculation (Eq. 11)	R_c*	Chemistry	Species Composition	LAI (for canopy and leaf-level emission potentials	Leaf Dry Mass (Keenan et al. 2009)	Calibration gas (from manufacturer)
Alice Holt, UK	629	±3%	±25%	±10%	±10%	±16.5%	±25%	±25%**
Bosco Fontana, Italy	571	±25%	±25%	±10%	±10%	±26%	±25%	±5%
Castelporziano, Italy	190	±16%	±25%	±10%	±10%	±26.25%	±25%	±5%
Ispra, Italy	1226	±8%	±25%	±10%	±10%	±18%	±25%	±5%
O3HP, France	176	±3%	±25%	±10%	±10%	±18.7%5	±25%	±5%

* R_c = 250 s m^{-1} (Karl et al., 2004)

** Instrument transmission efficiency used in the absence of a gas standard

5

Table 4. Average isoprene emission fluxes at the Alice Holt, Bosco Fontana, Castelporziano, Ispra forest and O3HP sites under a set of defined conditions.

	Alice Holt	Bosco Fontana	Castelporziano	Ispra	O3HP
Average Flux [μg m^{-2} h^{-1}]	2143	1911	83	9404	2649
σ [μg m^{-2} s^{-1}]	1075	599	102	3593	988
$\overline{RE}$ [μg m^{-2} h^{-1}]	142	443	31	1268	353
N [#]	9	17	5	19	4
Temperature range [K]	293-294	302-303	300-301	302-303	294 - 294
PPFD range [μmol m^{-2} s^{-1}]	800-1000	1800-2000	1400-1600	1600-1800	1800-2000
Mean Temperature [K]	293.4	302.5	300.5	302.6	293.7
Mean PPFD [μmol m^{-2} s^{-1}]	915	1902	1523	1703	1852
Mean 24 T [K]	290	299	295	298	290
Mean 240T[K]	290	299	295	297	290
Mean 24 PPFD [μmol m^{-2} s^{-1}]	432	680	424	556	625
Mean 240 PPFD [μmol m^{-2} s^{-1}]	415	659	452	553	591

32
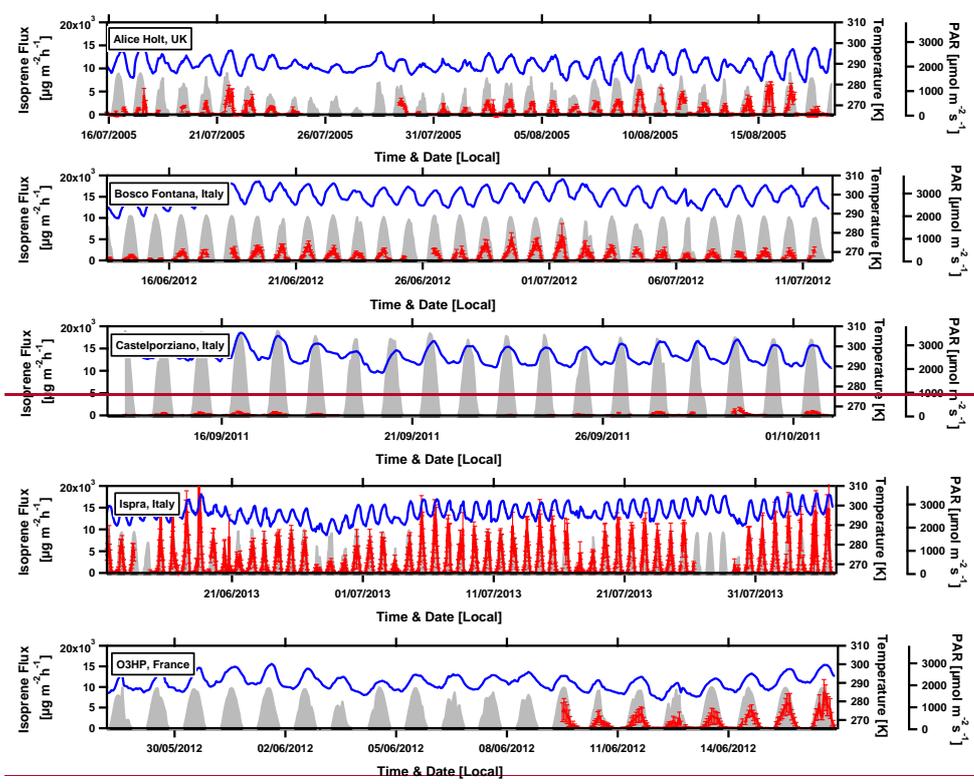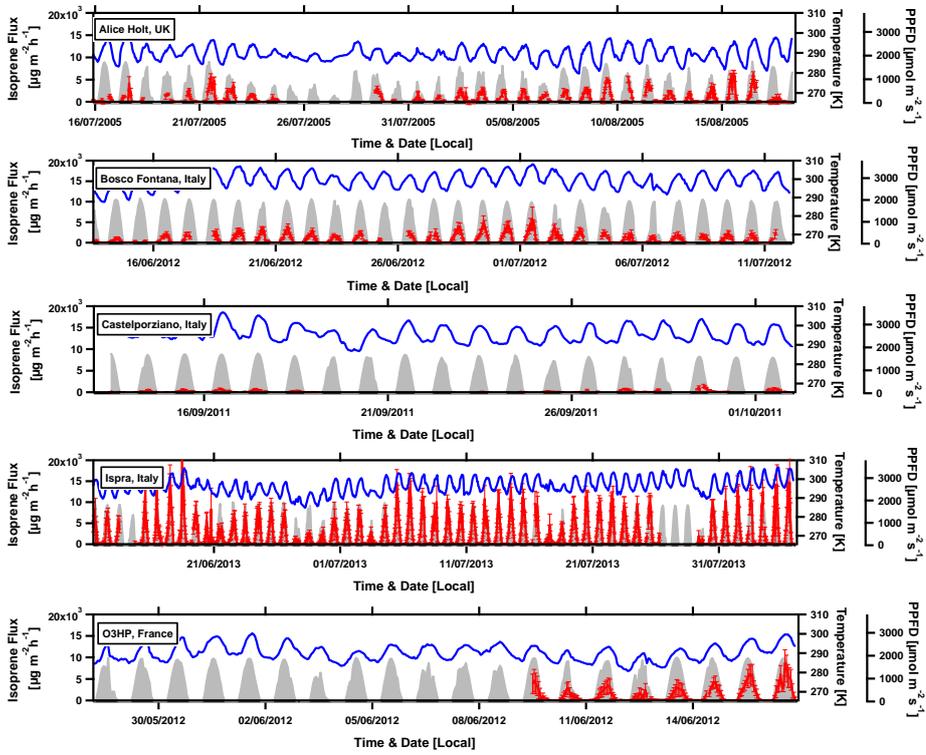
Figure 1. Time series of isoprene fluxes (red) in relation to temperature (blue) and ~~PAR~~ PPFD (grey) at the five measurement sites. Error bars show the calculated limit of detection for each individual flux measurement.
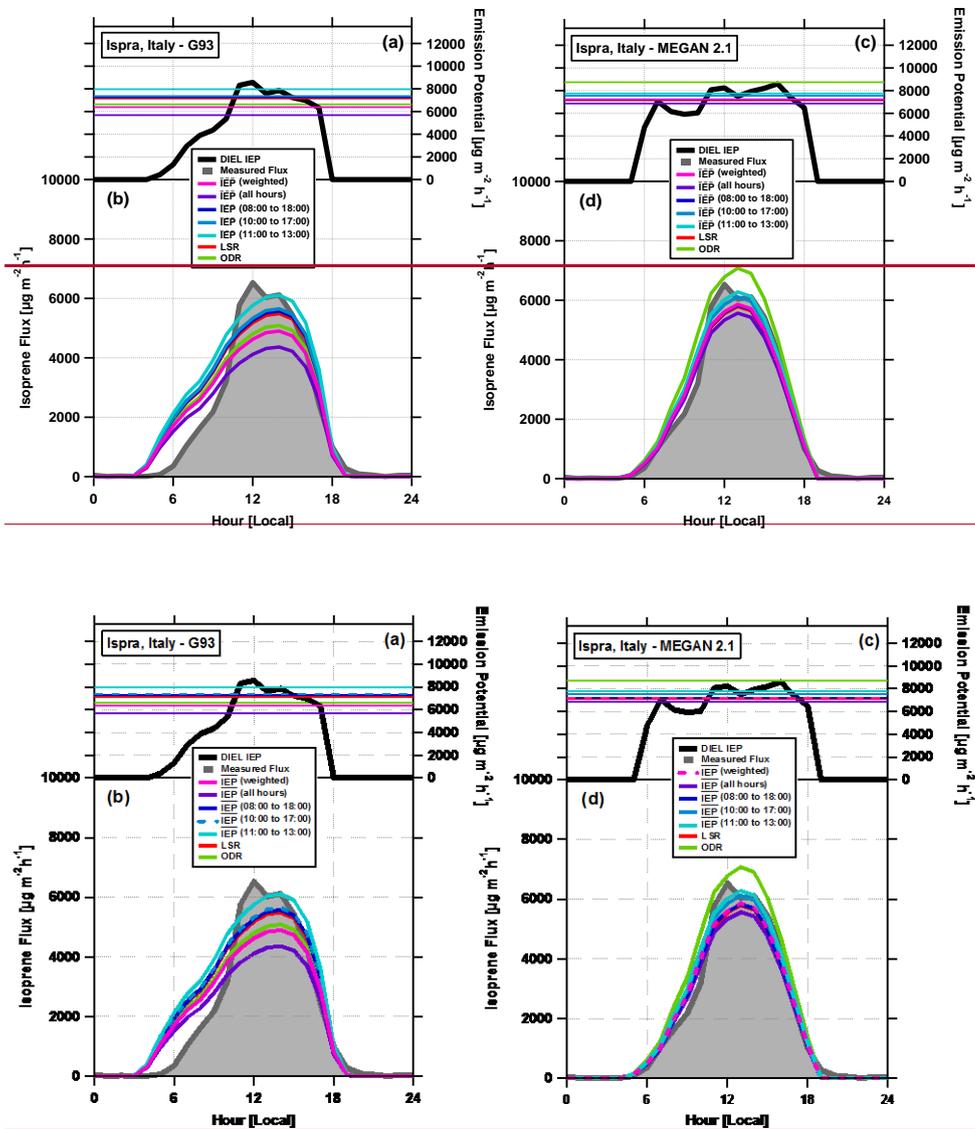
Figure 2 Panels (a) and (c) show the average diurnal cycle in the isoprene emission potential (e.g. $IEP = \overline{\left(\frac{F_{iso}}{\gamma}\right)}$) calculated for the Ispra forest site, Italy using the G93 (panel a) and MEGAN 2.1 (panel b) algorithms. Superimposed on top of these are the isoprene emission potentials calculated using the least square regression, orthogonal distance regression and average (with several averaging lengths) methods – see text for detailed description. Panels (b) and (d) show the average diurnal cycle of the measured fluxes and the average diurnal cycle of the fluxes modelled using the seven different isoprene emission potentials calculated for this data set.

34
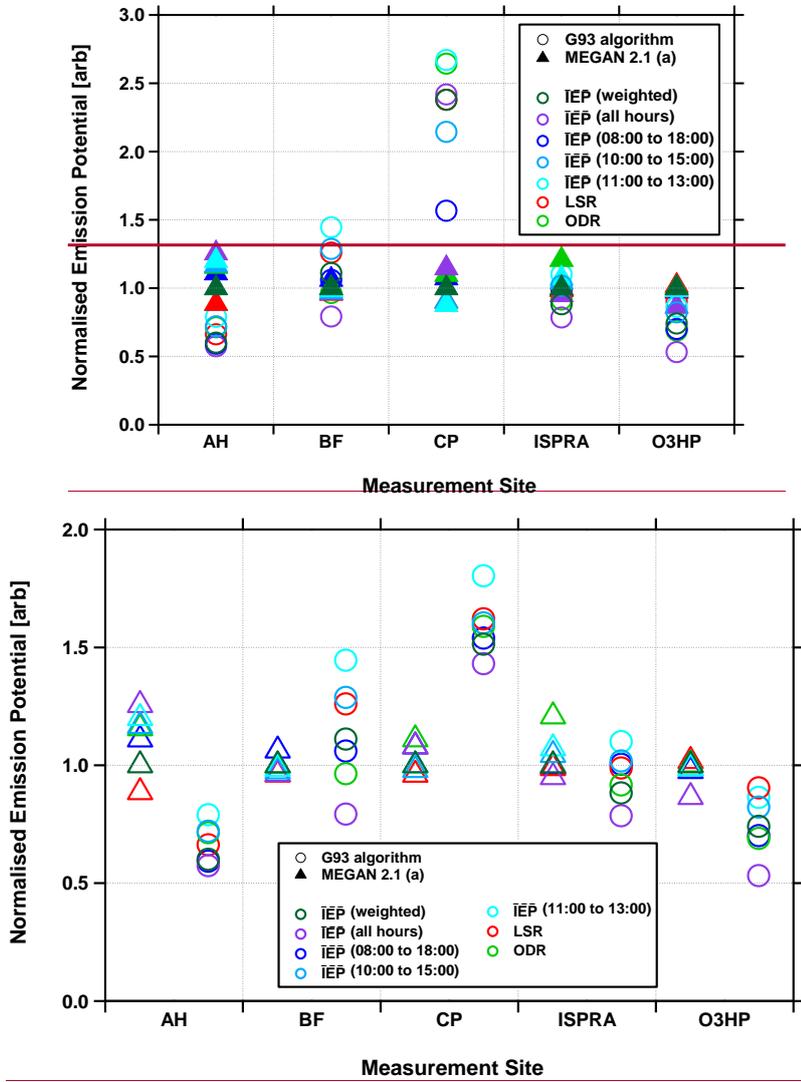
Figure 3 ~~Normalised~~ ~~I~~isoprene emission potentials (normalised to the MEGAN2.1 weighted average emission potential) calculated ~~calculated~~ for Alice Holt (AH), Bosco Fontana (BF), Ispra forest (ISPRA) and the Observatoire de Haute Provence (O3HP). Open circles show emission potentials calculated using the G93 algorithm and closed triangles show emission potentials calculated using the MEGAN model with method (a). For each algorithm, several different approaches were used to work back to an emission potential.
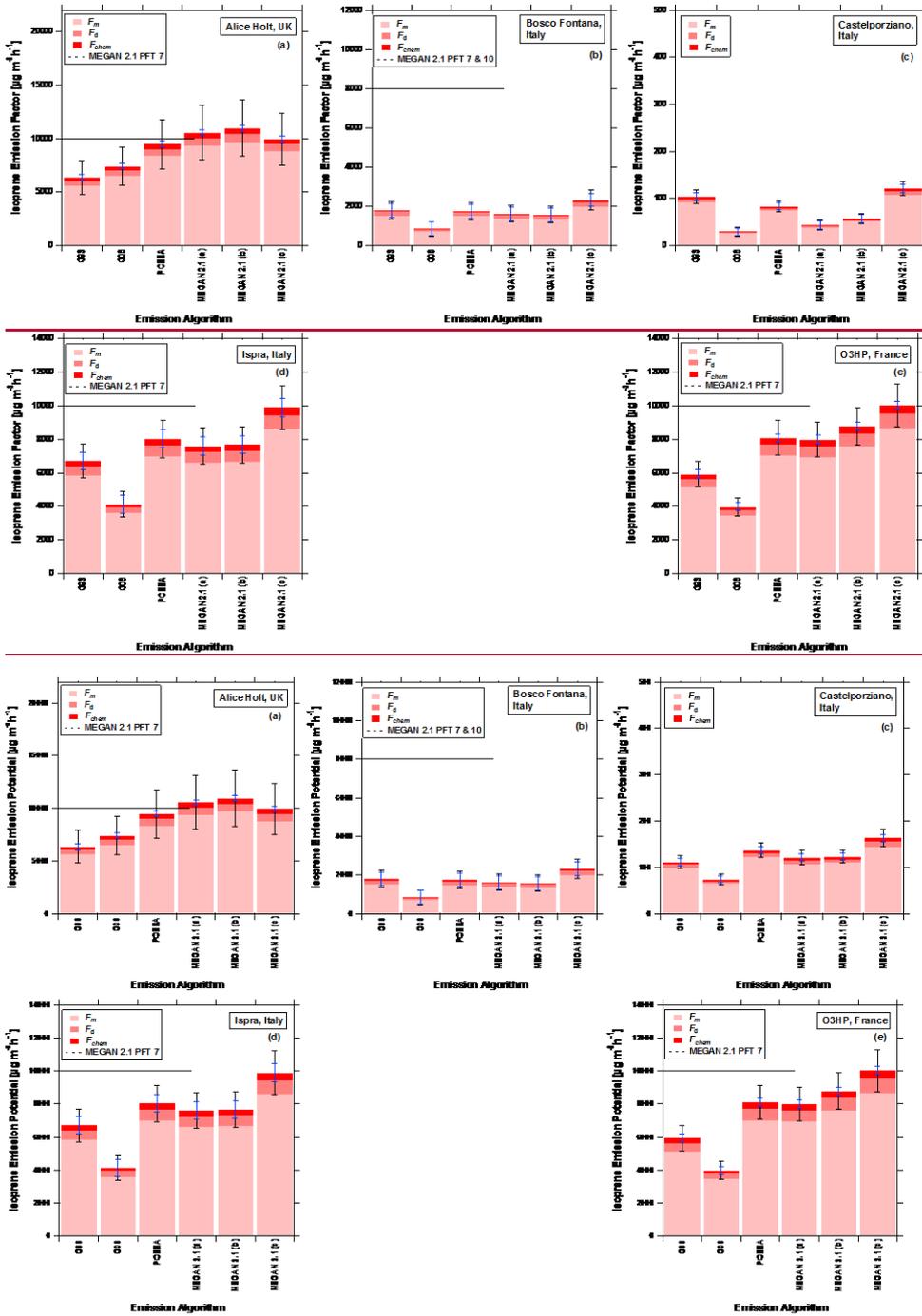
Figure 4. Graduated bars representing the ecosystem specific isoprene emission potentials (ε_{eco}) at each of the five measurement sites. Each bar shows (i) the calculated emission potential based on measured fluxes (F_m), (ii) the correction applied for dry deposition (F_d) and (iii) the correction applied for chemical flux divergence (F_{chem}). For each site emission potentials were calculated using six implementations of the Guenther algorithms (see Section 2.2 for details) and are shown relative to the relevant plant functional type emission potential in MEGAN 2.1 (black line). Note that for the Castelporziano site this value is at 1,839 ug m^{-2} h^{-1} and is off scale. The blue error bars show the uncertainty in the emission potential that relates to the random error in the observed flux measurements. The black error bars show the total uncertainty (random and systematic errors). MEGAN 2.1 (a) is the full implementation of the model using calculated leaf temperature. MEGAN 2.1 (b) is the full implementation of the model using air temperature. MEGAN 2.1 (c) is a version of the model where only the effects of current environmental conditions (e.g. light and air temperature) are used.

Formatted: Font: Italic, Subscript

37

Figure 5 Graduated bars representing an oak specific isoprene emission potentials (ε_{can}) at each of the five measurement sites. Each bar shows (i) the calculated emission potential based on measured fluxes (F_m), (ii) the correction applied for dry deposition (F_d) and (iii) the correction applied for chemical flux divergence (F_{chem}). For each site emission potentials were calculated using six implementations of the Guenther algorithms (see Section 2.2 for details) and are shown relative to the relevant plant functional type emission potential in MEGAN 2.1 (black line). The red error bars show the uncertainty in the emission potential that relates to the random error in the observed flux measurements. The black error bars show the total uncertainty (random and systematic errors). MEGAN 2.1 (a) is the full implementation of the model using calculated leaf temperature. MEGAN 2.1 (b) is the full implementation of the model using air temperature. MEGAN 2.1 (c) is a version of the model where only the effects of current environmental conditions (e.g. light and air temperature) are used.
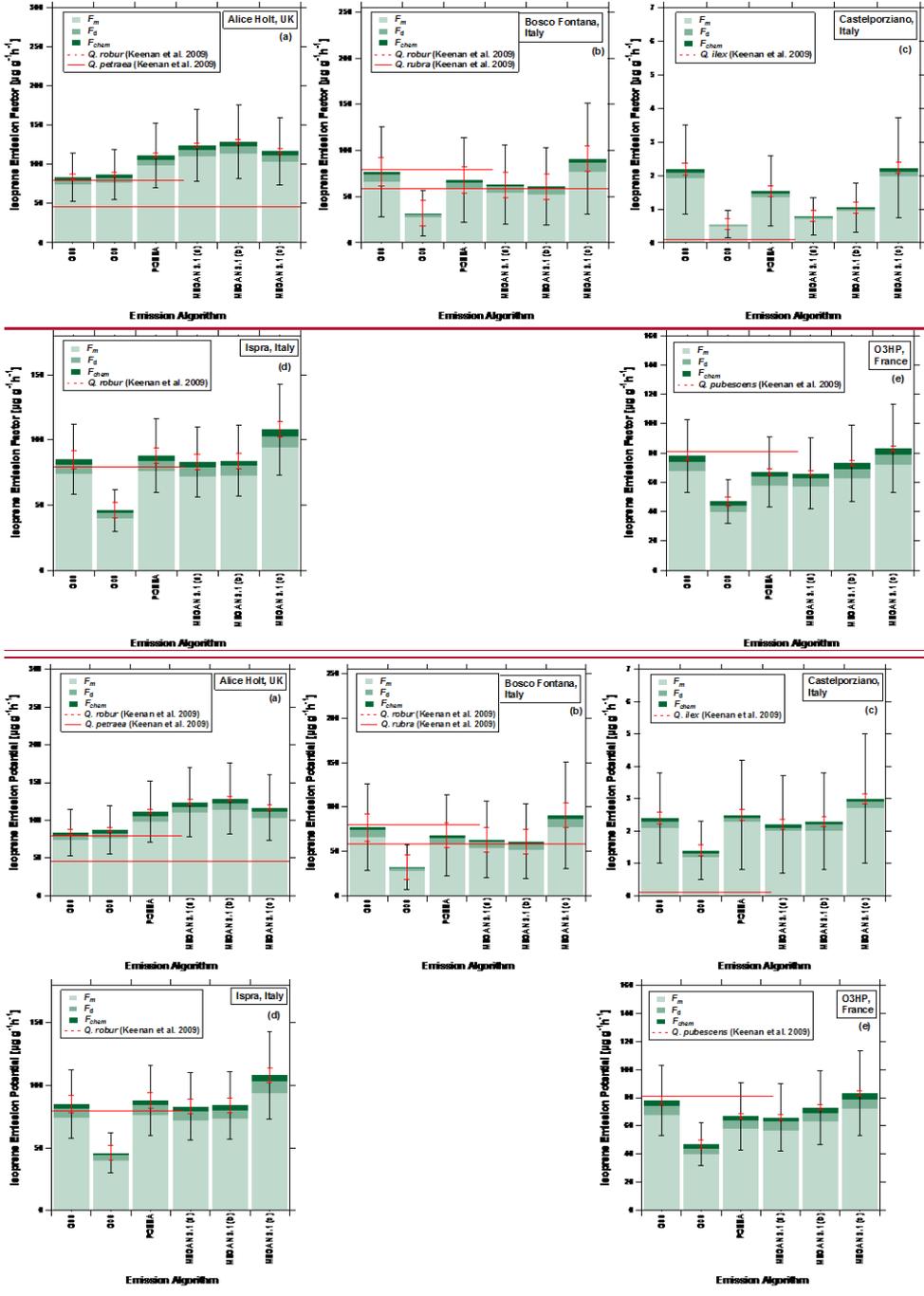
Figure 6. Graduated bars representing leaf-level equivalent isoprene emission potentials (ε_{LL}) at each of the five measurement sites. Each bar shows (i) the calculated emission potential based upon measured fluxes (F_m), (ii) the correction applied for dry deposition (F_d) and (iii) the correction applied for chemical flux divergence (F_{chem}). For each site emission potentials were calculated using six implementations of the Guenther algorithms (see Section 2.2 for details) and are shown relative to the leaf-level emission potentials reported by Keenan et al. (2009) (red line). The red error bars show the uncertainty in the emission potential that relates to the random error in the observed flux measurements. The black error bars show the total uncertainty (random and systematic errors). MEGAN 2.1 (a) is the full implementation of the model using calculated leaf temperature. MEGAN 2.1 (b) is the full implementation of the model using air temperature. MEGAN 2.1 (c) is a version of the model where only the effects of current environmental conditions (e.g. light and air temperature) are used. All algorithms have been optimised to equal unity at 1000 µmol m^{-2} s^{-1} of PAR and 303 K.

41
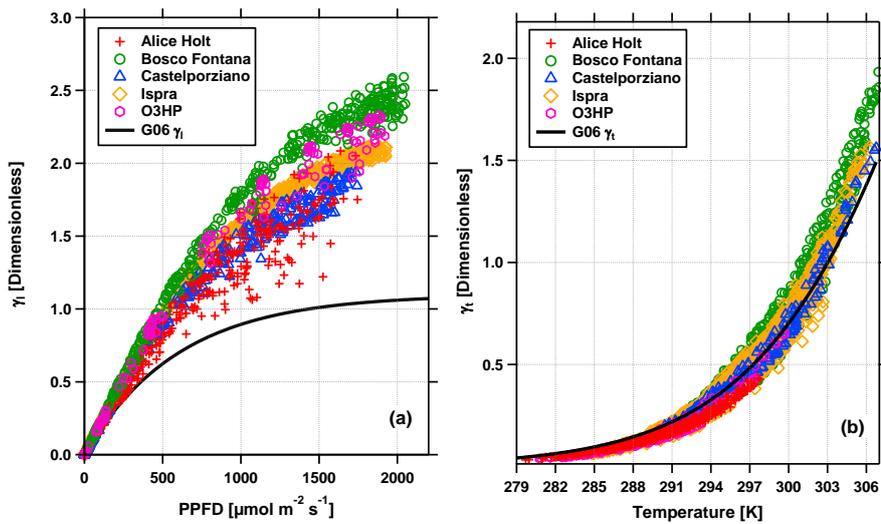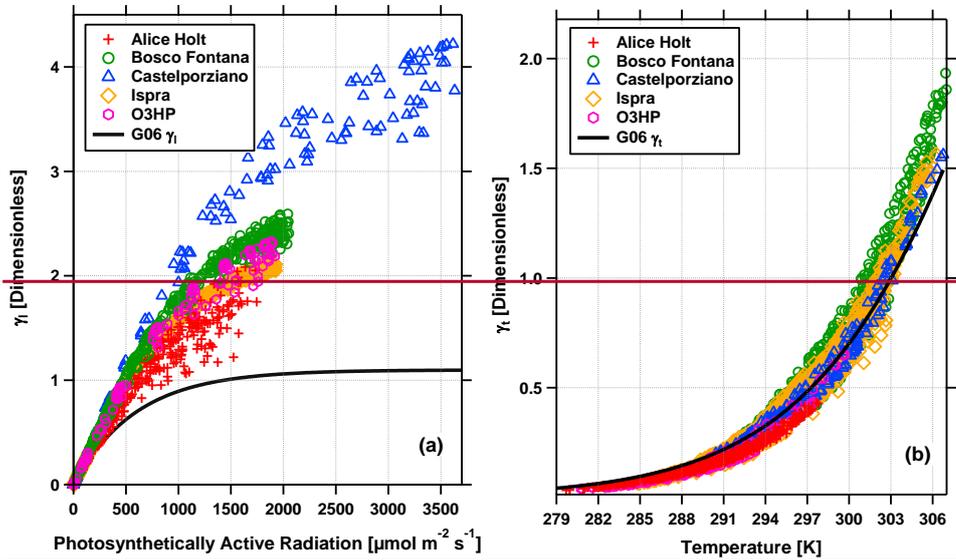
Figure 7. Light (a) and temperature (b) response curves from the G06 algorithm (see text for details) for the five measurement sites. The solid black lines show the light and temperature response curves when the previous light and temperature are held at standard conditions (200 μmol m^{-2} s^{-1} and 297 K for the previous 24 and 240 hours of light and temperature, respectively).

5

10

43

Isoprene emission potentials from European oak forests derived from canopy flux measurements: An assessment of uncertainties and inter-algorithm variability

Ben Langford[1], James Cash[1, 2], W. Joe F. Acton[3], Amy C. Valach[3*], C. Nicholas Hewitt[3], Silvano Fares[4], Ignacio Goded[5], Carsten Gruening[5], Emily House[1, 2, 3], Athina-Cerise Kalogridis[6**], Valérie Gros[6], Richard Schafers[1,2], Rick Thomas[7], Mark Broadmeadow[8] and Eiko Nemitz[1]

[1] Centre for Ecology & Hydrology, Edinburgh, EH26 0QB, U.K.
[2] School of Chemistry, University of Edinburgh, West Mains Road, Edinburgh, EH9 3JJ, U.K.
[3] Lancaster Environment Centre, Lancaster University, Lancaster, LA1 4YQ, U.K.
[4] Council for Agricultural Research and Economics - Research Centre for Forestry and Wood (CREA-FL), Arezzo, Italy
[5] European Commission, Joint Research Centre, Ispra, Italy
[6] Laboratoire des Sciences du Climat et de l'Environnement (LSCE-IPSL), Unite Mixte CEA-CNRS-UVSQ (Commissariat a l'Energie Atomique, Centre National de la Recherche Scientifique, Universite de Versailles Saint-Quentin-en-Yvelines), 91198 Gif-sur-Yvette, France
[7] School of Geography, Earth and Environmental Sciences, University of Birmingham, Edgbaston, Birmingham, B15 2TT

[8] Forestry Commission, Alice Holt Lodge, Farnham, Surrey, GU10 4LH, UK

* now at: British Antarctic Survey, Cambridge, UK
** now at N.C.S.R. "Demokritos", Institute of Nuclear and Radiological Sciences & Technology, Energy & Safety, 15341 Agia Paraskevi, Attiki, Greece

Correspondence to: Ben Langford (benngf@ceh.ac.uk)

Supplementary Information

S1.1 Alice Holt – Measurement setup

Above canopy-isoprene flux measurements at the Alice Holt forest site were made by combining fast measurements of isoprene made using a proton transfer reaction mass spectrometer (PTR-MS, Ionicon Analytik GmbH, Innsbruck, Austria), with measurements of the vertical wind velocity, made using a Gill Solent (R1012A) ultrasonic anemometer mounted atop a 25 m tall lattice tower at a height of 28.5 m. The PTR-MS was housed in a small container at the base of the tower and subsampled air from a 30 m PTFE tube (1/2" OD, 3/8" ID) which drew air from directly below the anemometer at a rate of 60 L min^{-1} to ensure turbulent flow was achieved.

1

The PTR-MS operating conditions were held constant throughout the measurement period to ensure the reduced electric field strength (E/N, where E is the electric field strength and N is the buffer gas density) was maintained at 127 Td. The drift tube pressure, temperature and voltage were set to 2.01 mbar, 45 °C and 550 V respectively. When operating in flux mode the PTR-MS sequentially measured eight mass to charge ratios including the isotope of the primary ion (m/z 21) and first water cluster (m/z 37) which were both sampled at a rate 20 ms and m/z 33, 45, 47, 59, 61, 69 and 71 which were all sampled at 50 ms. These dwell times are much shorter than is typical when measuring VOC fluxes by PTR-MS resulting in a lower signal-to-noise ratio than might be typical. This is because this campaign represented the first deployment of our flux system and therefore the optimal settings had not yet been determined. Here we only focus on the measurements of m/z 69 which we attribute entirely to isoprene. Typically the ion counts reported by the PTR-MS are converted to a meaningful concentration by first calculating the instrument sensitivity to a specific compound determined by sampling from a gas standard. During the Alice Holt campaign no gas standard was available. Consequently, the recorded ion counts of isoprene per second ($I(RH^+)$) were converted to a measurement of isoprene concentration in units of parts per billion as follows

$$[R] = \frac{1}{k\Delta t}\frac{I(RH^+)}{T(RH^+)}\left(\frac{I(H_3O^+)}{T(H_3O^+)}\right)^{-1},\tag{1}$$

where $I(RH^+)$ and $I(H_3O^+)$ are the isoprene and primary ion counts, respectively, k is the reaction rate constant taken from Zhao and Zhang (2004) which was modified to account for the typical fragmentation of isoprene to m/z 41 under the reported operating conditions and Δt is the reaction term which is dependent upon the length of the reaction chamber. $T(RH^+)$ and $T(H_3O^+)$ are the instrument specific transmission efficiencies for isoprene and the primary ions. The transmission efficiencies were determined experimentally at the end of the measurement campaign. According to Taipale et al., (2008) the use of transmission efficiencies rather than instrument sensitivities calculated using gas standards can result in uncertainties of ~25%. The instrument background was measured once per day by sampling ambient air through a Pt/Al$_2$O$_3$ catalyst heated to 200 ºC and these values were subtracted from the ambient concentration measurements. Fluxes of isoprene were calculated following the procedures outlined by Langford et al. (2009). A cross-correlation between the vertical wind velocity and isoprene concentration was calculated for each averaging period to determine the time-lag between the two datasets which arises due to the spatial separation between ultrasonic anemometer and PTR-MS. Due to the low signal-to-noise ratio of the raw isoprene data (<10), the Following the recommendations of Langford et al. (2015) were followed to avoid systematic bias in the reported fluxes which involved the use of we calculated a prescribed time-lag which changed each day to reflect the average day-time (11:00 to 14:00) time-lag of that day.

S1.2   Ispra – Measurement setup

Isoprene flux measurements were made from June 11 to August 12, 2013 at the Ispra firest field station. The forest is further characterized with a different focus in Ferrea et al. (2012). More technical information on the general setup of the Ispra forest station can be found in Putaud et al. (2014).

For the turbulent flux measurements of isoprene, 10 Hz measurement data from a sonic anemometer (Gill, HS-100) were combined with 10 Hz concentration data from a fast isoprene sensor (FIS, Hills Scientific) mounted aloft a 37 m measurement tower . For the latter, air was drawn into a sampling line located 30 cm away from the sonic anemometer and carried at a flow rate of 25 slpm through a Teflon tube with 6 mm inner diameter to the FIS located inside an air conditioned container on the ground.

The FIS measurements are based on the detection of chemiluminescence occurring during the reaction of isoprene with ozone. Ambient air with a flow rate of 4-5 slpm and a 4 % mixture of ozone at 0.8 slpm in O$_2$ from an ozoniser (Hills Scientific) are mixed inside the reaction cell of the instrument. Following the reaction of isoprene with ozone, light is emitted at a characteristic wavelength and detected using single-photon counting at near-zero background. Instrument calibration to obtain

2

isoprene concentrations was done using zero air from a gas cylinder and air with certified isoprene concentrations on a weekly basis confirming practically no drift of the zero signal and little variation in the span during the measurement campaign.

The covariances between the high frequency wind data and isoprene concentration data were calculated using the EdiRe software package (University of Edinburgh). The median time lag between vertical wind speed and concentration measurements was 4.7 s with little fluctuation during the measurement campaign. This value was used in the final data processing.

S2.   Isoprene Emission Potentials

Ecosystem (E_{eco}), oak canopy (E_{can}) and leaf-level (E_{LL}) equivalent isoprene emission potentials (IEPs) and uncertainties for each of the five measurement sites are listed below. The IEPs were calculated using the six different implementations of the Guenther algorithm described in the manuscript. In each case the final IEP was determined using the weighted average IEP method.

S2.1   Alice Holt

Emission factors derived for Alice Holt are summarised in Tables S1 to S3.

Table S1 Ecosystem-Scale isoprene emission potentials at Alice Holt

Algorithm	E_{eco}	E_{eco+Fd}	$E_{eco+Fd+chem}$
G93	5613	6045	6347±1552
G06	6542	7046	7398±1802
PCEEA	8368	9013	9464±2296
MEGAN 2.1 (a)	9333	10052	10555±2557
MEGAN 2.1 (b)	9686	10433	10955±2653
MEGAN 2.1 (c)	8781	9458	9931±2424

Table S2 Oak canopy isoprene emission potentials at Alice Holt

Algorithm	E_{can}	E_{can+Fd}	$E_{can+Fd+chem}$
G93	6237	6717	7053±2154
G06	7269	7829	8220±2505
PCEEA	9298	10014	10515±3196
MEGAN 2.1 (a)	10370	11169	11727±3562
MEGAN 2.1 (b)	10762	11592	12172±3695
MEGAN 2.1 (c)	9757	10509	11034±3352

Table S3 Leaf-level equivalent isoprene emission potentials at Alice Holt

Algorithm	E_{LL}	E_{LL+Fd}	$E_{LL+Fd+chem}$
G93	74	80	84±31
G06	77	8̶83	87±32
PCEEA	98	106	111±41
MEGAN 2.1 (a)	110	118	124±46
MEGAN 2.1 (b)	114	123	129±47
MEGAN 2.1 (c)	103	111	117±43

S2.1   Bosco Fontana

Emission factors derived for Bosco Fontana are summarised in Tables S4 to S6.

Table S4 Ecosystem-Scale isoprene emission potentials at Bosco Fontana

Algorithm	E_{eco}	E_{eco+Fd}	$E_{eco+Fd+chem}$
G93	1529	1722	1791±440
G06	720	810	843±375
PCEEA	1488	1675	1742±441
MEGAN 2.1 (a)	1376	1550	1612±428
MEGAN 2.1 (b)	1338	1507	1578±424
MEGAN 2.1 (c)	1980	2230	2319±493

Table S5 Oak canopy isoprene emission potentials at Bosco Fontana

Algorithm	E_{can}	E_{can+Fd}	$E_{can+Fd+chem}$
G93	5663	6378	6633±4002
G06	2667	3000	3120±2212
PCEEA	5511	6204	6452±3906
MEGAN 2.1 (a)	5096	5741	5970±3648
MEGAN 2.1 (b)	4956	5581	5805±3560
MEGAN 2.1 (c)	7333	8259	8590±5069

Table S6 Leaf-level equivalent isoprene emission potentials at Bosco Fontana

Algorithm	E_{LL}	E_{LL+Fd}	$E_{LL+Fd+chem}$
G93	66	74	77±49
G06	28	31	32±25
PCEEA	58	65	68±46
MEGAN 2.1 (a)	54	61	63±43
MEGAN 2.1 (b)	52	59	61±42
MEGAN 2.1 (c)	77	87	91±60

5

S2.3   Castelporziano

Emission factors derived for Bosco Fontana are summarised in Tables S7 to S9.

Table S7 Ecosystem-Scale isoprene emission potentials at Castelporziano

Algorithm	E_{eco}	E_{eco+Fd}	$E_{eco+Fd+chem}$
G93	~~91~~99	~~98~~106	~~103~~111±14
G06	~~26~~66	~~28~~70	~~29~~74±9~~11~~
PCEEA	~~74~~122	~~79~~130	~~83~~137±12~~16~~
MEGAN 2.1 (a)	~~38~~107	~~41~~115	~~43~~121±10~~15~~
MEGAN 2.1 (b)	~~51~~110	~~54~~117	~~57~~123±10~~14~~
MEGAN 2.1 (c)	~~107~~144	~~115~~155	~~121~~163±15~~19~~

10   **Table S8 Oak canopy isoprene emission potentials at Castelporziano**

Algorithm	E_{can}	E_{can+Fd}	$E_{can+Fd+chem}$
G93	~~331~~360	~~356~~385	~~374~~405±214~~232~~
G06	~~95~~240	~~102~~255	~~107~~267±68~~156~~
PCEEA	~~269~~444	~~287~~473	~~302~~496±175~~285~~
MEGAN 2.1 (a)	~~138~~389	~~149~~418	~~157~~439±94~~251~~
MEGAN 2.1 (b)	~~185~~400	~~196~~425	~~206~~447±122~~257~~
MEGAN 2.1 (c)	~~389~~524	~~418~~564	~~439~~592±251~~337~~

Table S9 Leaf-level equivalent isoprene emission potentials at Castelporziano

Algorithm	E_{LL}	E_{LL+Fd}	$E_{LL+Fd+chem}$
G93	~~1.9~~2.1	2.~~1~~3	~~2.2~~2.4±~~1.3~~1.4
G06	~~0.5~~1.2	~~0.5~~1.3	~~0.6~~1.4±~~0.4~~0.9
PCEEA	~~1.4~~2.3	~~1.5~~2.4	~~1.5~~2.5±~~1~~1.7
MEGAN 2.1 (a)	~~0.7~~2.0	~~0.8~~2.1	~~0.8~~2.2±~~0.6~~1.5
MEGAN 2.1 (b)	~~0.9~~2.0	~~1.0~~2.2	~~1.0~~2.3±~~0.7~~1.5

4

MEGAN 2.1 (c)	2.~~07~~	2.~~19~~	~~2.23.0±1.5~~2.0

S2.4   Ispra

Emission factors derived for Ispra are summarised in Tables S10 to S12.

Table S10 Ecosystem-Scale isoprene emission potentials at Ispra

Algorithm	E_{eco}	E_{eco+Fd}	$E_{eco+Fd+chem}$
G93	5824	6385	6704±983
G06	3591	3937	4133±748
PCEEA	6975	7646	8029±1120
MEGAN 2.1 (a)	6599	7234	7596±1074
MEGAN 2.1 (b)	6670	7312	7678±1082
MEGAN 2.1 (c)	8598	9426	9897±1321

5

Table S11 Oak canopy isoprene emission potentials at Ispra

Algorithm	E_{can}	E_{can+Fd}	$E_{can+Fd+chem}$
G93	7281	7981	8380±2073
G06	4489	4921	5167±1391
PCEEA	8719	9558	10036±2443
MEGAN 2.1 (a)	8249	9042	9495±2321
MEGAN 2.1 (b)	8338	9140	9597±2344
MEGAN 2.1 (c)	10748	11782	12371±2969

Table S12 Leaf-level equivalent isoprene emission potentials at Ispra

Algorithm	E_{LL}	E_{LL+Fd}	$E_{LL+Fd+chem}$
G93	74	81	85±27
G06	40	44	46±16
PCEEA	76	84	88±28
MEGAN 2.1 (a)	72	79	83±27
MEGAN 2.1 (b)	73	80	84±27
MEGAN 2.1 (c)	94	103	108±35

10

S2.4   O3HP

Emission factors derived for O3HP are summarised in Tables S13 to S15.

Table S13 Ecosystem-Scale isoprene emission potentials at O3HP

Algorithm	E_{eco}	E_{eco+Fd}	$E_{eco+Fd+chem}$
G93	5135	5642	5924±771
G06	3439	3779	3967±551
PCEEA	7018	7710	8096±1026
MEGAN 2.1 (a)	6926	7610	7990±1014
MEGAN 2.1 (b)	7606	8357	8775±1107
MEGAN 2.1 (c)	8684	9541	10018±1255

15   **Table S14 Oak canopy isoprene emission potentials at O3HP**

Algorithm	E_{can}	E_{can+Fd}	$E_{can+Fd+chem}$
G93	6847	7523	7899±1945
G06	4586	5038	5290±1328
PCEEA	9357	10280	10794±2639
MEGAN 2.1 (a)	9235	10146	10654±2605
MEGAN 2.1 (b)	10142	11142	11699±2857
MEGAN 2.1 (c)	11579	12721	13357±3256

Table S15 Leaf-level equivalent isoprene emission potentials at O3HP

Algorithm	E_{LL}	E_{LL+Fd}	$E_{LL+Fd+chem}$
G93	68	74	78±25
G06	40	44	47±15
PCEEA	58	64	67±24
MEGAN 2.1 (a)	57	63	66±24
MEGAN 2.1 (b)	63	69	73±26
MEGAN 2.1 (c)	72	79	83±29

5 **S3   Comparison of isoprene emission potentials**

Tables S16 to S25 show a comparison of IEPs calculated at each of the five measurement sites using seven different methods to derive the average isoprene emission potential. All emission potentials shown have been corrected for deposition and chemical losses. The data in these tables forms the basis of Fig. 3 in the main manuscript.

10

S3.1   Alice Holt, UK

Table S16 Comparison of isoprene emission potentials calculated using the MEGAN 2.1 (a) emission algorithm for Alice Holt in conjunction with the least square regression, orthogonal distance regression, weighted average and several variations of the midday
15 **average methods.**

	Fluxes	$\overline{IEP}$ (weighted)	$\overline{IEP}$ (all hours)	$\overline{IEP}$ (08 to 18)	$\overline{IEP}$ (10 to 15)	$\overline{IEP}$ (11 to 13)	LSR	ODR
IEP [µg m⁻² h⁻¹]	-	10555	13251	11712	12316	12671	9349	12217
Mean [µg m⁻² h⁻¹]	779	779	978	864	909	935	690	902
σ [µg m⁻² h⁻¹]	1066	**1097**	1378	1218	1281	1317	972	1270
r²	-	0.54	0.54	0.54	0.54	0.54	0.54	0.54
M score	-	1.37	1.34	1.31	1.31	1.32	1.53	**1.31**
Relative Bias [%]	-	**0**	26	11	17	20	-11	16

Table S17 Comparison of isoprene emission potentials calculated using the G93 emission algorithm for Alice Holt in conjunction with the least square regression, orthogonal distance regression, weighted average and several variations of the midday average
20 **methods.**

	Fluxes	$\overline{IEP}$ (weighted)	$\overline{IEP}$ (all hours)	$\overline{IEP}$ (08 to 18)	$\overline{IEP}$ (10 to 15)	$\overline{IEP}$ (11 to 13)	LSR	ODR
IEP [µg m⁻² h⁻¹]	-	6348	6062	6261	7607	8344	6995	7538
Mean [µg m⁻² h⁻¹]	779	779	744	768	933	1024	858	925
σ [µg m⁻² h⁻¹]	1327	915	874	902	1096	**1203**	1008	1086
r²	0.58	0.58	0.58	0.58	0.58	0.58	0.58	0.58
M score	-	1.239	1.315	1.260	1.065	**1.054**	1.121	1.069
Relative Bias [%]	-	**0**	-4	-1	20	31	10	19

S3.2   Bosco Fontana, Italy

6

Table S18 Comparison of isoprene emission potentials calculated using the MEGAN 2.1 (a) emission algorithm for Bosco Fontana in conjunction with the least square regression, orthogonal distance regression, weighted average and several variations of the midday average methods.

	Fluxes	$\overline{IEP}$ (weighted)	$\overline{IEP}$ (all hours)	$\overline{IEP}$ (08 to 18)	$\overline{IEP}$ (10 to 15)	$\overline{IEP}$ (11 to 13)	LSR	ODR
IEP [µg m^{-2} h^{-1}]	-	1550	1493	1647	1509	1527	1489	1547
Mean [µg m^{-2} h^{-1}]	862	862	830	916	839	849	828	860
σ [µg m^{-2} h^{-1}]	1113	1053	1015	1119	1026	1038	**1012**	1052
r^2	-	0.79	0.79	0.79	0.79	0.79	0.79	0.79
M score	-	0.347	0.356	0.347	0.353	**0.350**	0.357	0.347
Relative Bias [%]	-	**0**	-4	6	-3	-1	-4	0

Table S19 Comparison of isoprene emission potentials calculated using the G93 emission algorithm for Bosco Fontana in conjunction with the least square regression, orthogonal distance regression, weighted average and several variations of the midday average methods.

	Fluxes	$\overline{IEP}$ (weighted)	$\overline{IEP}$ (all hours)	$\overline{IEP}$ (08 to 18)	$\overline{IEP}$ (10 to 15)	$\overline{IEP}$ (11 to 13)	LSR	ODR
IEP [µg m^{-2} h^{-1}]	-	1722	1229	1643	1996	2240	1953	1495
Mean [µg m^{-2} h^{-1}]	862	862	615	822	999	1121	977	748
σ [µg m^{-2} h^{-1}]	1113	854	609	815	990	**1111**	968	741
r^2	-	0.75	0.75	0.75	0.75	0.75	0.75	0.75
M score	-	0.66	1.17	0.70	**0.59**	0.61	0.60	0.81
Relative Bias [%]	-	**0**	-29	-5	16	30	13	-13

S3.3   Castelporziano, Italy

Table S20 Comparison of isoprene emission potentials calculated using the MEGAN 2.1 (a) emission algorithm for Castelporziano in conjunction with the least square regression, orthogonal distance regression, weighted average and several variations of the midday average methods.

	Fluxes	$\overline{IEP}$ (weighted)	$\overline{IEP}$ (all hours)	$\overline{IEP}$ (08 to 18)	$\overline{IEP}$ (10 to 15)	$\overline{IEP}$ (11 to 13)	LSR	ODR
IEP [µg m^{-2} h^{-1}]	-	4374	4980	4680	3972	3874	3971	4782
Mean [µg m^{-2} h^{-1}]	44	44	5048	4748	4044	3944	4043	4949
σ [µg m^{-2} h^{-1}]	70	6157	6961	6561	5556	5456	5554	6763
r^2	-	0.5554	0.5554	0.5554	0.5554	0.5554	0.5554	0.5554
M score	-	1.265	1.19	1.201.19	1.381.28	1.421.28	1.381.31	1.201.18
Relative Bias [%]	-	**0**	148	78	-102	-120	-10-4	1011

Table S21 Comparison of isoprene emission potentials calculated using the G93 emission algorithm for Castelporziano in conjunction with the least square regression, orthogonal distance regression, weighted average and several variations of the midday average methods.

	Fluxes	$\overline{IEP}$ (weighted)	$\overline{IEP}$ (all hours)	$\overline{IEP}$ (08 to 18)	$\overline{IEP}$ (10 to 15)	$\overline{IEP}$ (11 to 13)	LSR	ODR

IEP [µg m⁻² h⁻¹]	-	103112	67105	11392	118114	13327	1193	11704
Mean [µg m⁻² h⁻¹]	44	44	4229	4540	4749	536	489	4745
σ [µg m⁻² h⁻¹]	70	4548	4529	4941	5150	577	510	5046
r²	-	0.4749	0.497	0.490.47	0.4947	0.497	0.497	0.497
M score	-	1.4841	1.512.72	1.3969	1.332	**1.224**	1.303	1.3445
Relative Bias [%]	-	**0**	-534	2-10	612	1924	711	52

S3.4   Ispra, Italy

Table S22 Comparison of isoprene emission potentials calculated using the MEGAN 2.1 (a) emission algorithm for Ispra in conjunction with the least square regression, orthogonal distance regression, weighted average and several variations of the midday average methods.

	Fluxes	*IEP* (weighted)	*IEP* (all hours)	*IEP* (08 to 18)	*IEP* (10 to 15)	*IEP* (11 to 13)	LSR	ODR
IEP [µg m⁻² h⁻¹]	-	7596	7212	7558	7928	8142	7504	9174
Mean [µg m⁻² h⁻¹]	2108	2108	2002	2098	2201	2261	2083	2546
σ [µg m⁻² h⁻¹]	3126	2940	2792	2925	3069	3152	2905	3551
r²	-	0.86	0.86	0.86	0.86	0.86	0.86	0.86
M score	-	0.28	0.32	0.29	**0.27**	**0.27**	0.29	0.31
Relative Bias [%]	-	**0**	-5	0	4	7	-1	21

Table S23 Comparison of isoprene emission potentials calculated using the G93 emission algorithm for Ispra in conjunction with the least square regression, orthogonal distance regression, weighted average and several variations of the midday average methods.

	Fluxes	*IEP* (weighted)	*IEP* (all hours)	*IEP* (08 to 18)	*IEP* (10 to 15)	*IEP* (11 to 13)	LSR	ODR
IEP [µg m⁻² h⁻¹]	-	6703	5969	7629	7733	8359	7512	6966
Mean [µg m⁻² h⁻¹]	2108	2108	1877	2399	2432	2629	2363	2190
σ [µg m⁻² h⁻¹]	3126	2401	2139	2733	2771	2995	2691	2496
r²	-	0.78	0.78	0.78	0.78	0.78	0.78	0.78
M score	-	0.51	0.65	0.44	**0.43**	0.44	0.44	0.48
Relative Bias [%]	-	**0**	-11	14	15	25	12	4

S3.5   O3HP, France

Table S24 Comparison of isoprene emission potentials calculated using the MEGAN 2.1 (a) emission algorithm for O3HP in conjunction with the least square regression, orthogonal distance regression, weighted average and several variations of the midday average methods.

	Fluxes	*IEP* (weighted)	*IEP* (all hours)	*IEP* (08 to 18)	*IEP* (10 to 15)	*IEP* (11 to 13)	LSR	ODR
IEP [µg m⁻² h⁻¹]		7991	6914	7795	7883	7889	8138	8018

Mean [µg m⁻² h⁻¹]	899	899	777	877	886	887	915	902
σ [µg m⁻² h⁻¹]	1371	1279	1107	1247	1262	1262	**1302**	1283
r²	-	0.90	0.90	0.90	0.90	0.90	0.90	0.90
M score	-	0.23	0.34	0.24	0.23	0.23	**0.22**	0.23
Relative Bias [%]	-	**0**	0	-13	-2	-1	0	2

Mean [$\mu g\ m^{-2}\ h^{-1}$]	899	899	777	877	886	887	915	902
σ [$\mu g\ m^{-2}\ h^{-1}$]	1371	1279	1107	1247	1262	1262	**1302**	1283
r^2	-	0.90	0.90	0.90	0.90	0.90	0.90	0.90
M score	-	0.23	0.34	0.24	0.23	0.23	**0.22**	0.23
Relative Bias [%]	-	**0**	0	-13	-2	-1	0	2

Table S25 Comparison of isoprene emission potentials calculated using the G93 emission algorithm for O3HP in conjunction with the least square regression, orthogonal distance regression, weighted average and several variations of the midday average methods.

	Fluxes	*IEP* (weighted)	*IEP* (all hours)	*IEP* (08 to 18)	*IEP* (10 to 15)	*IEP* (11 to 13)	LSR	ODR
IEP [$\mu g\ m^{-2}\ h^{-1}$]		5924	6894	5607	6576	6902	7225	5513
Mean [$\mu g\ m^{-2}\ h^{-1}$]	899	899	1046	851	998	1047	1096	836
σ [$\mu g\ m^{-2}\ h^{-1}$]	1371	1031	1200	977	1145	1201	**1258**	960
r^2	-	0.84	0.84	0.84	0.84	0.84	0.84	0.84
M score	-	0.43	0.34	0.49	0.36	0.34	**0.34**	0.52
Relative Bias [%]	-	**0**	16	-5	11	16	22	-7

5

10

15

20

9

S4 **Emission potential calculation assessment**

Figures S1 to S4 show the average diurnal profile of the isoprene emission potential that have been calculated by inverting the
5 G93 (Panel A) and MEGAN 2.1 (a) (Panel C) emission algorithms. Also shown are the average emission potential assigned to
each site which were calculated using seven different methods (see main text for details).

S4.1 **Alice Holt**
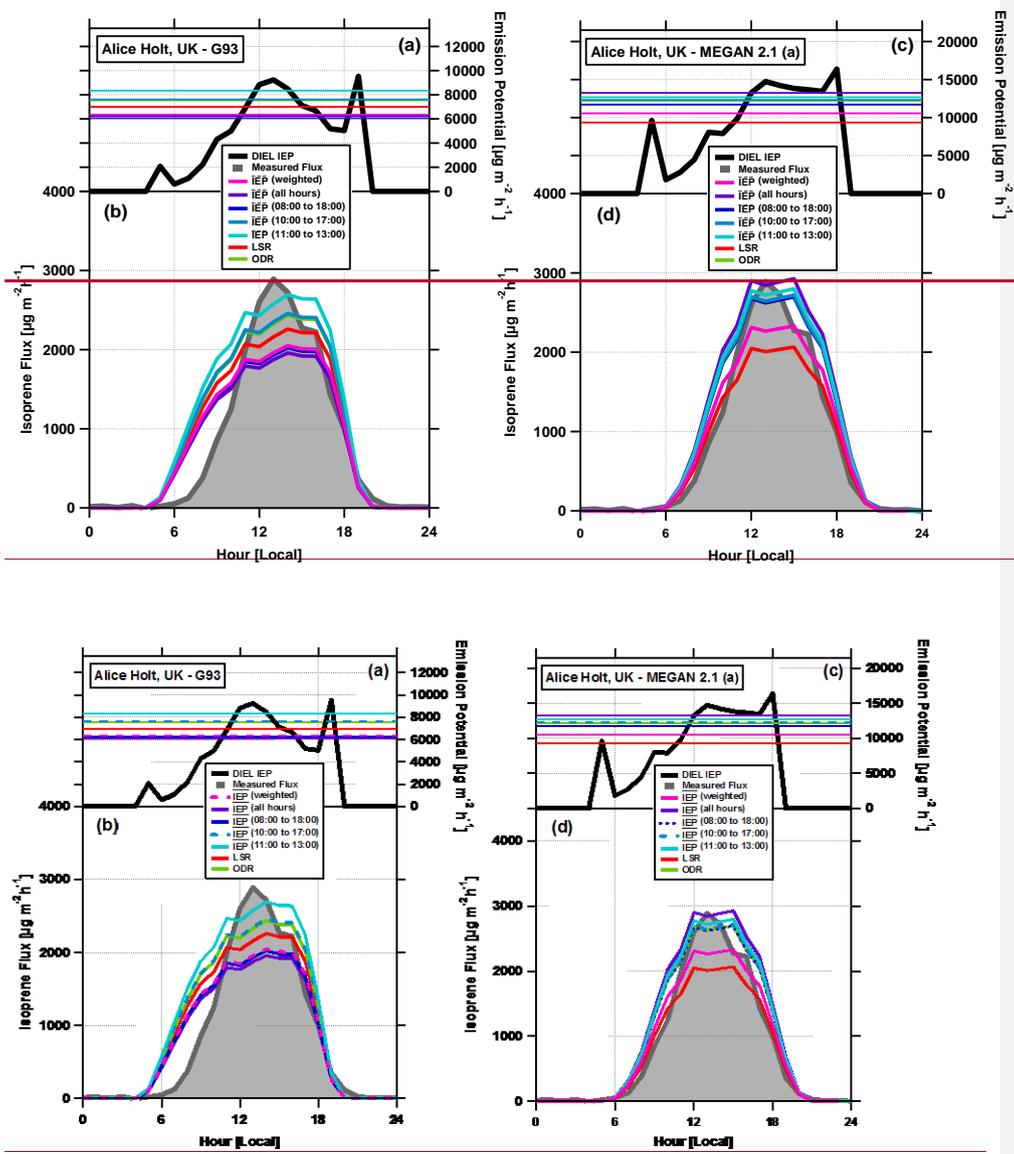
Figure S1 Panels A and C show the average diurnal cycle in the isoprene emission potential (e.g. $IEP = \overline{\left(\frac{F_{iso}}{\gamma}\right)}$**)** **calculated for the Alice Holt site, UK using the G93 (panel A) and MEGAN 2.1 (panel B) algorithms. Superimposed on top of these are the isoprene emission potentials calculated using the least square regression, orthogonal distance regression and average (with several averaging lengths) methods – see text for detailed description. Panels B and D show the average diurnal cycle of the measured fluxes and the average diurnal cycle of the fluxes modelled using the seven different isoprene emission potentials calculated for this data set.**
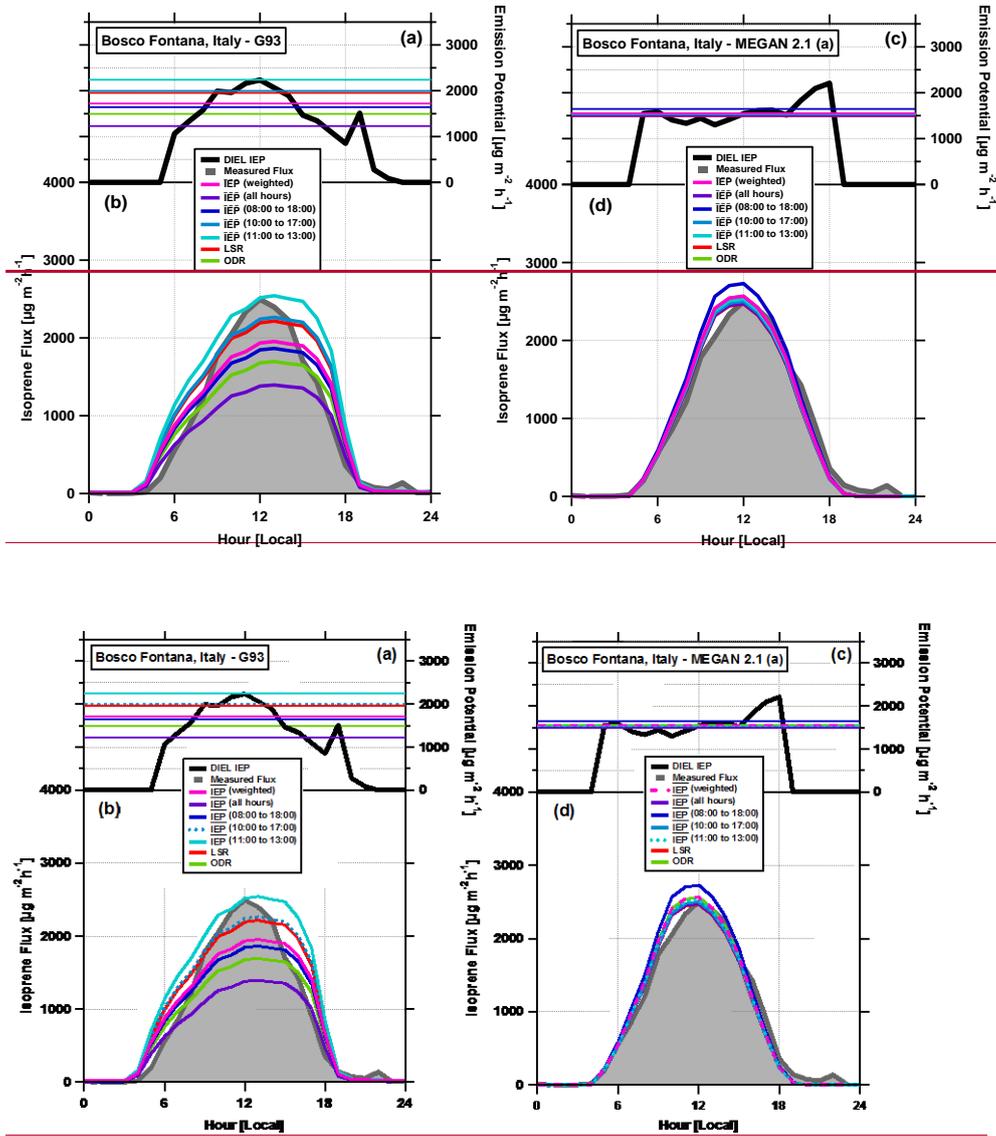
S4.2 Bosco Fontana

Figure S2 Panels A and C show the average diurnal cycle in the isoprene emission potential (e.g. $IEP = \overline{\left(\frac{F_{iso}}{\gamma}\right)}$**) calculated for the Bosco Fontana site, Italy using the G93 (panel A) and MEGAN 2.1 (panel B) algorithms. Superimposed on top of these are the isoprene emission potentials calculated using the least square regression, orthogonal distance regression and average (with several averaging lengths) methods – see text for detailed description. Panels B and D show the average diurnal cycle of the measured fluxes and the average diurnal cycle of the fluxes modelled using the seven different isoprene emission potentials calculated for this data set.**
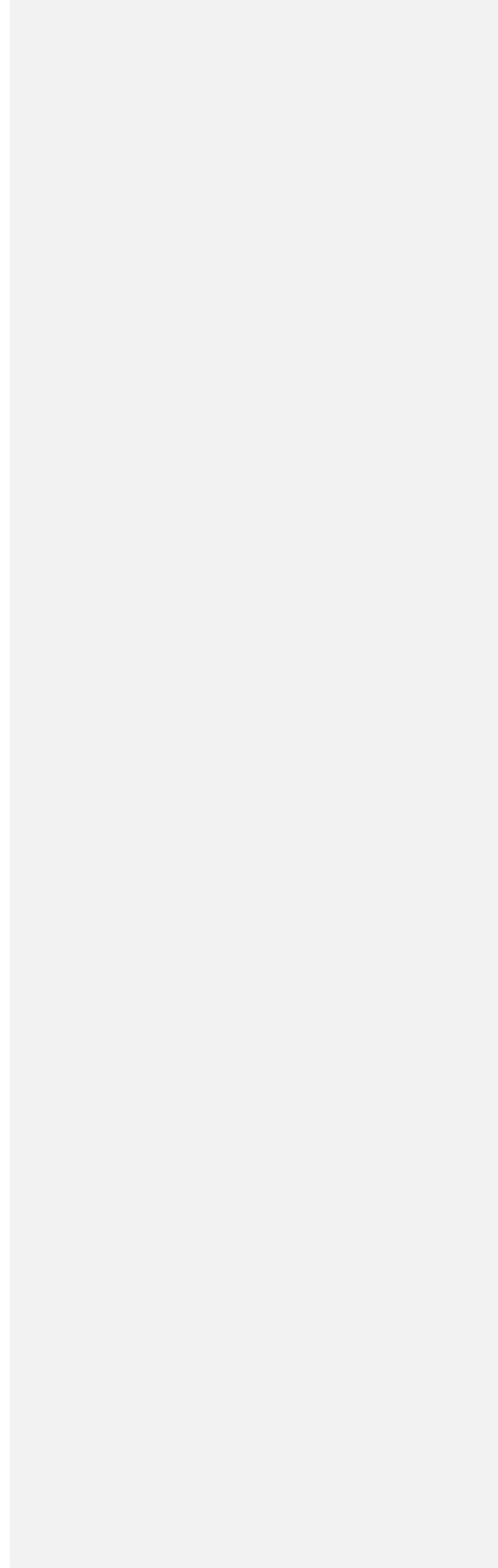
S4.3   Castelporziano
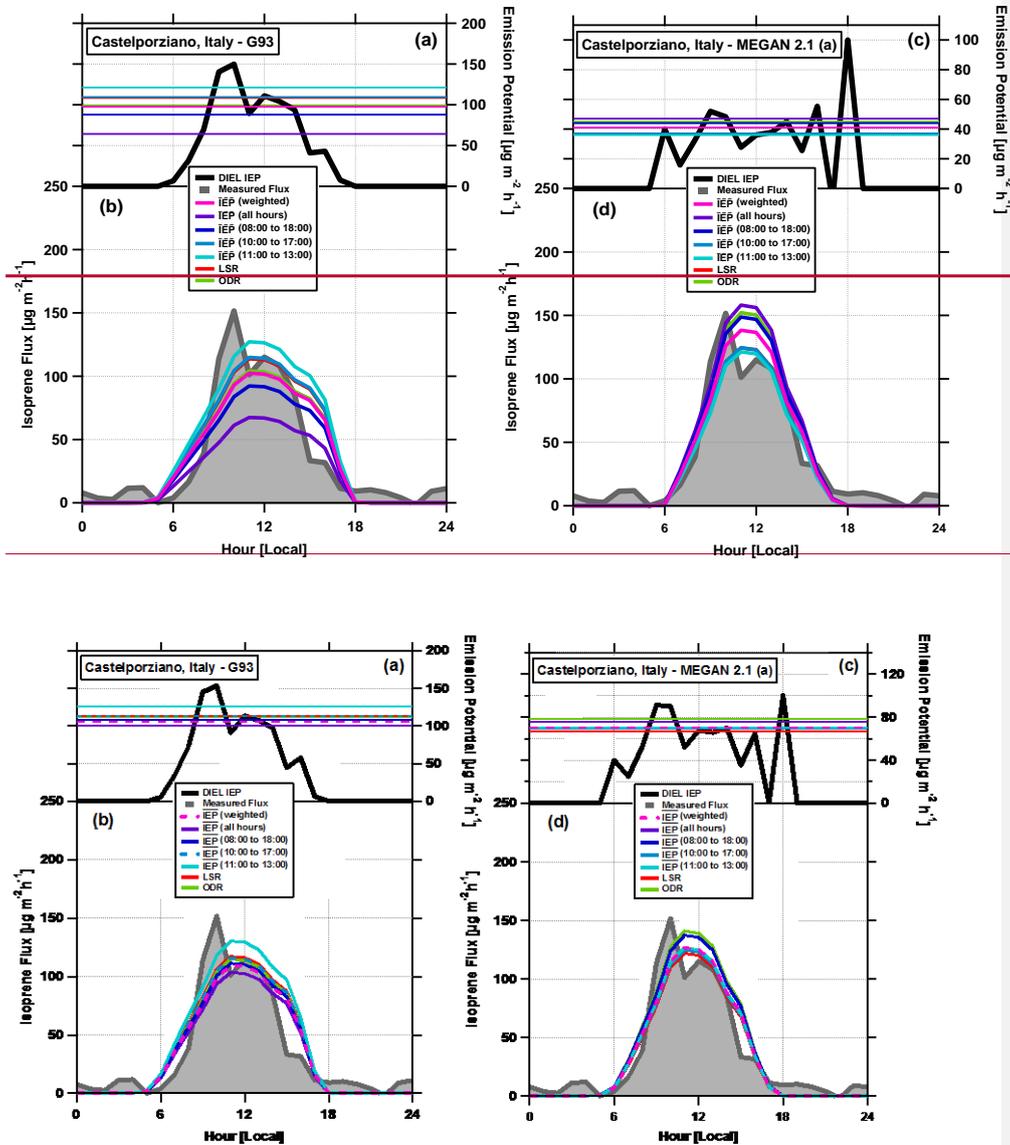
Figure S3 Panels A and C show the average diurnal cycle in the isoprene emission potential (e.g. $IEP = \overline{\left(\frac{F_{iso}}{\gamma}\right)}$)   calculated for the Castelporziano site, Italy using the G93 (panel A) and MEGAN 2.1 (panel B) algorithms. Superimposed on top of these are the isoprene emission potentials calculated using the least square regression, orthogonal distance regression and average (with several averaging lengths) methods – see text for detailed description. Panels B and D show the average diurnal cycle of the measured fluxes and the average diurnal cycle of the fluxes modelled using the seven different isoprene emission potentials calculated for this data set.

14
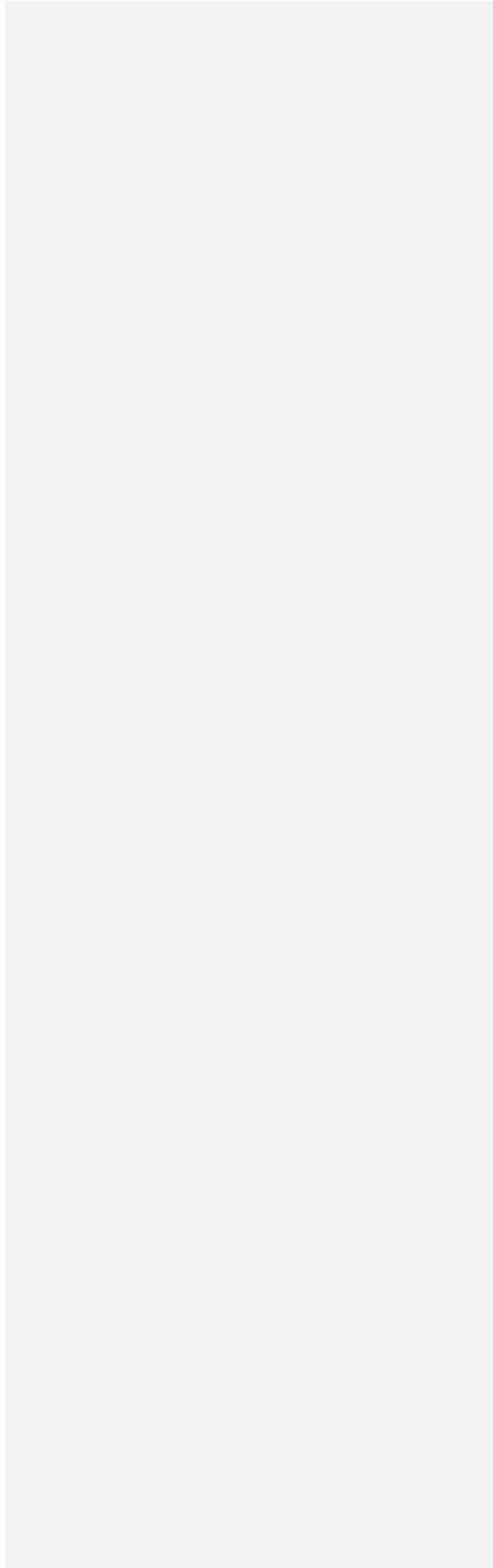
S4.4   O3HP
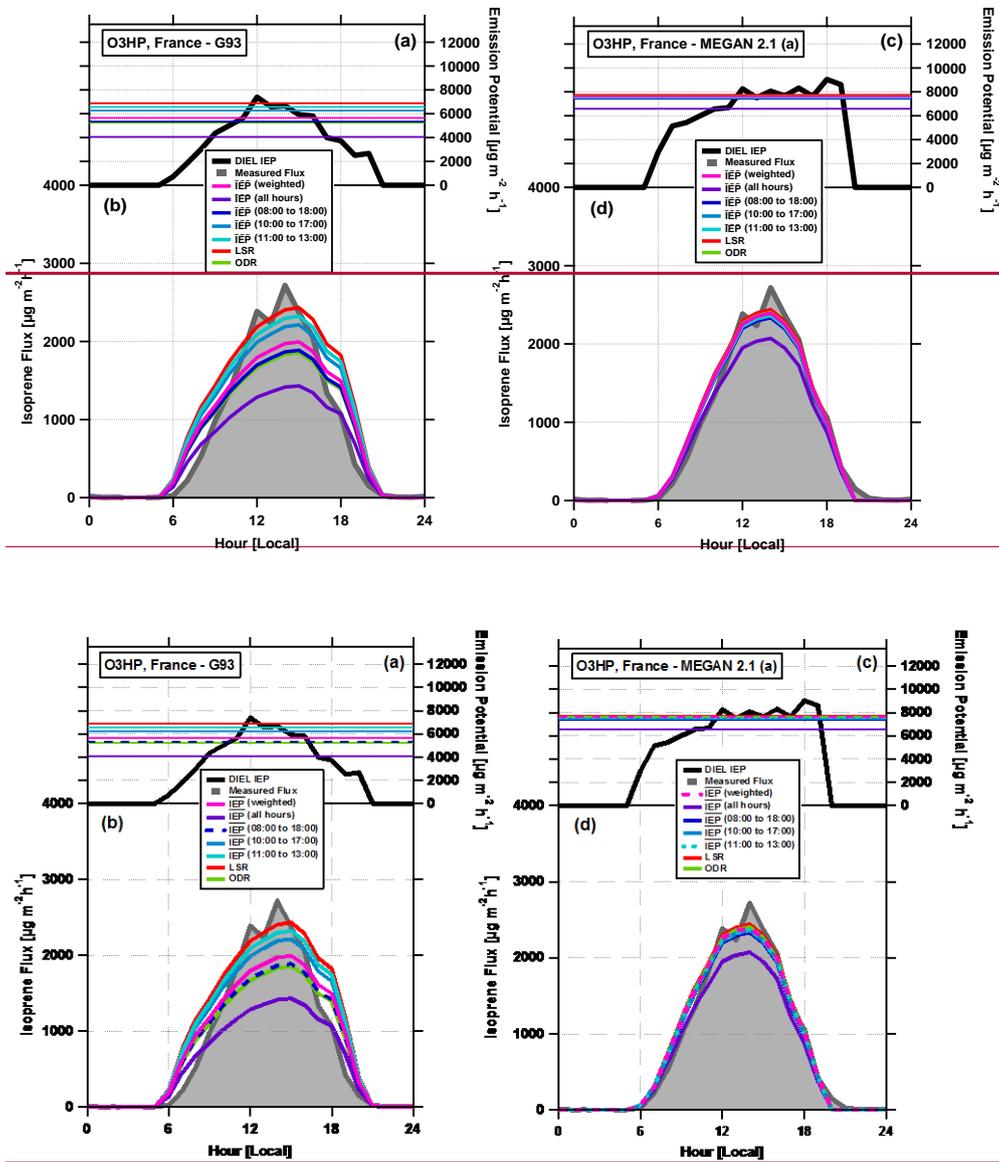
Figure S4 Panels A and C show the average diurnal cycle in the isoprene emission potential (e.g. $IEP = \overline{\left(\frac{F_{iso}}{\gamma}\right)}$)   calculated for the Observatoire de Haute Provance site, France using the G93 (panel A) and MEGAN 2.1 (panel B) algorithms. Superimposed on top of these are the isoprene emission potentials calculated using the least square regression, orthogonal distance regression and average (with several averaging lengths) methods – see text for detailed description. Panels B and D show the average diurnal cycle of the

measured fluxes and the average diurnal cycle of the fluxes modelled using the seven different isoprene emission potentials calculated for this data set.

5

10

15

20

S5   Influence of past light and temperature on calculated emission potential

Within the MEGAN model Tthe influence of past light and temperature on derived emission potentials using the MEGAN model is considered relative to a set of standard within canopy, leaf-level, conditions. When experimentalists use the MEGAN model in a big-leaf approach, these leaf-level conditions are typically calculated using measurements of PPFD and temperature made above the forest canopy. Figures S5 to S9 show the time series of the average 24 hour and 240 hour above canopy light PPFD and temperature for each of the five sites relative to the leaf-level standard conditions used in MEGAN. Typically the past 24 and 240 hour PPFD is considerably higher than the standard conditions which results in a much larger gamma factor and a reduced emission potential. For this reason, it is our recommendation that the MEGAN model should not be used to derive emission potentials unless coupled to an appropriate canopy environment model.

S5.1   Alice Holt
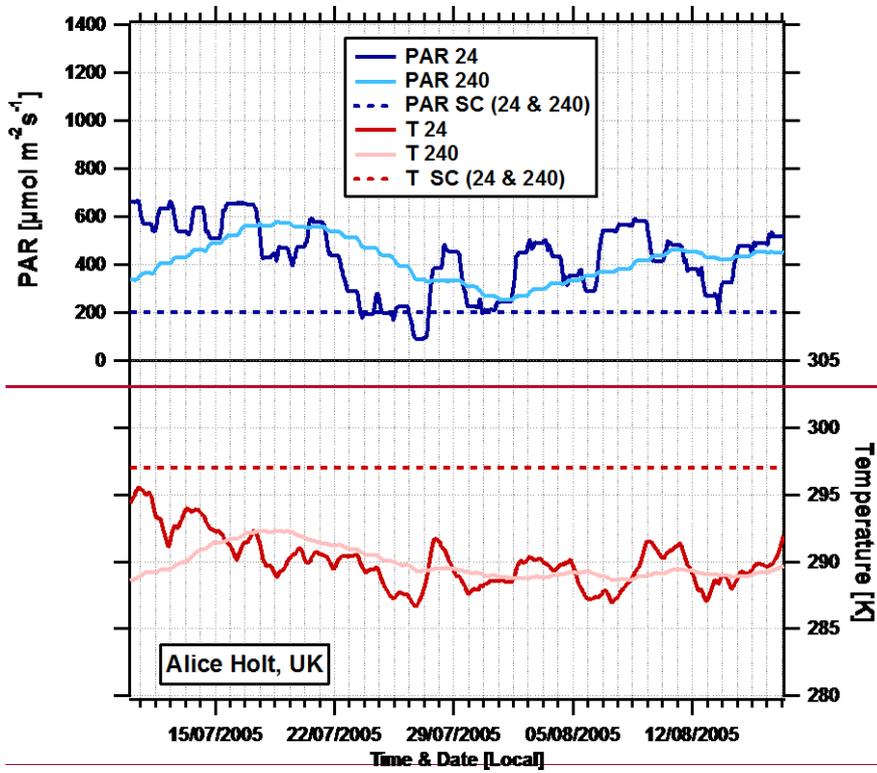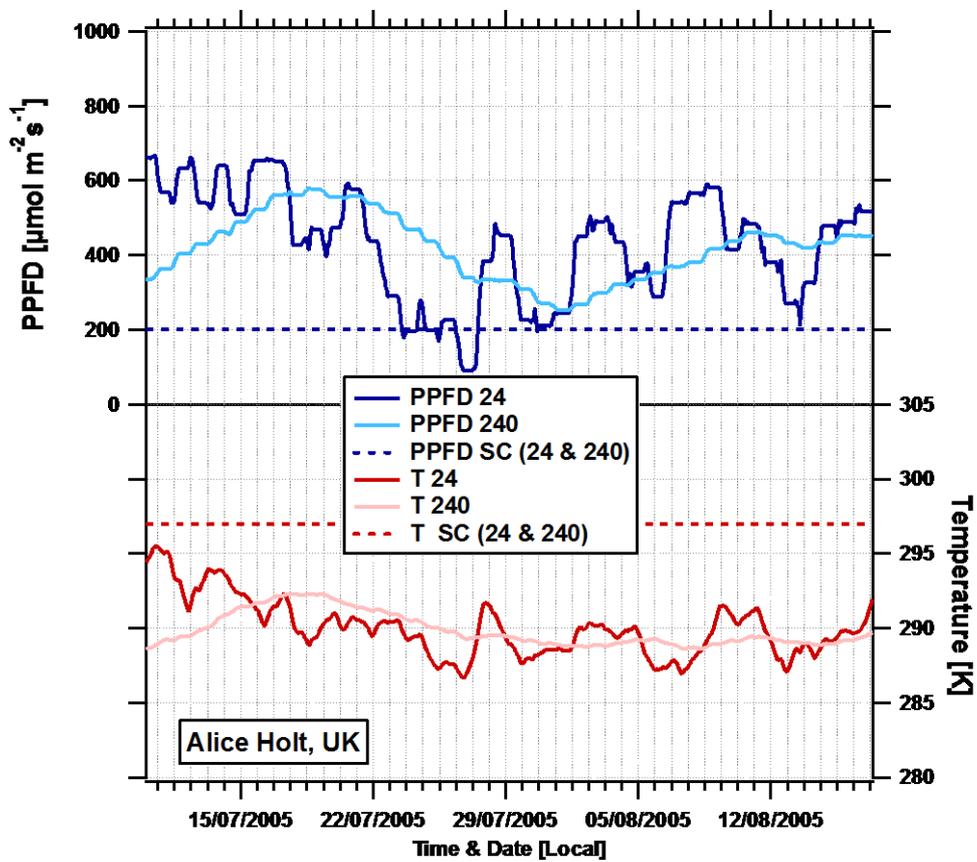
Alice Holt, UK

Figure S5. Time series of the previous (24 and 240 hours) above canopy light and temperature measurements made at the Alice Holt site relative to the standard conditions used in the Model of Emission of Gases and Aerosols from Nature (dashed lines) for leaf-level canopy average temperature and light.

5

S5.2   **Bosco Fontana**

Bosco Fontana, Italy
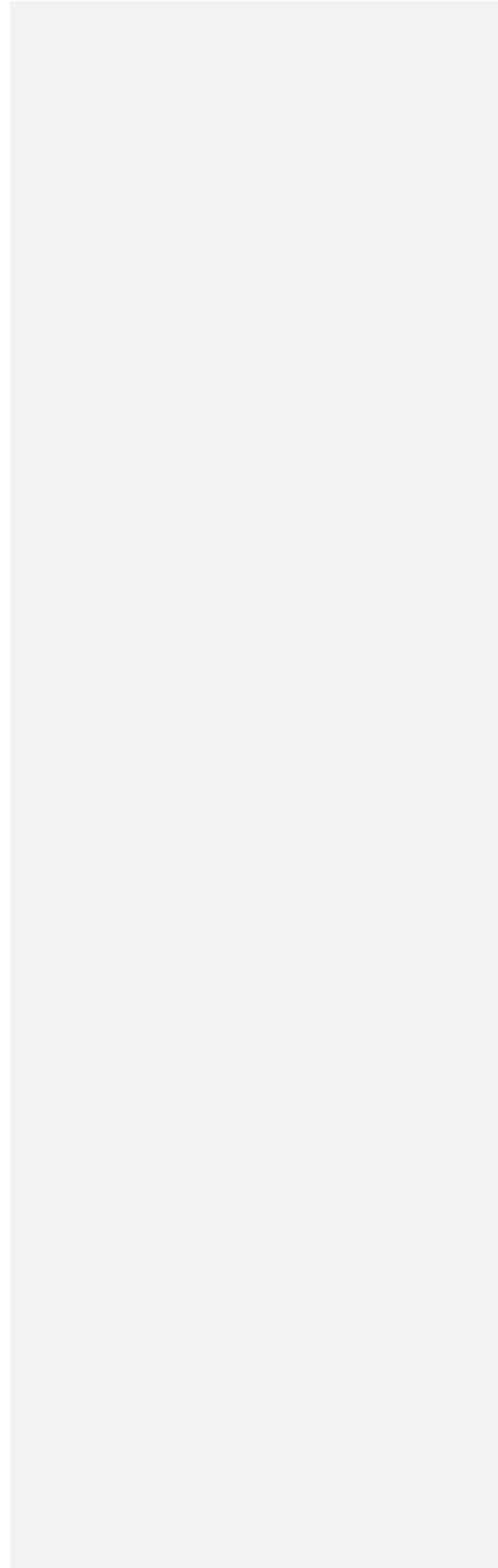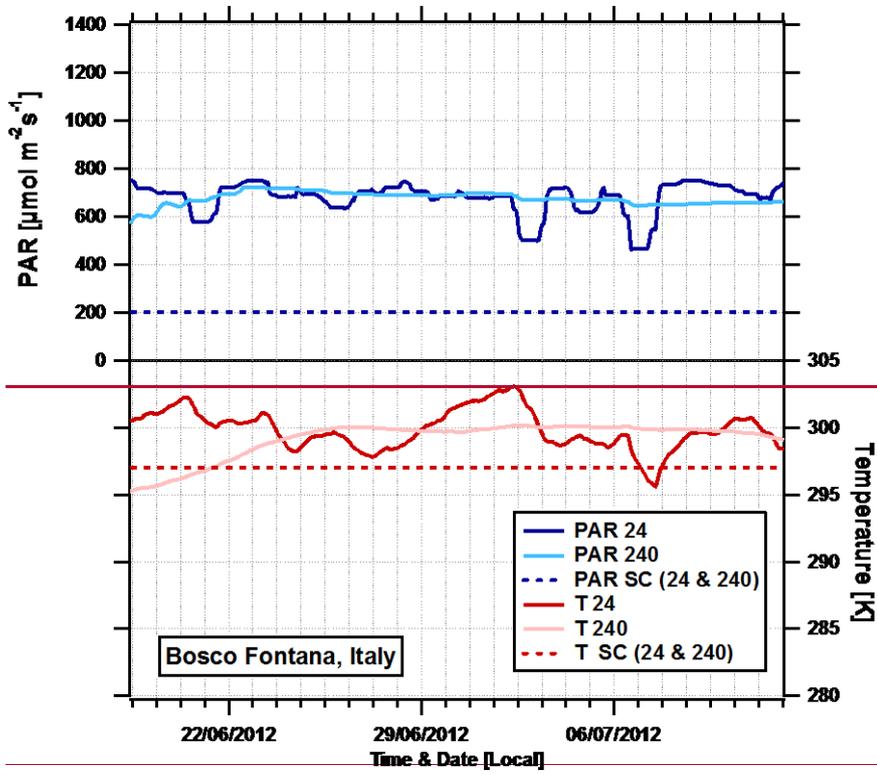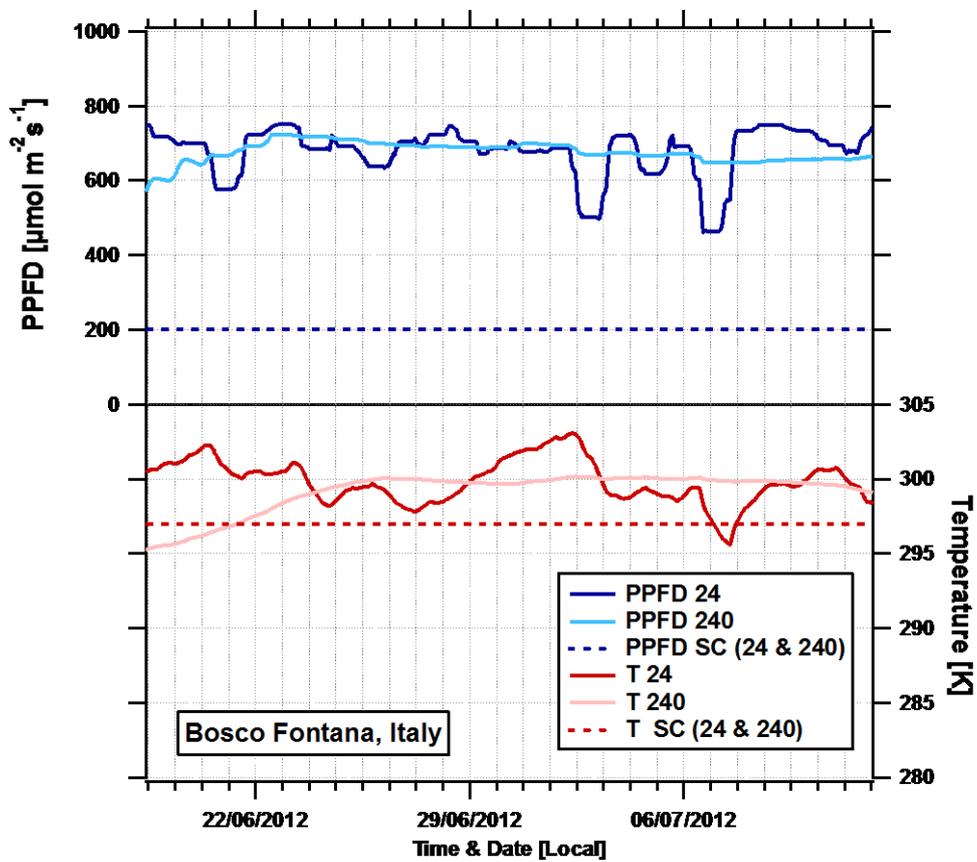
Figure S6. Time series of the previous (24 and 240 hours) above canopy light and temperature measurements made at the Bosco Fontana site relative to the standard conditions used in the Model of Emission of Gases and Aerosols from Nature (dashed lines) for leaf-level canopy average temperature and light.

22

S5.3   Castelporziano

Castelporziano, Italy
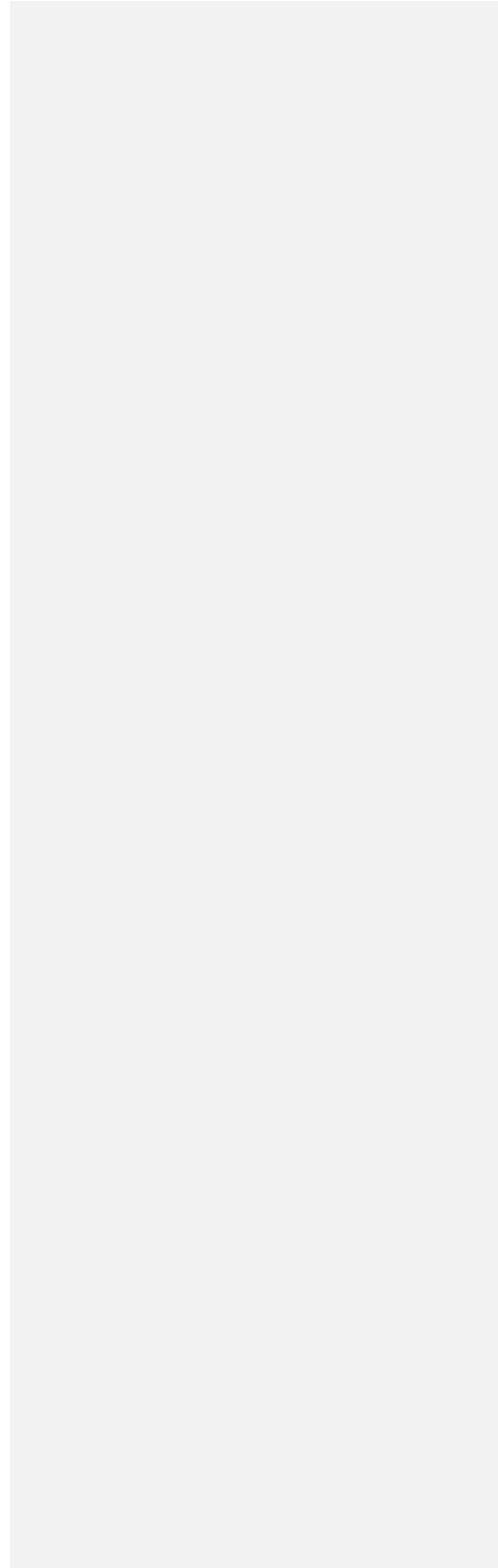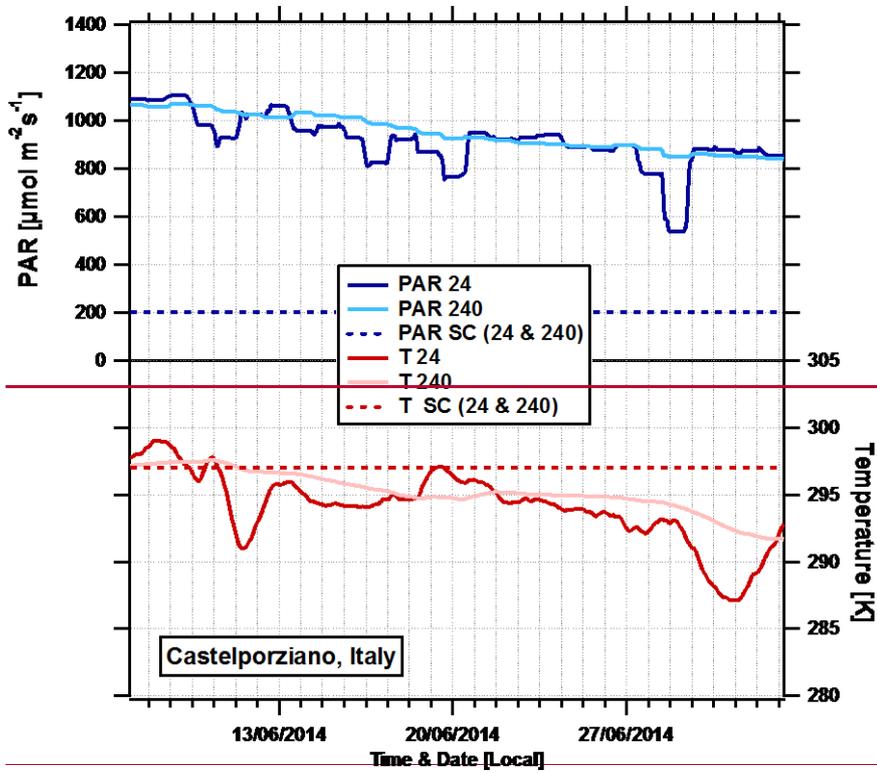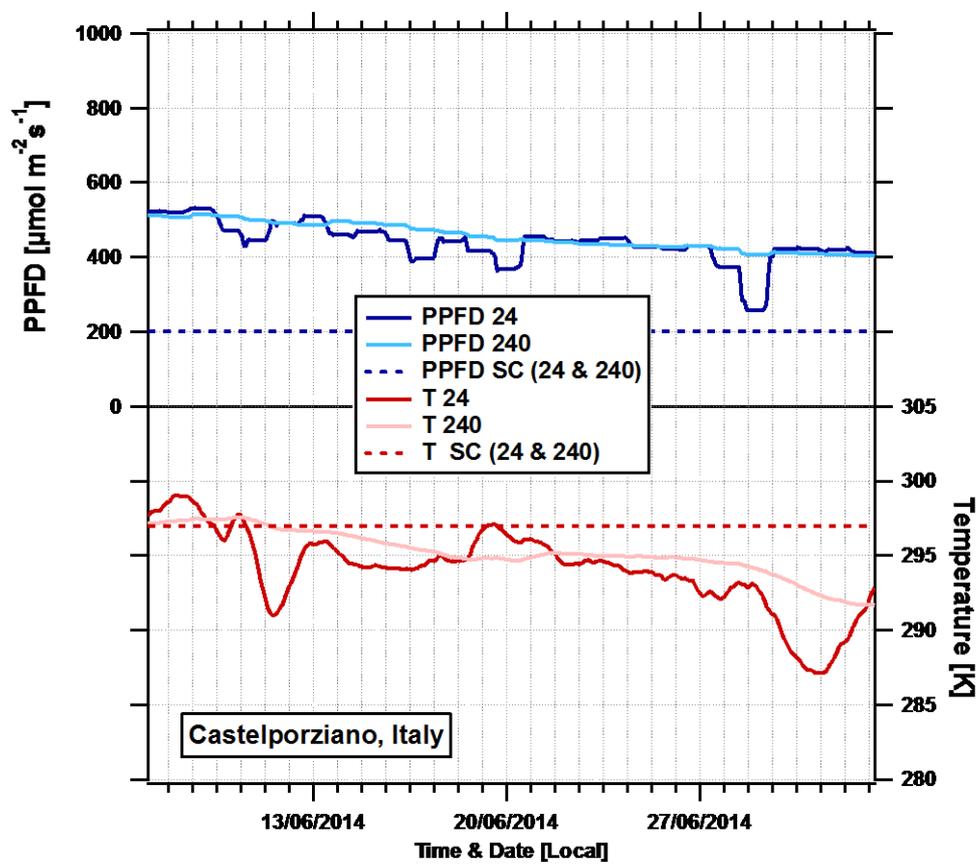
Figure S7. Time series of the previous (24 and 240 hours) above canopy light and temperature measurements made at the Castelporziano site relative to the standard conditions used in the Model of Emission of Gases and Aerosols from Nature (dashed lines) for leaf-level canopy average temperature and light.

25

S5.4   Ispra
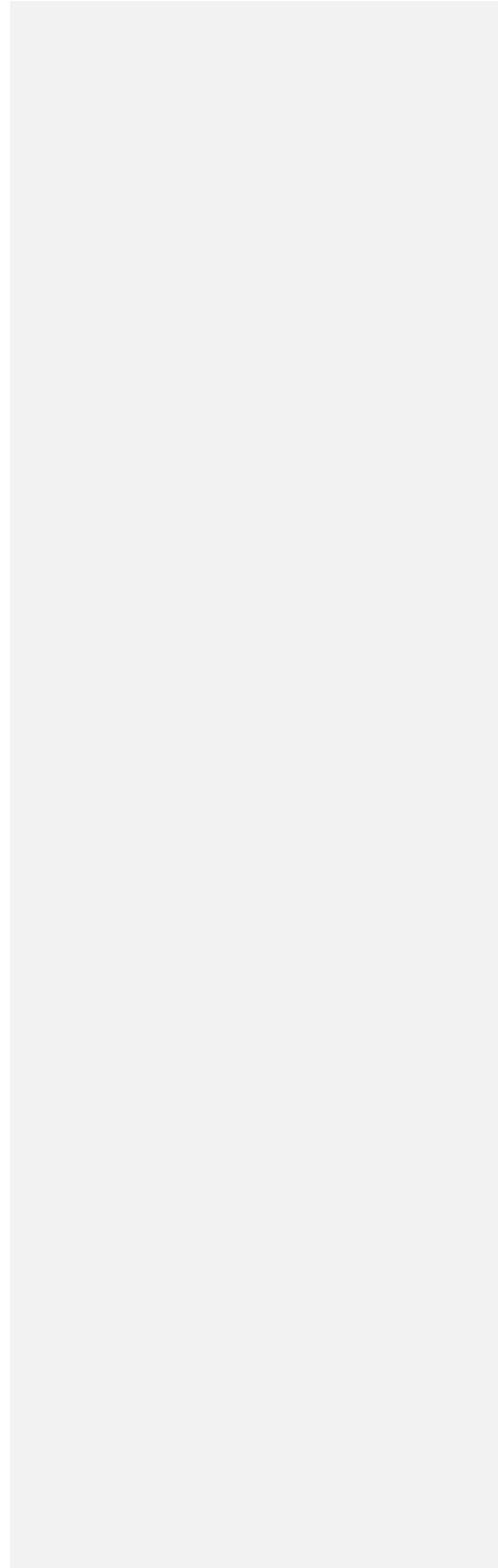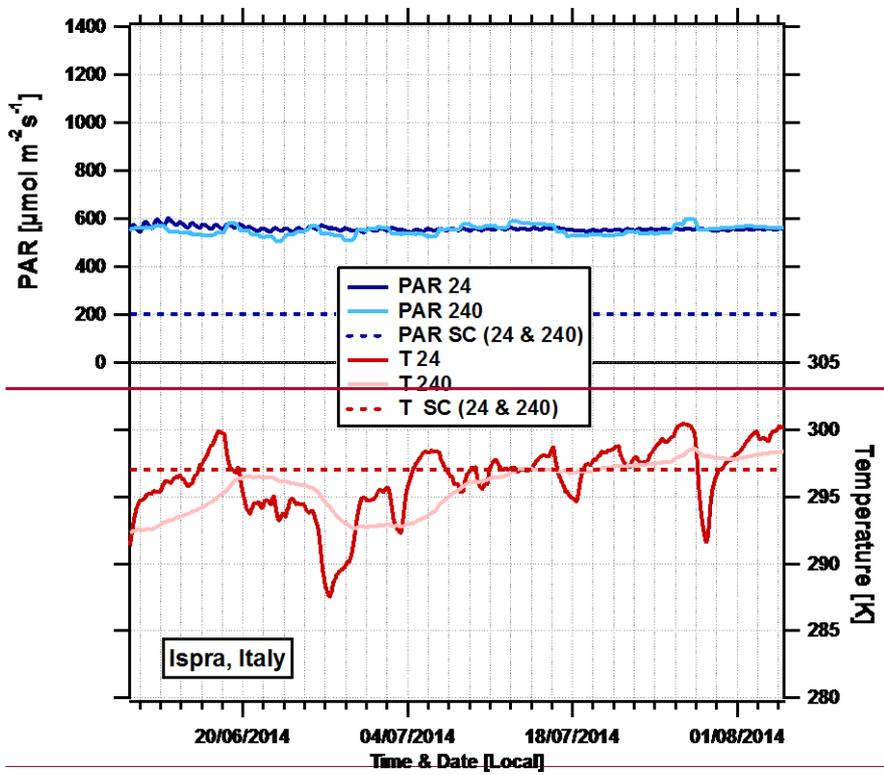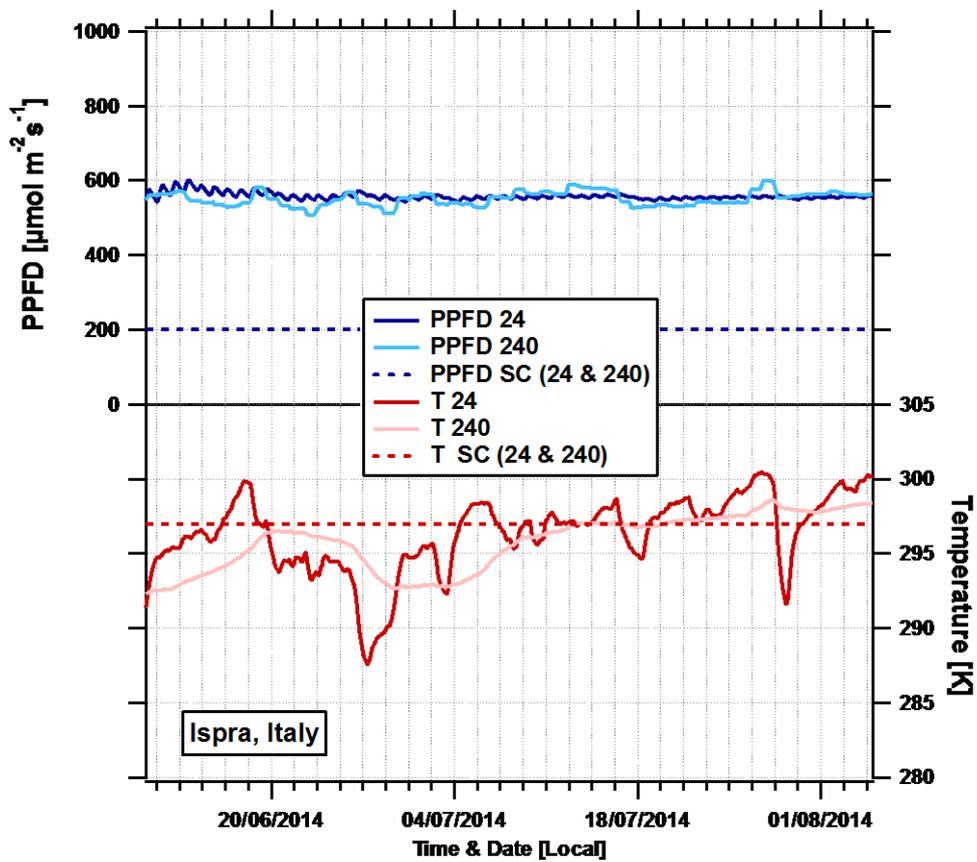
Figure S8. Time series of the previous (24 and 240 hours) above canopy light and temperature measurements made at the Ispra forest site relative to the standard conditions used in the Model of Emission of Gases and Aerosols from Nature (dashed lines) for leaf-level canopy average temperature and light.

S5.5   O3HP
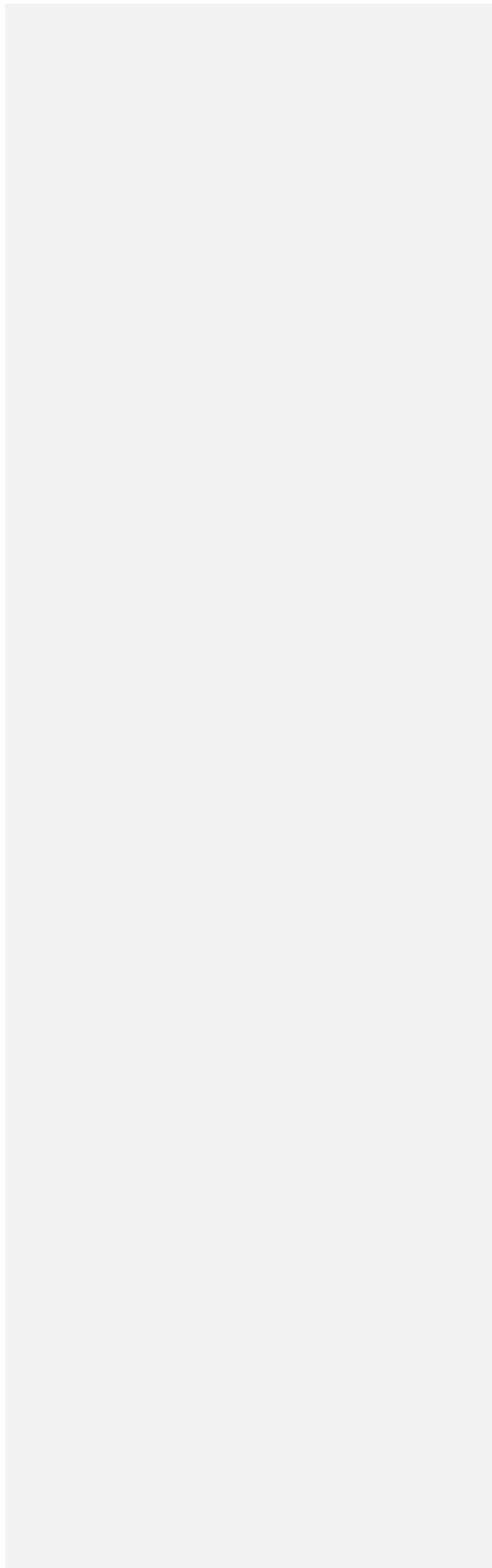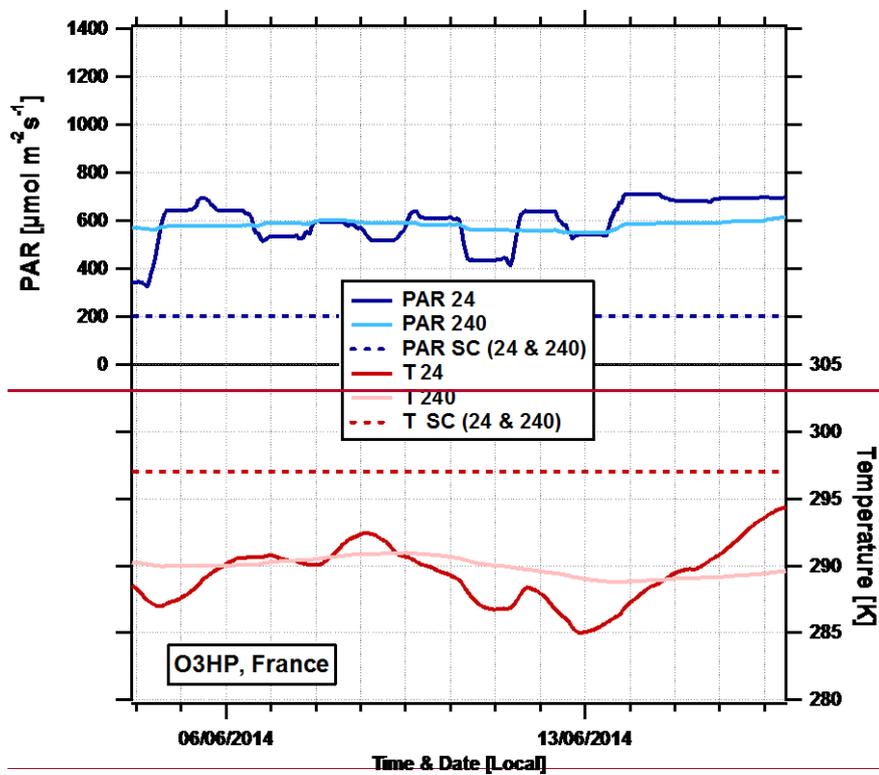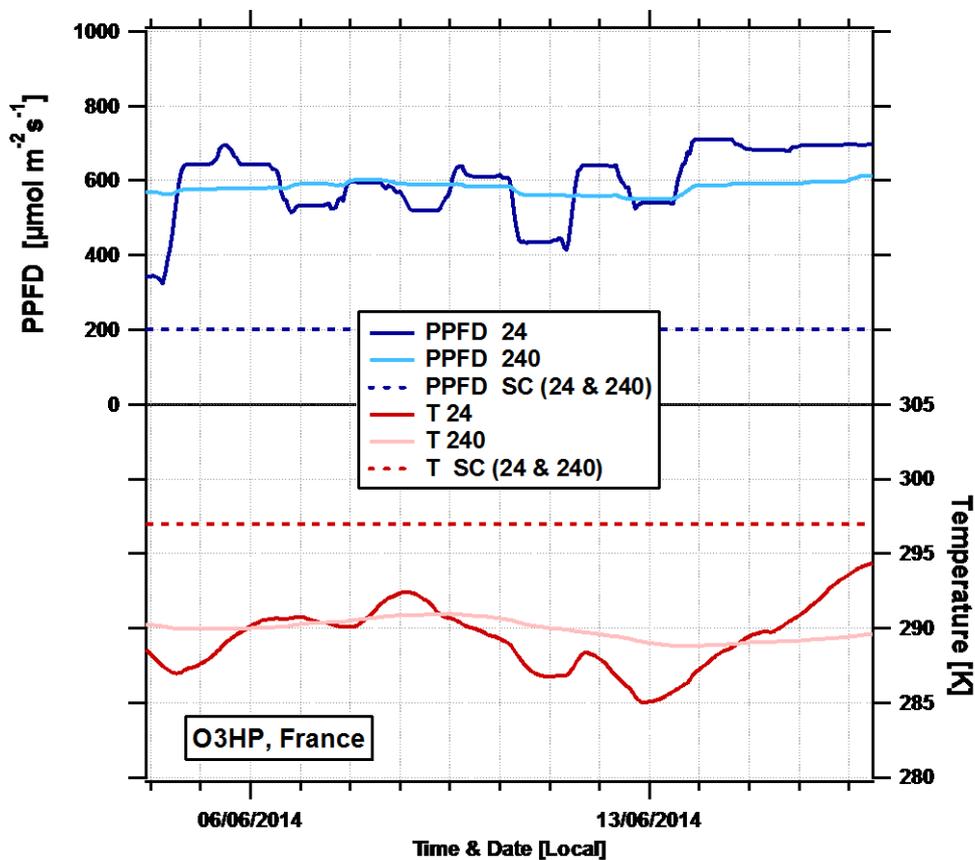
Figure S9. Time series of the previous (24 and 240 hours) above canopy light and temperature measurements made at the Observatoire de Haute Provence site relative to the standard conditions used in the Model of Emission of Gases and Aerosols from Nature (dashed lines) for leaf-level canopy average temperature and light.

S6   Species composition uncertainty

Species composition data for each of the five measurement sites was available, but no uncertainties were stated. Here, we attempt to assess the uncertainty by performing wind rose analysis of the isoprene emission potentials to assess how they vary spatially. Figure S10 shows the isoprene emission potential wind rose for the Alice Holt, Bosco Fontana and Ispra forest sites relative to the average isoprene emission potential. This analysis showed the spatial variation to range from 14% at Alice Holt to 20% at Bosco Fontana. For the remaining two sites, Castelporziano and O3HP, where there was insufficient data to perform a detailed wind rose analysis, uncertainties of 20% were assigned.
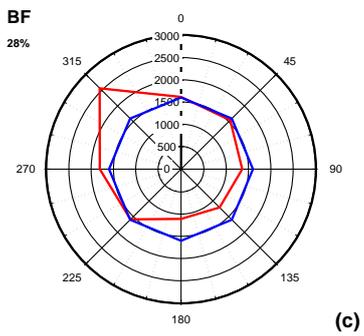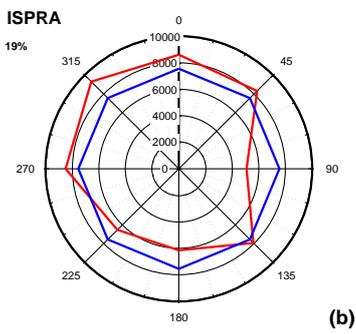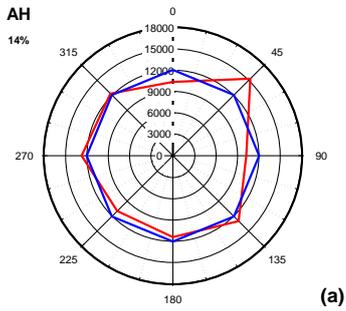
Figure S10 Calculated isoprene emission potential by wind sector (red) and site average (blue) for the Alice Holt (a), Ispra (b) and Bosco Fontana (c) measurement sites.

S7   Reporting fluxes for a set of defined conditions

Above canopy flux measurements may be used to determine an emission potential for a specific set of defined conditions. We used two-dimensional histograms to determine the most common set of light and temperature conditions observed during day time at each of the five measurement sites. The histograms binned the number of flux averaging periods that corresponded to specific bin ranges of light ($\pm$ 200 μmol m^{-2} s^{-1}) and temperature ($\pm$ 1 K). The results for the are shown in figures S11 to S14
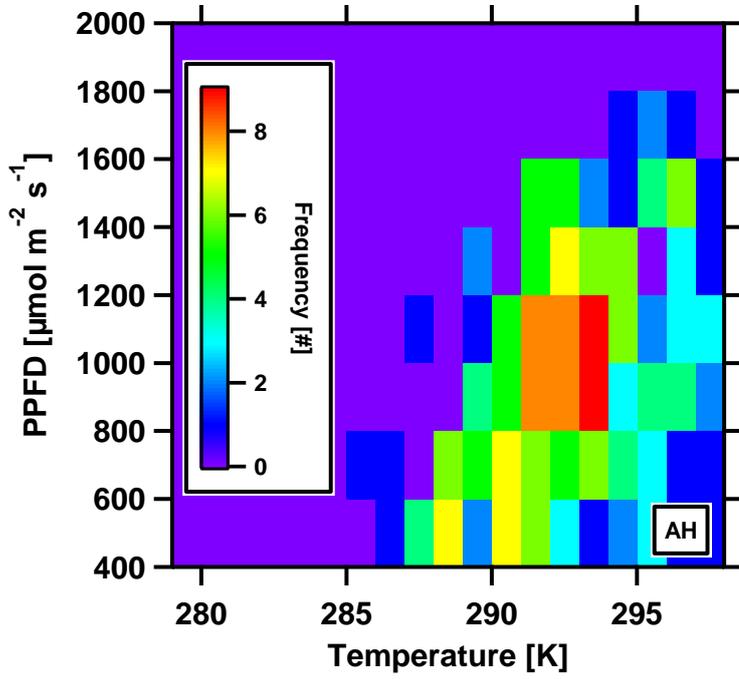
Figure S11 Two dimensional histogram plot of flux averaging periods that correspond to bins of light ($\pm$ 200 μmol m^{-2} s^{-1}) and temperature ($\pm$ 1 K) at the Alice Holt measurement site.
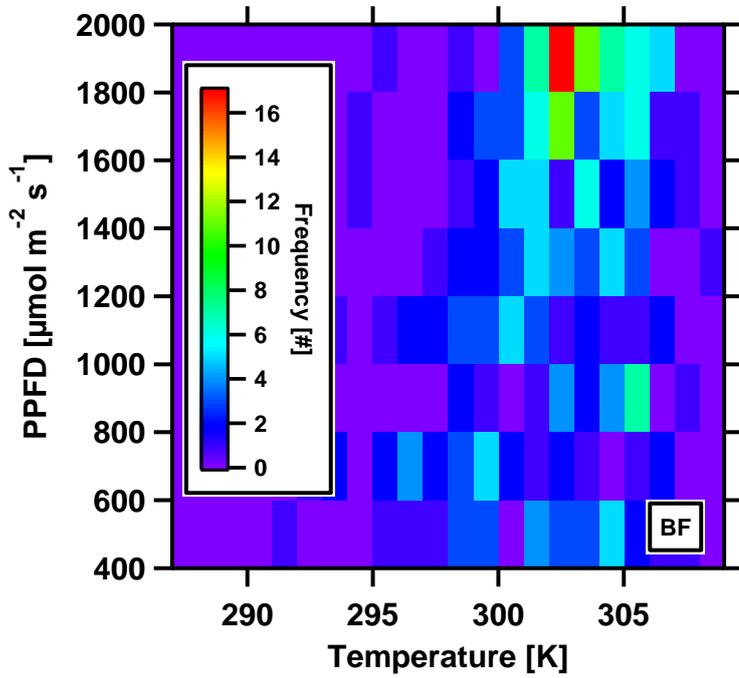
Figure S12 Two dimensional histogram plot of flux averaging periods that correspond to bins of light (± 200 µmol m^{-2} s^{-1}) and temperature (± 1 K) at the Bosco Fontana measurement site.
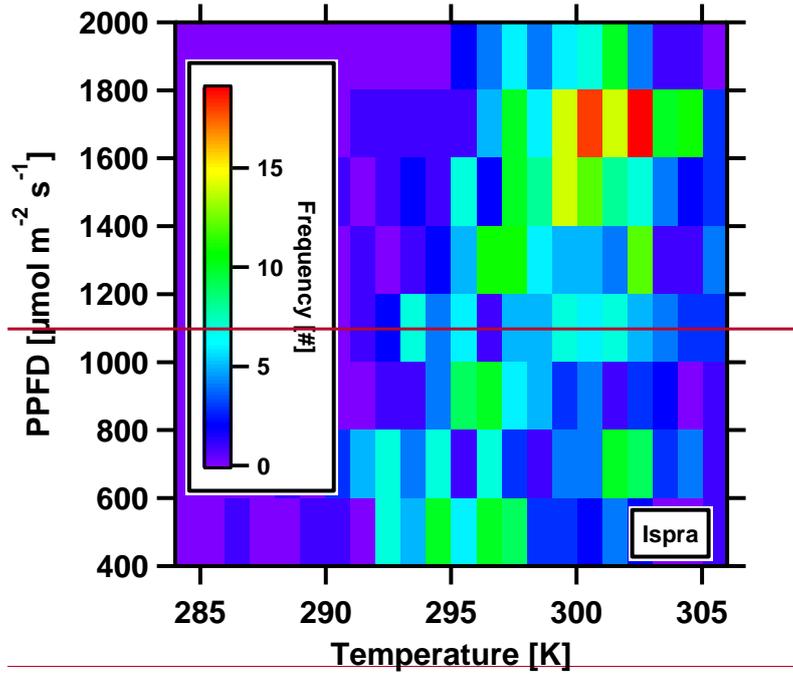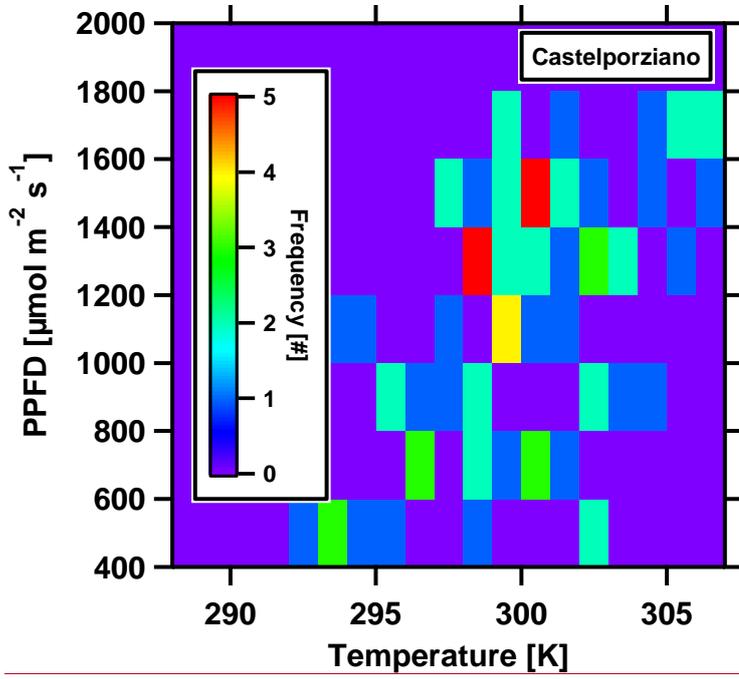
Figure S13 Two dimensional histogram plot of flux averaging periods that correspond to bins of light ($\pm$ 200 μmol m^{-2} s^{-1}) and temperature ($\pm$ 1 K) at the Castelporziano measurement site.
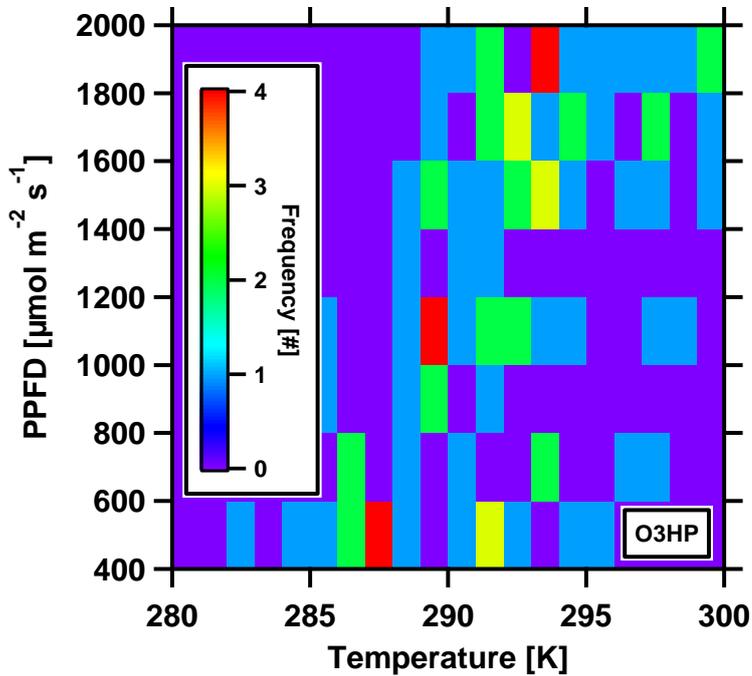
Figure S14 Two dimensional histogram plot of flux averaging periods that correspond to bins of light (± 200 µmol m^{-2} s^{-1}) and temperature (± 1 K) at the O3HP measurement site.

5

References

Ferrea, C., Zenone, T., Comolli, R., Seufert, G.: Estimating heterotrophic and autotrophic soil respiration in a semi-natural forest of Lombardy, Italy, Pedobiologia 55 (2012) 285– 294.

10

Langford, B., Davison, B., Nemitz, E., and Hewitt, C. N.: Mixing ratios and eddy covariance flux measurements of volatile organic compounds from an urban canopy (Manchester, UK), Atmos. Chem. Phys., 9, 1971-1987, doi:10.5194/acp-9-1971-2009, 2009.

15 Langford, B., Acton, W., Ammann, C., Valach, A., and Nemitz, E.: Eddy-covariance data with low signal-to-noise ratio: time-lag determination, uncertainties and limit of detection, Atmospheric Measurement Techniques, 8, 4197-4213, 10.5194/amt-8-4197-2015, 2015.

Putaud, J. P., Bergamaschi, P., Bressi M., Cavalli, F., Cescatti, A., Daou, D., Dell'Acqua, A., Douglas, K., Duerr, M.,
20 Fumagalli, I., Goded, I., Grassi, F., Gruening, C., Hjorth, J., Jensen, N. R., Lagler, F., Manca, G., Martins Dos Santos, S., Matteucci, M., Passarella, R., Pedroni, V., Pokorska, O., Roux, D., JRC – Ispra Atmosphere – Biosphere – Climate Integrated monitoring Station 2013 Report,, EUR 26995 EN, doi: 10.2788/926761, 73-93.

Taipale, R., Ruuskanen, T. M., Rinne, J., Kajos, M. K., Hakola, H., Pohja, T., and Kulmala, M.: Technical Note: Quantitative long-term measurements of VOC concentrations by PTR-MS - measurement, calibration, and volume mixing ratio calculation methods, Atmospheric Chemistry and Physics, 8, 6681-6698, 2008.

Zhao, J., and Zhang, R. Y.: Proton transfer reaction rate constants between hydronium ion (H_3O^+) and volatile organic compounds, Atmospheric Environment, 38, 2177-2185, 2004.